ACCUMBENS-PROJECTING LATERAL HYPOTHALAMIC MELANIN CONCENTRATING HORMONE NEURONS INTERACT WITH OVARIAN HORMONES TO MODULATE MOTIVATED FOOD-SEEKING

Ву

Lauren Marie Raycraft

A DISSERTATION

Submitted to
Michigan State University
in partial fulfillment of the requirements
for the degree of

Psychology – Doctor of Philosophy

2023

ABSTRACT

Food intake requires a complex interplay of signals from central and peripheral systems as well as external stimuli, which are integrated across multiple timescales to coordinate feeding behavior. Individuals make numerous decisions about food each day, including what to eat, how much to eat, and when. Traditionally, research examining the timing of food intake has done so on a 24-hour scale, examining the influence of appetite-stimulating and satiety signals on circadian rhythms of feeding behavior. However, individuals can keep track of time on multiple scales including in the milliseconds to minutes range, a form of timing known as interval timing. This perception of brief intervals supports associative learning and the formation of predictive relationships (C. V. Buhusi & Meck, 2005). Thus, interval timing is critical for learning and decision-making. However, despite the role of interval timing in decision-making and the frequency of food-related decisions, few studies have examined the relationship between appetitive signals and interval timing. Appetitive signals, including the neuropeptide Melanin concentrating hormone (MCH), are predominantly produced in the lateral hypothalamic area (LHA), a heterogenous brain region characterized by its role in energy homeostasis. I previously provided the first evidence that LHA neurons that produce MCH (LHAMCH neurons) influence time-dependent food-seeking in a manner that depends on LHA subregion, sex, and estrous cycle stage. In particular, excitation of anterior LHAMCH neurons selectively prolonged motivated food-seeking in females tested during diestrus, the period of the rodent estrous cycle when levels of circulating gonadal hormones are typically lower. This suggested a role for the nucleus accumbens (NAc), a ventral striatal region critically involved in reward processing, and

circulating gonadal hormones like estradiol. This dissertation extends these findings by examining the role of LHAMCH neurons that project to the nucleus accumbens (LHAMCH → NAc) on time-dependent food-seeking. Specifically, I separately examined the effects of chemogenetic excitation of NAc-projecting neurons from posterior (LHAp; Chapter 2) and anterior (LHAa; Chapter 3) subregions of the LHA in intact female rats. While chemogenetic excitation of LHAp^{MCH} → NAc neurons failed to produce behavioral effects on time-dependent food-seeking, excitation of LHAa^{MCH} > NAc neurons influenced responding selectively during diestrus. Interestingly, however, these effects were in the opposite direction than expected: chemogenetic excitation of LHAa^{MCH} > NAc neurons *reduced* food-seeking after the omission of an expected food reward. Finally, I directly examined the influence of estrogen on LHAa^{MCH} →NAc neuronal excitation by ovariectomizing rats (OVX) and testing them with and without estradiol replacement. Contrary to expectations, chemogenetic excitation of LHAa^{MCH} → NAc reduced post-criterion food-seeking in OVX rats treated with estradiol, rather than without. In short, the removal of peripheral estrogen through ovariectomy does not recapitulate effects of LHAa^{MCH} → NAc excitation during diestrus. This data indicates that motivational effects of LHAa^{MCH} > NAc neurons are sensitive to circulating gonadal hormones, including estrogen. Furthermore, these data indicate a role for LHAaMCH > NAc neurons in guiding decisions to persevere or attenuate effortful food-seeking after the omission of an expected food reward.

This disse (10/16/1928 – 3/1	ertation is dedicate 17/2023). Whip-sm	ed to my Granmo nart and well-rea in all of us.	om, Marjorie "Mar id, she instilled the	j" Raycraft e value of learning

ACKNOWLEDGEMENTS

As it turns out, the acknowledgments are nearly as hard to write as the dissertation itself – especially given how many people have supported me throughout graduate school and the years leading up to it. First and foremost, thank you Alex, for accepting me into the lab as a naïve and enthusiastic undergrad, and then back into the lab as a PhD student. Often, it's the small, unassuming moments that irrevocably change the course of your life – for me, this includes the decision to take your Neurobiology of Food Intake course, and that day I stayed after class to ask if I could work in your lab. Thank you, thank you, thank you, not only for saying yes then, but for welcoming me back into the lab as a PhD student and then investing six years into mentoring and supporting me as I chased this dream. I would, quite literally, not be a behavioral neuroscientist without you.

Thank you also to my committee, including Drs. Alexa Veenema, Kelly Klump, and Gina Leinninger, for your steadfast support throughout the chaos and uncertainty of graduate school. Knowing I had a great committee in my corner was reassuring in even the toughest times.

I am also grateful to have made lifelong friends in the Johnson lab over the last six years, including especially Jenna Lee, Kate Sapkowski, and Nicollette Russell.

These women worked side-by-side with me through tears and dance parties and just about everything else you can think of. I love you all and am so grateful to know you.

I would also like to thank Maria and David, Chase and Shay, and all of the other support staff in the building and animal facilities. These individuals not only made this

work possible, but also provided kindness and a bright spot – and even delicious baked goods! – on long days in the lab.

Thank you to all of my BNS friends, from my initial cohort – Ben Fry, Jenny Gerena, and Henry Yang – to the cohort who adopted me – Jessica Lee, Samantha Bowden, Taryn Meinhardt, and Allie Costello – for providing solidarity, support, and humor as we navigated grad school through moving buildings, a global pandemic and more. I am also grateful to have found mentors and friends in BNS post docs Katie Yoest, Christina Reppucci, and Jenna Lee.

Beyond MSU, thank you to each and every mentor I've had over the years, especially my first – Dr. Ján Pékarovic, who inspired my initial passion for research. Thank you to the friends who've indulged me in continuing school for so long, especially those that have stood by me since high school – Mallory Busso Wollerman, Alex Liou, Colleen Unsworth, Kyle Mulvaney and Becca Jacobs – and college – Taylor McEvilly, Erin VanBuskirk, Sarah Schulte, Megha Patel and Amanda Ahrens. Thanks also to Keenan Scribner and Erica Tooker. I'm so grateful to each and every one of you.

I am phenomenally lucky to call Dodie and Jay Raycraft Mom and Dad, and Meghan my sister. Their influence on me – and my education – can't be captured in words. I am also lucky to have the support of my (future) mother-in-law, Janet Kerber. I could not have done this without them. I love you all dearly.

Finally, thank you to my fiancé, Mitch Lindstrom. You have had unwavering confidence in me since I first entertained the idea of applying to graduate school, and have been my rock throughout. Thank you for believing in me, even when I didn't. I love you.

TABLE OF CONTENTS

CHAPTER 1: Introduction	1
CHAPTER 2: Accumbens-projecting Melanin Concentrating Hormone neurons that originate in the posterior Lateral Hypothalamic Area do not influence motivation or time perception	
CHAPTER 3: MCH Neurons in the anterior LHA interact with estrous cycle stage to influence motivation in a time-dependent manner	66
CHAPTER 4: Estrogen is necessary for LHAa ^{MCH} →NAc neuronal effects on post-criterion responding	95
CHAPTER 5: Overall Discussion	20
BIBLIOGRAPHY12	28
APPENDIX14	45

CHAPTER 1: Introduction

The ability to perceive time is integral to our daily lives. Time perception enables us to respond to changing environments and make predictions about future events, such as food availability. Time is perceived on multiple scales, including within the seconds to minutes range. This distinct form of timing known as **interval timing** supports associative learning and the formation of predictive relationships by providing temporal contiguity (Balsam et al., 2010; C. V. Buhusi & Meck, 2005). Interval timing can contribute to the ability of an individual to learn about their food environment through the acquisition of predictive associations between environmental stimuli and food. As such, interval timing has the potential to greatly impact decisions associated with the acquisition and ingestion of food. Despite this, few studies have examined the relationship between interval timing and feeding behavior.

The lateral hypothalamic area (LHA) is a regulatory brain region ideally situated to integrate a variety of physiological signals with information from higher-order brain regions involved in timing and reward processing. As such, it has been described as an "integrator," "hub," and "motivation-cognition interface" for its role in motivated decision making (Berthoud & Münzberg, 2011; Bonnavion et al., 2016; Mogenson et al., 1980; Petrovich, 2018). A subset of neurons within the LHA synthesize the appetite-stimulating (i.e., orexigenic) neuropeptide, Melanin Concentrating Hormone (MCH). Like the LHA, MCH has also been described as an "integrative peptide" for its role in synthesizing information from various homeostatic and hedonic neurochemical signals to coordinate motivated behavior (Diniz & Bittencourt, 2017). Notably, LHA neurons that synthesize MCH, herein referred to as LHA^{MCH} neurons, influence learned food intake in

tasks that inherently rely on the ability to perceive time in the seconds-to-minutes range (Noble et al., 2019; Sherwood et al., 2012, 2015; Subramanian et al., 2023).

Previously, I examined whether neurons in the LHA that produce MCH could influence time-dependent food-seeking in an interval timing task. The peak interval (PI) paradigm is a duration reproduction task in which animals are trained that lever presses result in reinforcement only after a criterion duration (e.g., after 20s) has elapsed. Using chemogenetics to selectively excite LHAMCH neurons during the PI paradigm, I revealed that LHA^{MCH} neurons potentially modulate time perception and/or motivation within this food-seeking task. However, the effects of LHA^{MCH} neuronal excitation depended on the extent of LHAMCH neuronal excitation within the LHA (i.e., targeting of a more anterior vs posterior subset of LHAMCH neurons, LHAa and LHAp, respectively) and sex of the animals. Excitation of LHAp^{MCH} neurons putatively changed time perception, an effect that was subtle in male rats but pronounced in females. In contrast, excitation of LHAaMCH neurons had no effect on time perception, per se. Instead, excitation of LHAaMCH neurons robustly increased responding after the omission of an expected food reward in female – but not male – rats. This prolongation of high rate responding after the criterion had elapsed indicates increased motivation to continue food-seeking. In other words, LHAaMCH neuronal excitation increased motivation to continue foodseeking in female, but not male, rats.

Given that the rodent estrous cycle is known to modulate food intake in female rats, we next examined whether the influence of LHA^{MCH} neuronal excitation on time-dependent food-seeking was modulated by estrous cycle stage. The rodent estrous cycle is characterized by fluctuating gonadal hormones which typically peak during

proestrus and estrus (P/E) and then fall rapidly during metestrus and diestrus (M/D) (Goldman et al., 2007). Strikingly, in the PI paradigm, the effects of LHA^{MCH} neuronal excitation on temporally mediated food-seeking were dependent on the estrous cycle stage in which rats were tested. Excitation of LHAa^{MCH} neurons produced a robust increase in temporally mediated motivated responding only when rats were tested during M/D. This effect reveals a role for LHA^{MCH} neurons in coordinating motivated behavior based on information about the timing of food availability (i.e., the temporal context) and in manner that depends on estrous cycle stage. However, the potential circuitry underlying these effects has not yet been identified.

As a key mesolimbic brain region involved in motivated behavior, including in aspects of both food intake and interval timing, the Nucleus Accumbens (NAc) is a potential downstream target of LHA^{MCH} neurons (Kelley, 2004; Kurti & Matell, 2011; MacDonald et al., 2012). Indeed, the MCH receptor, MCH1R, is densely expressed in the NAc and infusion of the MCH peptide to the NAc increases feeding (Georgescu et al., 2005). In addition, the estrogen receptor ER- α is densely expressed in the NAc with MCH1R, providing a potential mechanism through which fluctuating estrogen levels could influence MCH activity (Terrill et al., 2020). As such, projections from LHA^{MCH} neurons to the NAc might underlie the effects of LHA^{MCH} neuronal excitation on temporally mediated food-seeking in female rats. To explore this possibility, this dissertation examines the effects of chemogenetic excitation of anterior and posterior LHA^{MCH} neurons that project to the NAc (LHA^{MCH} →NAc) on time-dependent food-seeking in the PI task. In addition, I examine the role of the estrous cycle in mediating the influence of these LHA^{MCH} →NAc neurons on this motivated behavior. Finally, I

directly manipulate estrogen to isolate a potential role for this hormone in moderating the effects of LHA^{MCH} →NAc neuronal excitation on motivated behavior. Together, these studies will explore a role for LHA^{MCH} →NAc neurons in modulating time-dependent motivated behavior and describe whether these effects are influenced by estrous cycle stage and/ or estrogen.

To place these results in context, this first dissertation chapter will provide insight into the traditional view of food intake from a circadian perspective as well as describe alternative models of interval timing. I will then describe the role of the lateral hypothalamic area (LHA) in food intake as well as the Melanin Concentrating Hormone (MCH) neuropeptide system and its interactions with the nucleus accumbens (NAc) in motivated feeding behavior. Finally, I will discuss the interactions of the estrous cycle with MCH and describe how these effects are accounted for in these dissertation studies. These data provide a novel framework through which LHA^{MCH} neurons may coordinate behavior based on information from a broader temporal context.

1.1 Feeding behavior is coordinated across multiple timescales

(i) Circadian Timing

Traditionally, research has primarily examined the timing of food intake on a 24-hour scale, examining the influence of circadian rhythms on food intake (Bass & Takahashi, 2010; W. Huang et al., 2011; ter Haar, 1972). Circadian timing relies on a "master clock" in the suprachiasmatic nucleus (SCN) of the hypothalamus, which integrates light cues via the retinohypothalamic tract (RHT) to synchronize the transcription of so-called "clock genes." The lateral hypothalamic area (LHA) receives input from the SCN to coordinate arousal and sleep-wake cycles via neuropeptide and

hormonal signaling (Arrigoni et al., 2019; Brown et al., 2015; Goodless-Sanchez et al., 1991). Thus, damage to the LHA disrupts the sleep/wake cycle (Mistlberger et al., 2003; Pfeffer et al., 2012) in part due to the influence of MCH expressing cells. Accordingly, during REM sleep, MCH production increases and a subset of MCH neurons become active (Blouin et al., 2013; Hassani et al., 2009; Jego et al., 2013). Furthermore, acute optical stimulation of LHA MCH cells promotes REM sleep (Jego et al., 2013).

Although MCH has been critically implicated in the sleep-wake cycle, findings suggest that this does not extend to an influence of MCH in modulating food intake over protracted time frames. Animals will evoke an increase in motoric behavior in the period preceding predictable food availability; this food-anticipatory activity (FAA) is under the control of a circadian-like time-keeping mechanism that prepares organisms for meal intake (Challet, 2019). Although the brain mechanisms underlying FAA are independent of the SCN, they are influenced by neurons in the LHA (Mieda & Yanagisawa, 2002); however, this does not appear to require the MCH system as deletion of MCH1R has no influence over FAA (Zhou et al., 2005). Thus, while MCH is important for regulating sleep-wake cycles, it's influence in guiding appetite through timing likely involves mechanisms that control shorter duration timescales.

(ii) Interval Timing

Interval timing refers to the ability to perceive time in the seconds to minutes range and is functionally and molecularly distinct from circadian timing. Rather than rely on the SCN, the perception of time in this brief range involves a distributed network of corticostriatal circuits, the basal ganglia (BG), and the substantia nigra (SN) (C. V. Buhusi & Meck, 2005; Meck, 1996, 2005). In the lab, interval timing is studied through

the use of duration reproduction tasks, which train animals to reproduce a criterion time through operant responding. One such procedure is the Peak Interval (PI) paradigm, a classic interval timing task.

The PI paradigm is modified from Fixed Interval (FI) procedures, in which animals learn that instrumental responding (i.e., lever pressing) results in reinforcement only after a particular criterion duration has elapsed (Balcı & Freestone, 2020; C. V. Buhusi & Meck, 2006; Rakitin et al., 1998; Roberts, 1981). During FI trials, animals can respond on the lever at any point in time, but only responses that occur after the FI duration (e.g., after 20s) are reinforced. Thus, animals typically respond intermittently throughout the trial and accelerate their response rate around the time of expected reinforcement (Skinner, 1938). Thus, lever responding is characterized by a "breakthen-run" pattern, where low rates of lever responding abruptly increase in anticipation of reinforcement (Balcı, 2014; Schneider, 1969). This transition from a low to high rate of responding is conceptualized as the "start" function and reflects an increase in reward expectancy as the time of reinforcement approaches (Balcı, 2014; Gibbon, 1977). Acquisition of this "start" function depends on the dorsal striatum (MacDonald et al., 2012).

While FI trials enable responding prior to reinforcement to be examined, reward delivery and trial offset prevents the ability to examine responding at or after the criterion time. Thus, Peak interval paradigms are unique from FI paradigms in that they also include probe trials (Balcı & Freestone, 2020; C. V. Buhusi & Meck, 2006; Rakitin et al., 1998; Roberts, 1981). Following the acquisition of FI responding, probe trials are intermixed during PI training. Probe trials onset in the same manner as FI trials and are

initially indistinguishable from FI trials. However, during probe trials no reinforcement is delivered, even after the criterion time has elapsed. Instead, probe trials typically last at least 3x the length of the FI criterion and randomly offset without reward delivery. Thus, after sufficient FI training, probe trials can be randomly intermixed with FI trials in order to examine how animals respond across time without the contamination of reward delivery.

During probe trials, animals exhibit a break-run-break pattern of responding, with a "start" transition into high-rate responding before the criterion (similar to FI trials) and a "stop" transition back to low-rate responding after (Balcı, 2014; Church et al., 1994; Church & Broadbent, 1991; Gallistel & Gibbon, 2000). In other words, during probe trials animals increase their response rate to a peak (peak rate) at the time of expected reinforcement, then attenuate high rate responding after the perceived time of reinforcement has elapsed. The actual time at which peak response rate occurs is *peak* time, and under normal conditions this will approximately equal the criterion time (Balcı, 2014; Gibbon, 1977). When responses are plotted across time as a proportion of peak rate, the resulting proportion of peak rate function forms an approximately normal distribution centered around the criterion time with a slight negative skew. Early in PI training, when probe trials are first introduced, this negative skew is considerable, with high rate responding persisting long after the omitted food reward. The negative skew of the proportion of peak rate response function is reduced as animals learn to attenuate high rate responding and the "stop" function is acquired. Thus, the right-hand side of the proportion of peak rate response function narrows as the "stop" function is acquired. The "start" and "stop" functions are viewed as distinct features of responding that reflect

independent, time-mediated decision processes and that are acquired during different phases on the PI task (C. V. Buhusi & Meck, 2009). Consistent with this idea, unlike the "start" function that is mediated by the dorsal striatum, the decision to stop responding once the criterion duration has elapsed reflects control by the ventral striatum (MacDonald et al., 2012).

Once the "start" and "stop" functions have been acquired, the overall width of the response function that is generated varies proportionally with the length of the criterion being timed. This in part reflects errors in timing that increase in proportion to the length of the duration being timed (Balsam et al., 2009; Gibbon, 1977; Malapani & Fairhurst, 2002; Meck, 1996, 2005). This property forms the basis of Scalar Expectancy Theory (SET; also known as Scalar Timing Theory or the scalar property) and is reflected in a proportional broadening or narrowing of the response function with longer or shorter intervals, respectively. (Church, 1984; Gibbon, 1977; Malapani & Fairhurst, 2002; Meck, 1996). The scalar property is an important feature of timing, as it enables confirmation of changes in time perception. While the "start" and "stop" functions represent discrete behavioral states that can be separately influenced, changes to time perception proportionally alter these functions and shift the response function. For example, if time perception is sped up (i.e., clock speed increases), high rate responding will "start," peak, and "stop" earlier than under normal conditions, resulting in a proportional leftward shift of the response function that coincides with a reduction in peak time. In addition, the width of the "run" period (i.e., the length of high rate responding around the peak) follows the scalar property and thus would proportionally narrow when clock speed is increased (Gibbon, 1977).

(iii) Models and Mechanisms of Interval Timing

Conceptual models of interval timing posit that an *internal clock* keeps track of time in the seconds-to-minutes range. This clock is molecularly and functionally discrete from the SCN "master clock" of circadian timing. Unlike the circadian master clock, which reliably syncs to light as a zeitgeber and accurately tracks long periods of time in the ~24-hour range, adjusting timing slowly (such as through a gradual phase shift), the internal clock of interval timing can time any number of meaningful events rapidly and flexibly (Meck, 1996). Indeed, it is posited that the internal clock can time multiple arbitrary intervals simultaneously, with seemingly no limit aside from those imposed by attentional processes (Balsam et al., 2009; Gibbon, 1977; Malapani & Fairhurst, 2002; Meck, 1996, 2005). However, unlike the circadian clock, which is incredibly accurate over the course of many hours, the internal clock of interval timing is susceptible to variance, which increases in proportion to the duration being time. Thus, the internal clock varies from the circadian clock in at least three ways: (1) the internal clock is more flexible, (2) the internal clock is less precise, and (3) the internal clock displays the scalar property (Gibbon, 1977; Meck, 1996).

While there are multiple models of interval timing, most of them share three key components: a clock or accumulator, a decision-making comparator mechanism, and a memory component. The Pacemaker-Accumulator model is perhaps the most influential model of interval timing (Meck, 1996). This information-processing model posits that the firing of dopaminergic cells in the substantia nigra pars compacta (SNpc) results in the release of striatal dopamine (DA) which in turn acts as an internal clock or "accumulator." This accumulation of striatal DA serves as an indicator for when

meaningful events occur. An attentional gate or "switch" closes when salient events occur (e.g., when a discriminative stimulus is presented) and the amount of DA that has accumulated before another meaningful event (e.g., food reward delivery) can thus be measured. In this example, the duration between when the stimulus is presented and when actions (e.g., lever presses) result in reinforcement can be stored as a reference memory of the amount of DA that accrued during this interval. In the future, when the same stimulus is presented, this reference memory for time is recalled into working memory and compared to the amount of DA currently accruing as time passes. This is the "comparator" component of the Pacemaker-Accumulator information processing model. When the amount of DA that has accrued matches the reference memory, a decision is made and behavior changes accordingly; this is the decision component. For example, the decision to start responding at a high rate is made when the reference memory for time approximately matches the current perception of time. Likewise, the decision to stop responding at a high rate occurs when the current time exceeds the reference time.

Given that the internal clock relies on accumulating DA, changes to the rate of DA accumulation can alter clock speed (i.e., the perception of how quickly time passes). As such, drugs that increase striatal DA (e.g., methamphetamine) result in a decrease in peak time that coincides with a leftward shift and proportional narrowing of the response function (Matell et al., 2006; Meck, 1983). Together, these features indicate an increase in clock speed. In contrast, drugs that decrease DA accumulation (e.g., the D2R antagonist haloperidol) delay peak time as well as produce a rightward shift and proportional broadening of the response curve, indicating a decrease in clock speed (C.

V. Buhusi & Meck, 2002; Meck, 1983, 2006). Together, these studies provide evidence for the dopaminergic nature of the internal clock. On the other hand, the memory component of the internal timing system appears to depend on intact cholinergic signaling, as disrupting acetylcholine interrupts memory formation and/ or recall, depending on the timing of disruption in memory consolidation or retrieval (Meck, 1983, 1996; Meck & Church, 1987).

While the pacemaker-accumulator model of interval timing provides a succinct theoretical framework, one criticism of the model is that its molecular underpinnings remain unclear and – at times – in contrast to its theoretical components. For example, how the pacemaker-accumulator process begins (i.e., to what is the initial duration compared?) remains murky. In addition, the ability to simultaneously time multiple intervals challenges the idea of a single internal clock.

The striatal beat frequency (SBF) model integrates new evidence regarding the neurobiology of interval timing with the conceptual framework provided by SET and pacemaker-accumulator models (C. V. Buhusi & Meck, 2005). As in the pacemaker accumulator model, SBF ascribes a clock function to both the SNpc and striatum, but in this case timekeeping relies on coincidence-detection by multiple neurons (C. V. Buhusi & Meck, 2005; Matell et al., 2003; Matell & Meck, 2004). Fundamental to the SBF model is the assumption that neurons oscillate at a given frequency – albeit not always synchronously – and that their coincident activation can be used to measure time across multiple intervals (Matell et al., 2003). In other words, the perception of a given interval is associated with a broad neural activation pattern, during which some neurons are activated and others are not (C. V. Buhusi & Meck, 2005; Hinton & Meck, 2004;

Matell et al., 2003; Merchant et al., 2013). From this perspective, the striatum acts as a perceptual filter, integrating the pulsatile activation of SNpc with meaningful events and stimuli via coincident activation in the striatum. These activation patterns are learned through Hebbian strengthening; thus, the memory for a learned interval in this model depends on long term potentiation or depression (LTP or LTD, respectively) within corticostriatal circuits (C. V. Buhusi & Meck, 2005; Matell et al., 2003).

The SBF model has gained traction as electrophysiological and fMRI studies have revealed corticostriatal activation increases around the time of expected reward (C. V. Buhusi & Meck, 2005; Matell et al., 2003). It is also supported by studies of reward prediction error, where DA activity has been recorded during trials in which initially neutral stimuli are learned to predict reinforcement (Fiorillo et al., 2003; Hollerman & Schultz, 1998). While DA initially fires robustly to reinforcement delivery, learning quickly shifts this neuronal response to the earliest stimuli that predicts future reinforcement (Fiorillo et al., 2003; Hollerman & Schultz, 1998). Thus, DA activity encodes the time of expected reward via predictive cues. In the PI paradigm, stimuli that indicate trial onset act as this predictive cue, and the DA pulse that occurs may serve to initiate timing during the trial (Matell et al., 2003).

Despite the accruing neurobiological support for the SBF model, it still cannot fully account for interval timing processes. For example, although SBF attempts to account for biological variability and the scalar property of timing by adding sources of variance to the model, the neurobiological basis of this variability and how to best incorporate it remains unclear. Nevertheless, the SBF model may provide the neural underpinnings of the conceptual model described by the pacemaker-accumulator (C. V.

Buhusi & Meck, 2005). Furthermore, when considered together, these models provide a framework through which corticothalamic oscillations acting as the "clock" work in concert with striatal MSNs, which in turn filter or integrate timed signals within a broader context to modify behavior (Matell et al., 2003). Specifically, striatal activation is relayed through basal ganglia output nuclei to the thalamus and motor cortex to coordinate timed behaviors (Matell et al., 2003).

Regardless of the model ascribed, there is significant evidence to suggest that interval timing mechanisms involve a distributed network of thalamo-corticostriatal circuits. Given that the hypothalamus also contacts corticostriatal circuits involved in timing, I hypothesize that cells within this region may be capable of influencing time in the seconds-to-minutes range. Integration of the temporal context in the seconds-to-minutes range could inform a variety of food related behaviors, such as predicting when food will be available or when to initiate or terminate a meal. Thus, it follows that hypothalamic neurons that coordinate food intake behaviors might use this temporal information to appropriately facilitate feeding. As such, let us discuss the anatomy of the LHA and evidence suggesting LHA^{MCH} neurons may guide appetitive behavior through temporally mediated processes.

1.2 Lateral Hypothalamic Regulation of Feeding Behavior

(i) The Lateral Hypothalamic Area in Food Intake

The neural control of food intake is primarily localized within the hypothalamus, a diencephalic region critically involved in energy homeostasis. Classically, the hypothalamus was conceptualized as a "feeding center" after its stimulation was observed to produce voracious food intake (Hoebel & Teitelbaum, 1962). However, the

functional heterogeneity of the LHA has been apparent from its discovery. For example, in addition to promoting feeding, stimulation of the LHA also augments a variety of behaviors including drinking and gnawing (Valenstein et al., 1968), copulation (Caggiula & Hoebel, 1966) and aggression (Hutchinson & Renfrew, 1966) as reviewed in (Stuber & Wise, 2016). In fact, the behavioral output of LHA stimulation appears to depend on the state of the animal, the experimental parameters, and previous learning, which led to the view that this stimulation could generally augment arousal and modulate reward processes (Stuber & Wise, 2016). In addition, these studies also revealed a direct role for the LHA in reward, as rats would continuously lever press for LHA self-stimulation (Berridge & Valenstein, 1991; Hoebel & Teitelbaum, 1962; Olds & Milner, 1954). These additional findings provided the first indication that classification of the LHA solely as a "feeding center" did not account for its complex and varied roles in motivated behavior. Instead, these findings alluded to the diverse functions of the LHA supported by its underlying physiological complexity.

(ii) Anatomical and molecular complexity of the LHA

The LHA forms a bed nucleus for two large bundles of fibers which pass through it rostrocaudally: the fornix (fx) and the median forebrain bundle (mfb), the latter of which is instrumental in reward signaling (Nieuwenhuys et al., 1982; Saper et al., 1979). The mfb contains dense bundles of dopaminergic axons extending from the brainstem and midbrain to the forebrain, including fibers separately comprising the nigrostriatal (substantia nigra to dorsal striatum) and mesolimbic (ventral tegmental area to ventral striatum and basal ganglia) reward pathways (Nieuwenhuys et al., 1982; Qualls-Creekmore & Münzberg, 2018). The LHA is thus ideally situated to act as a relay station

capable of integrating central and peripheral energy balance signals with higher-order brain regions involved in affective processing, decision-making, reward and timing (Berthoud & Münzberg, 2011; Bonnavion et al., 2016; Petrovich, 2018; Saper et al., 2002; Stuber & Wise, 2016).

Despite its easily identifiable location relative to the mfb and fx, the LHA is complicated by a lack of clear and discernable anatomical bounds (Hahn & Swanson, 2010; Saper et al., 1979). In the rat, the LHA extends rostrocaudally from about -1.30 mm to -4.80 mm relative to Bregma (Paxinos & Watson, 1998) and is typically described as being constrained by anterior and posterior boundaries in the preoptic area (POA) and ventral tegmental area (VTA), respectively (Berthoud & Münzberg, 2011; Hahn & Swanson, 2010; Stuber & Wise, 2016). Recent advances in neuroscience have enabled further delineation of the cytoarchitecture of the LHA. Notably, tract tracing studies have been used to identify and describe more than twenty LHA subregions (Hahn & Swanson, 2010, 2015; Swanson et al., 2005) while molecular profiling of the various cell types identified within the LHA – of which there are many – has highlighted its heterogeneity (Bonnavion et al., 2016; Mickelsen et al., 2017, 2019). Within the LHA, one of the best characterized subpopulations of cells are those that produce the orexigenic (i.e., appetite-stimulating) neuropeptide Melanin concentrating hormone (MCH) (Bittencourt et al., 1992; Qu et al., 1996). Like the LHA, MCH has also been described as an "integrative peptide" for similarly integrating the homeostatic and rewarding features of feeding behavior (Diniz & Bittencourt, 2017). In the following sections, I will discuss this system in more detail.

1.3 LHA Melanin Concentrating Hormone

(i) The MCH peptide

MCH is a cyclic 19-amino acid protein, the production of which is driven by the pMCH promoter, which also encodes neuropeptides EI and GE (Broberger et al., 1998; Pissios et al., 2006; Qu et al., 1996). As an orexigenic peptide, central infusions of MCH increase food intake (Baird et al., 2006; Della-Zuana et al., 2002; Gomori et al., 2023). In addition, genetic overexpression of the pMCH promoter in mice leads to obesity whereas deletion of the peptide or its receptor both result in hypophagia (Ludwig et al., 2001; Shimada et al., 1998). Recall also that MCH plays a role in arousal by increasing REM sleep to support energy conservation (Monti et al., 2013). In line with this, mice with a genetic deficiency of the MCH receptor, MCH1R, are hyperactive and lean (Marsh et al., 2002). The orexigenic and rewarding actions of MCH are thought to occur through the nucleus accumbens (NAc), where infusions of the MCH peptide also increase food intake (Georgescu et al., 2005). In the following section, I will describe the anatomy and physiology of the MCH system, with a particular emphasis on its role in temporally mediated food intake and actions in the NAc.

(ii) LHA^{MCH} Neurons: Anatomy & Physiology

Within the LHA, MCH neurons are capable of synthesizing both GABA and glutamate, however the majority of these neurons are likely glutamatergic, as they lack the vesicular transporters vGAT and vMAT necessary for GABA release (Bonnavion et al., 2016; Mickelsen et al., 2017, 2019). Indeed, at least in the lateral septum (LS), stimulation of LHA^{MCH} neurons leads to the release of glutamate (Chee et al., 2015). Based on their co-expression of additional peptide markers, Mickelsen et al. (2019)

suggest that glutamatergic LHAMCH neurons can be further categorized into two subclusters, defined in part by whether or not they co-express the anorexigenic signal CART (i.e., CART+ or CART-). The CART+ subcluster robustly expresses CART as well as Tacr3, and Nptx1, which encode tachykinin receptors and neuronal pentraxin, respectively (Mickelsen et al., 2019; Stelzer et al., 2016). In contrast, the CARTsubcluster instead moderately expresses Scq2 and Nrxn3, which encode secretogranin II and neurexin 3, respectively. These proteins are involved in receptor function and cell adhesion, as well as the sorting and packaging of peptide hormones (Mickelsen et al., 2019; Stelzer et al., 2016). In addition, LHAMCH neurons express receptors for GABA, glutamate, glucocorticoids, NPY, melanocortins, and leptin, although whether the expression of these receptors varies between subclusters of LHA^{MCH} neurons remains unclear (Bäckberg et al., 2004; Harthoorn et al., 2005; Huang & van den Pol, 2007; Lee et al., 2021; Mickelsen et al., 2019). Finally, early immunochemical work provides ample evidence that LHA^{MCH} neurons also express α -melanocyte hormone (α -MSH), corticotrophin releasing hormone (CRH) and growth hormone releasing hormone (GHRH) (Bittencourt et al., 1992). However, the extent to which the synthesis and release of these hormones by LHAMCH neurons varies by subcluster – if at all – remains unclear. Nevertheless, the molecular heterogeneity of LHAMCH neurons speaks to the robust potential of these neurons to interact with a variety of brain systems to modulate behavior.

(iii) The MCH Receptor System

In rodents, the MCH peptide exerts its actions through the MCH1R receptor (Hawes et al., 2000; Saito et al., 1999; Tan et al., 2002). Although a second MCH

receptor (MCH2R) has been identified in humans, it is either absent or non-functional in rodents (Tan et al., 2002). The MCH peptide binds MCH1R with a high affinity and selectivity: nanomolar concentrations of MCH strongly activate MCH1R, while neuropeptide EI, which is also produced by the pMCH promoter, does not (Saito et al., 1999). MCH1R is a G-protein coupled receptor (GPCR) first identified as the orphan GPCR known as SLC1 or GPR24 (Hawes et al., 2000; Saito et al., 1999; Tan et al., 2002). GPCRs are typically grouped into subclasses based on their α-subunit and denoted as Gi/o, Gs, or Gq. The MCH1R can be coupled to multiple G protein subtypes, including both Gi/o and Gq. Activation of MCH1R by MCH inhibits cyclic AMP (cAMP) production, induces a transient increase in calcium concentration ([Ca²⁺]), increases mitogen-activated protein kinase (MAPK), and increases inositol phosphate (IP), a marker of increased phospholipase C (PLC) (Chambers et al., 1999; Hawes et al., 2000; Saito et al., 1999). The effects of MCH1R activation on cAMP and MAPK production can be blocked by pretreatment with pertussis toxin (PTX), which inactivates Gi/o proteins, indicating that these MCH1R effects on intracellular signaling are Gi/o mediated. On the other hand, PTX pretreatment does not fully abolish the effects of MCH1R activation on the stimulation of PLC, indicating that this mechanism is mediated at least in part by Gq receptors (Hawes et al., 2000). Thus, MCH1R functionally couples to both Gi/o and Gq receptors and can therefore exert both inhibitory and excitatory effects on cellular activity. To date, little is known about what determines which signaling mechanisms are initiated following MCH1R binding. These intracellular mechanisms may vary by brain region, function, or any number of other properties that

determine what molecular components are present in a given MCH1R⁺ cell (Hawes et al., 2000).

MCH1R is expressed extensively throughout the CNS, as demonstrated by *in situ* hybridization and RT-qPCR of MCH1R mRNA as well as by protein immunoreactivity (Bittencourt et al., 1992; Hervieu et al., 2000). Bittencourt et al. report that MCH immunoreactive (MCH-ir) fibers are found in nearly "every commonly recognized cell group and cortical field" (Bittencourt et al., 1992), including throughout the diencephalon, mesencephalon, and rhombencephalon (Hervieu et al., 2000). In addition, MCH signaling also occurs through volume transmission in the cerebrospinal fluid, which indicates that the MCH peptide can also influence brain regions which are not directly innervated by MCH-ir fibers (Noble et al., 2018).

Within the CNS, MCH1R expression is particularly dense in the hypothalamus, including both within the LHA and ZI. MCH1R is also evident throughout the olfactory system, the hippocampus, and the amygdala. It is densely expressed in the caudate putamen, substantia nigra, and striatum, each of which are important for interval timing (C. V. Buhusi & Meck, 2005; Hervieu et al., 2000; Meck, 1996, 2005). The expression of MCH1R in the ventral striatum is of particular interest, given the role of the nucleus accumbens (NAc) in motivated behavior, timing, and food intake.

1.4 Interim Summary

Now that I have described the interval timing system, the LHA, and the MCH system, let's reconsider the preliminary data indicating a potential role for LHA^{MCH} in time-dependent food-seeking. As described above, I previously examined the influence of LHA^{MCH} neurons on time-dependent food-seeking by chemogenetically exciting these

neurons in the anterior or posterior LHA (LHAa or LHAp, respectively) during the peak interval paradigm. Using male and female rats, I found that LHAp^{MCH} neuronal excitation putatively increased clock speed in male and female rats, an effect that may have been driven by responding in females. In contrast, chemogenetic excitation of LHAa^{MCH} neurons did not influence time perception *per se* in male or female rats. Rather, in female rats this manipulation robustly delayed the "stop" function, resulting in prolonged high rate responding after the omission of an expected reward. In contrast to the LHAp^{MCH} neuronal excitation, these effects occurred selectively during M/D, indicating an ability for LHAa^{MCH} neuronal excitation to increase motivation only during periods of the estrous cycle when circulating gonadal hormone levels are typically lower.

Together, these findings indicate a role for LHA^{MCH} neurons in modulating time-dependent motivated responding in females, in a manner that depends on estrous cycle stage. In particular, LHAa^{MCH} neurons robustly increased motivated responding during M/D by delaying the "stop" function after the omission of an expected reward. Given that the ventral striatum is important in determining the "stop" function during interval timing tasks, this suggests that these LHA^{MCH} neurons may exert their actions through signaling in the ventral striatum (i.e., in the NAc). In addition, these LHA^{MCH} neurons may interact with circulating gonadal hormones like estrogen to modulate motivated responding. As such, I will next describe the role of MCH in the NAc, as well as evidence indicating that MCH supports temporally mediated food intake. Finally, I will describe the rodent estrous cycle and evidence for interactions between the MCH system and estrogen.

1.5 MCH in motivated and time-dependent feeding behavior

(i) MCH activity in the NAc

The striatum, which I have previously described above in terms of its dorsal and ventral portions and their discriminable roles in interval timing, can alternatively be described by its various nuclei, including those within the basal ganglia (BG). While the dorsal striatum consists of the caudate and putamen, the ventral striatum typically refers to the nucleus accumbens (NAc), which can itself be divided into two distinct subregions: the core and shell (Kelley, 2004; Mogenson et al., 1980, 1983). The NAc has long been associated with motivated behavior and described as an interface between motivation and action (Mogenson et al., 1980). Primarily composed of Median Spiny Neurons (MSNs), the NAc responds to both glutamatergic and GABAergic modulation to alter neural activity and modify motivated behaviors (Mogenson et al., 1980).

The NAc both sends and receives projections from the LHA (Haemmerle et al., 2015; O'Connor et al., 2015). Both glutamatergic antagonists and GABAergic agonists infused to the NAc potently increase feeding (Kelley, 2004). MCH1R is expressed on the majority of MSNs in the NAc, including on both DA receptor-1 (DR1) and receptor-2 (DR2)-expressing neurons (Pissios et al., 2008) as well as on those that express enkephalin or dynorphin (Georgescu et al., 2005). Expression of MCH1R is especially dense in the NAc shell, where infusion of the MCH peptide increases feeding (Georgescu et al., 2005). Similarly, infusion of an MCH1R antagonist in this region instead decreases feeding (Georgescu et al., 2005). Although this group does not specify the sex of the animals used in this study, others report that infusion of MCH

peptide to the NAc shell increases feeding only in male – but not female – rats (Terrill et al., 2020), suggesting this site as a potential mediator of sex differentiated feeding effects. In line with this, when circulating ovarian hormones were removed via ovariectomy in females, infusion of MCH to the NAc increased food intake in oil, but not estradiol, treated rats (Terrill et al., 2020). Together, these data point to a role for the NAc and MCH in mediating sex- and estradiol-dependent effects on food intake.

In addition to its role in MCH-dependent, sex-differentiated feeding behavior, a role for the NAc in "computing coincident events [to] enhance the probability that temporally related actions and [events become] associated" in feeding behavior has also been proposed (Kelley, 2004). Notably, these temporal relationships inherently involve time perception in the seconds to minutes range (i.e., they depend on interval timing). As described previously (section 1.1, above), corticostriatal circuits are integral to interval timing, and coincident activation of these neurons may underlie time perception in this range. Thus, interactions between the LHA and this corticostriatal network may support learning about food-predictive cues by integrating temporal information to inform behavior. Thus, the LHA and NAc may work together to influence food intake through either or both the modulation of time perception and motivation. In particular, given that the ventral striatum (i.e., the NAc) is specifically involved in acquisition of the "stop" function in interval timing paradigms, contacts with the NAc may be responsible for the effects of chemogenetic LHA^{MCH} neuronal excitation on prolonging high rate responding after the criterion duration.

(ii) LHA^{MCH} in learned food intake

MCH is important for learning about food-predictive cues, which inherently involves understanding temporal relationships between initially neutral stimuli and reinforcing outcomes. MCH increases food intake primarily through alterations in the duration of consumption, which can be analyzed via licking microstructure (Davis & Smith, 1988, 1992; Johnson, 2018; Smith, 2001). Within a meal, individual bursts of licking behavior can be described in terms of their frequency (i.e., burst number) and duration (i.e., burst size) (Davis & Smith, 1988, 1992; Johnson, 2018; Smith, 2001). Intracerebroventricular (ICV) infusions of MCH increase burst size, which is typically interpreted as an increase in the perceived palatability of the food being consumed (Baird et al., 2006). MCH therefore supports consumption by enhancing hedonic taste evaluation (Baird et al., 2006), thereby supporting learning about the rewarding properties of food.

While changes in burst size are typically interpreted in terms of hedonic evaluation (i.e., longer burst size implies increased hedonic value), they could alternatively reflect a delay in the "stop" mechanism. As a decision process guided by both time perception and motivation (MacDonald et al., 2012; Matell et al., 2006), either or both of these processes could delay the "stop" function to prolong consumption.

Thus, an increased burst size following MCH peptide infusion could alternatively indicate that MCH delays the "stop" function as a result of altered time perception or motivation.

Consistent with the idea that MCH modulates the "stop" function to change consumption patterns, MCH1R antagonism decreases lick burst size in response to a food-paired cue (Sherwood et al., 2015). In other words, MCH1R antagonism disrupts

the expression of learned overeating, specifically by decreasing the duration of bouts of consumption. In addition, both pharmacological antagonism and genetic deletion of MCH1R disrupt the ability of a reinforcing conditioned cue to support new learning (Sherwood et al., 2012), again indicating a role for MCH neurons in learning about food predictive cues.

Importantly, MCH influences food intake primarily through changes the *duration* of individual bouts of consumption. In addition, the influence of MCH appears to be temporally constrained to the beginning of a meal and/ or within ongoing consumption. For example, optogenetic stimulation of LHA^{MCH} neurons potently increases feeding only when stimulation is applied during consumption, revealing a role for MCH in prolonging – but not initiating – food intake (Dilsiz et al., 2020). Similarly, calcium imaging reveals that LHA^{MCH} neurons are activated in response to food cues and during consumption (Subramanian et al., 2023). However, the activity of these neurons wanes over the course of a meal, again indicating a temporal specificity to their role in feeding behavior. Similarly, the influence of MCH peptide infusion on burst size is also greater at the beginning of a meal (Baird et al., 2006). In each case, the influence of MCH is temporally specific. Effects occur during ongoing consumption to increase the length of bouts of consumption, primarily at the beginning of a meal.

In addition, LHA^{MCH} neurons that project to the ventral hippocampus (HPc) have also been shown to increase early responding for food in a task that requires instrumental responding to be inhibited until a criterion duration has elapsed (the differential reinforcement of low rates of responding or DRL task) (Noble et al., 2019). While this effect was interpreted as an increase in behavioral impulsivity, it could

alternatively reflect a change in time perception resulting in increased early responding.

Notably, in each of these examples, timing matters. Importantly, the PI paradigm

(described in 1.1 ii, above) enables the examination of effects of both timing and

motivation within the same task.

1.6 Estrogen Modulates the Influence of MCH on Food Intake

It is well-established that food intake in females fluctuates with the estrous cycle, an effect largely attributed to circulating levels of estrogen (i.e, 17- β-estradiol benzoate, EB) (Blaustein & Wade, 1976; López & Tena-Sempere, 2015; Morin & Fleming, 1978; ter Haar, 1972; Varma et al., 1999). The rodent estrous cycle is typically divided into four stages: metestrus, diestrus, proestrus, and estrus (M, D, P, and E, respectively) (Goldman et al., 2007). Generally speaking, EB and other circulating gonadal hormones are typically highest during proestrus and behavioral estrus (i.e., the period when rats are sexually receptive) and then fall rapidly during the day of estrus and then remain low throughout metestrus and early diestrus (Goldman et al., 2007). In addition to EB, these hormones include progesterone and luteinizing hormone (LH), which peak in proestrus, as well as follicle stimulating hormone (FSH), which rises and falls rapidly during estrus. Ovulation typically occurs ~10-12 hours after the peak in LH, during the dark phase of estrus (Goldman et al., 2007).

Removal of peripheral hormones through adult ovariectomy (OVX) results in a robust increase in food intake and body weight. However, this effect can be normalized to the level of intact, cycling animals through cyclic replacement of estrogen (Asarian & Geary, 2002; Geary & Asarian, 1999). Accordingly, estrogen has been posited to act as an anorexigenic signal, inhibiting food intake (Asarian & Geary, 2002; Eckel, 2011;

Geary & Asarian, 1999). The effects of EB on food intake may be mediated at least in part by MCH, as EB inhibits the orexigenic effects normally seen following MCH peptide administration (Santollo & Eckel, 2008, 2013).

In addition to influencing food intake behavior, estrogen also influences time perception (Bayer et al., 2020; M. Buhusi et al., 2017; Morita et al., 2005; Sandstrom, 2007; Williams, 2011). Acute EB treatment in OVX rats proportionally shifts the response function to the left, suggesting an increase in clock speed (Pleil et al., 2011; Sandstrom, 2007). However, when administered on subsequent days, the effect of EB treatment wanes after the first session (Pleil et al., 2011). This transient effect further supports the notion that EB increases clock speed, as new learning under EB conditions would allow rats to adjust the reference memory for time. Interestingly, in intact female mice, responding occurs later than in males, although the authors suggest that this effect may be driven by a delayed "start" function and general decrease in incentive motivation rather than an effect on timing, *per se* (Gür et al., 2019). Although there are only a handful of studies examining estrous cycle or EB in time perception, and the role of gonadal hormones is not yet clear, it is evident that EB is capable of exerting effects on timing and/or motivation (Panfil et al., 2023).

Estrogen acts by binding its receptors, estrogen receptors (ERs), in both the CNS and periphery. There are two classic ERs, ER- α and ER- β , which are located in the cytoplasm and nucleus, where they act as transcription factors (Toran-Allerand, 2004). ERs are widely distributed throughout the CNS, and densely expressed throughout the rostrocaudal extent of the hypothalamus. In 1997 Shughrue et al. provided an in-depth overview of the relative distributions of ER- α and ER- β mRNA

throughout the rat brain and reported that the relative proportion of ER- α and ER- β differs in various brain regions, including throughout the hypothalamus. However, there is somewhat conflicting evidence regarding the expression of ER- α and ER- β in the LHA and NAc. For example, while Shughrue et al., 1997 reported that only ER- β is expressed in the LHA, ZI, and NAc, others provide evidence of ER- α in the LHA and ZI of both mice (Couse et al., 1997) and rats (Muschamp & Hull, 2007). Similarly, recent evidence has identified ER- α mRNA in the NAc (Muschamp & Hull, 2007; Terrill et al., 2020).

The timeframe of effects mediated by nuclear ER-α and ER-β depend on the rate of translocation to the nucleus, transcription, and degradation of various protein products. These effects are therefore typically slow to onset and long lasting. However, the effects of EB application can also occur rapidly, within seconds to minutes (Boulware et al., 2005; McEwen, 2002). These rapid effects of estrogen are typically referred to as non-genomic and are thought to occur via membrane-bound rather than nuclear ERs. Recent evidence has indicated that ER-α and ER-β are also associated with the cellular membrane as homo- and heterodimers, where their effects may occur more rapidly (Almey et al., 2015; Toran-Allerand, 2004). In addition, a third ER membrane-bound receptor, ER-X, has also been putatively identified (Toran-Allerand et al., 2002). Estrogen also interacts with G-protein coupled receptors, of which there are three subtypes: the excitatory mGlurl (mGluR1 and mGluR5, which are Gq receptors), and inhibitory mGluRII and mGluRIII (including mGluR 2 and 3 and mGluR 4-7, respectively, which are Gi/o receptors) (Almey et al., 2015). There has been at least one GPCR ER identified, GPER1, but estrogen has also been shown to act in vitro on

mGluR1 and 2 in hippocampal neurons (Boulware et al., 2005) and on mGluR5 in striatal neurons (Grove-Strawser et al., 2010). Thus, estrogen may exert both excitatory and inhibitory effects on a variety of neurons through GPCRs. Rapid effects of estradiol mediated through these non-genomic mechanisms may include changes in membrane permeability and activation of multiple signaling pathways, including cyclic AMP/ protein kinase A (PKA), mitogen-activated protein kinase (MAPK) and phospholipase C (PLC) (Almey et al., 2015; Boulware et al., 2005).

The MCH system is robustly modulated by the estrous cycle, and MCH may in turn regulate hormonal fluctuations across the cycle. For example, low levels of MCH peptide, receptor, and MCH-ir fibers have been reported during proestrus and estrus (P/E) (Murray et al., 2000; Santollo & Eckel, 2013). Indeed, the density of MCH-ir fibers rapidly decreases from the morning of proestrus to the evening, as circulating levels of estrogen and progesterone rapidly rise (Gallardo et al., 2004). Additionally, this decrease in MCH signaling has been suggested as a mechanism controlling the release of LH, indicating that MCH may also influence gonadal hormones (Gallardo et al., 2004). Through ovariectomy and estrogen replacement, Santollo & Eckel (2013) have isolated estrogen as the hormone responsible for reducing MCH expression during P/E. However, the mechanism by which estrogen regulates MCH remains unclear, as it is commonly accepted the LHA^{MCH} neurons do not express ER-α (Muschamp & Hull, 2007) and are unlikely to express ER-β based on its distribution (Li et al., 1997).

However, the potential action of estrogen on the MCH system via GPCRs has not been ruled out. Given that the MCH1R receptor is a GPCR that couples to both Gi and Gq proteins (Hawes et al., 2000), it is possible that estrogen may compete with

circulating MCH to bind MCH1R. Estrogen may also bind directly to LHA^{MCH} neurons through mGlur1 (Huang & van den Pol, 2007). Alternatively, estrogen could mediate the effects of MCH indirectly, as the expression of MCH1R and ER-α are similarly distributed throughout the CNS (Bittencourt et al., 1992; Muschamp & Hull, 2007; Shughrue et al., 1997) and even colocalized in non-MCH neurons, including throughout the LHA and NAc (Muschamp & Hull, 2007; Terrill et al., 2020). In addition, MCH1R is more densely colocalized with ER-α in female rats compared to their males counterparts, providing a potential mechanism for sex- and estrous-cycle effects on MCH mediated behaviors coordinated by the NAc (Terrill et al., 2020).

1.7 Overview of dissertation chapters

Given the evidence of sex-dependent effects on MCH-mediated food intake in the NAc, as well as my own findings that LHA^{MCH} neurons modulate time-dependent food-seeking in a sex- and estrous-cycle dependent manner, I hypothesized that LHA^{MCH} neurons that project to the NAc may account for these effects. Support for this hypothesis comes from an extensive literature indicating a role for the NAc in motivated food intake (Kelley, 2004) as well as evidence suggesting that the NAc modulates the "stop" function of time-dependent food-seeking in interval timing tasks (MacDonald et al., 2012), perhaps by communicating the incentive value of reward (Kurti & Matell, 2011) As an integrative peptide, MCH activity in the LHA and NAc may link the temporal context of a changing environment to motivation in order to inform behavior.

While a functional role of MCH neurons that project to the NAc from the posterior LHA has been previously described (Terrill et al., 2020), I first sought to confirm that LHA^{MCH} neurons in the anterior LHA also project to the NAc. To do so, I examined

projections from the LHAa and LHAp to this region using a retrograde viral tracing technique. Using a non-specific retrograde adeno-associated virus expressing GFP, I identified a dense expression of MCH-ir fibers in the NAc that originate from the LHAa. In line with the reports of others (Pissios et al., 2008), our retrograde tracing from the anterior LHA indicates that LHAa projections primarily contact the NAc shell, rather than core.

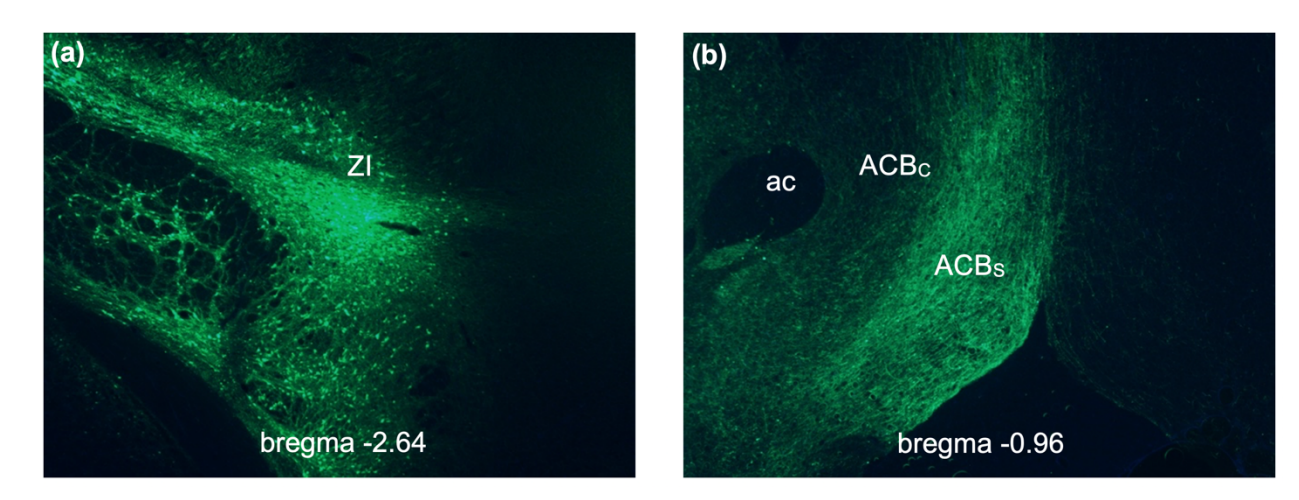


Figure 1.1 Representative image of eGFP expression in the (a) anterior, dorsolateral LHA injection site and (b) the ACB_S following infusion of AAV2-hSyn-eGFP. ac=anterior commissure; ACB_c= Nucleus accumbens core; ACB_S= Nucleus accumbens shell; ZI = zona incerta.

In this dissertation, I separately examined the effects of chemogenetic excitation of NAc-projecting neurons from posterior (LHAp; Chapter 2) and anterior (LHAa; Chapter 3) subregions of the LHA. I hypothesized that while chemogenetic excitation of LHAp-MCH → NAc neurons would fail to influence time-dependent food-seeking, excitation of LHAa-MCH → NAc neurons would prolong highly motivated food-seeking in female rats. In addition, I hypothesized that LHAa-MCH → NAc excitation would produce effects only when rats were tested during diestrus, the period of the rodent

estrous cycle when levels of circulating gonadal hormones are generally lower. Finally, in Chapter 4, I hypothesized that removal of peripheral gonadal hormones through ovariectomy would recapitulate the behavioral effect of LHAa-MCH \rightarrow NAc excitation during diestrus, while estradiol replacement in ovariectomized (OVX) rats would blunt these effects.

As expected, chemogenetic excitation of posterior LHA^{MCH} → NAc neurons failed to produce behavioral effects on time-dependent food-seeking (Chapter 2). In addition, excitation of anterior LHA^{MCH} → NAc neurons selectively produced post-criterion behavioral effects during diestrus (Chapter 3). Interestingly, however, these effects were in the opposite direction than hypothesized: chemogenetic excitation of LHAa^{MCH} > NAc neurons reduced food-seeking after the omission of an expected food reward. Finally, removal of peripheral gonadal hormones through ovariectomy (OVX) failed to recapitulate the effects of LHAa^{MCH} → NAc excitation observed during diestrus (Chapter 4). In oil pretreated rats, chemogenetic excitation of LHAa^{MCH} → NAc neurons failed to influence PI responding, whereas this excitation reduced post-peak responding in EB pretreated rats. Thus, excitation of LHAa^{MCH} → NAc neurons in EB pretreated rats produced a behavioral phenotype similar to that observed in diestrus females. These results suggest that estradiol is necessary for the behavioral effects of LHAa^{MCH} → NAc neurons, but raise new questions about the timing of estradiol in its influence on MCH. Implications of these results are discussed in Chapter 5.

CHAPTER 2: Accumbens-projecting Melanin Concentrating Hormone neurons that originate in the posterior Lateral Hypothalamic Area do not influence motivation or time perception

Abstract

Temporal information can be processed across a wide range of timescales, endowing the capacity for an organism to regulate its internal milieu as well as predict and adapt to the external environment. Previously, I demonstrated that neurons that produce the orexigenic peptide Melanin Concentrating Hormone (MCH) may putatively influence time perception. Specifically, chemogenetic excitation of MCH neurons in the posterior lateral hypothalamic area (LHApMCH neurons) altered the timing of responding in a time-dependent food-seeking task, the Peak Interval (PI) paradigm. Excitation of LHApMCH neurons resulted in responding that reached a peak rate at an earlier time (i.e., peak time) and attenuated more quickly compared to when rats were tested under control conditions. These effects were significant in female – but not male – rats, and potentially driven by a subtle decrease in post-peak responding that occurred after the criterion duration. To examine the circuitry underlying these effects in female rats, I examined whether LHApMCH neurons that project to the nucleus accumbens – a ventral striatal region important for motivated behavior, feeding and timing - could influence how female rats perform in the PI paradigm. Using a dual virus approach, I selectively excited LHApMCH neurons that project to the NAc and examined their influence on behavior in the PI task across the estrous cycle. I hypothesized that LHApMCH neurons that project to the NAc would not influence time perception in the PI paradigm, per se, but could potentially modulate motivated responding by influencing the "stop" function.

Chemogenetic excitation of LHAp^{MCH} neurons failed to influence time-dependent food seeking behavior in the PI task. Moreover, there were no effects of this excitation on either peak time or on motivated responding as revealed by the "stop" function. Thus, the effects of LHAp^{MCH} neurons on interval timing do not rely on efferents to NAc and may instead reflect control from alternative downstream dorsal striatal or hippocampal targets.

Introduction

Core components of metabolic regulation have traditionally been studied within the context of circadian timing, whereby biological rhythms are evoked by brain oscillations coupled to the 24-hr light-dark cycle (Bass & Takahashi, 2010; Turek et al., 2005) via orchestration of the suprachiasmatic nucleus (SCN) (Reppert & Weaver, 2002). Alternatively, interval timing operates in the seconds-to-minutes range, and depends on corticostriatal rather than SCN-dependent modulation (Lewis & Miall, 2003; Mello et al., 2015). The ability to perceive time in the seconds-to-minutes range enables animals to learn predictive relationships and adapt to a changing environment. Importantly, time perception in this range supports temporal contiguity, learning, and decision making (Kacelnik & Brunner, 2002; Marshall, Smith, & Kirkpatrick, 2014; Meck et al., 2012). The Peak Interval (PI) paradigm is an interval timing task in which animals learn to predict when food reinforcement will be available based on the temporal context provided by a discriminative stimulus. Adept time perception in this task allows an animal to coordinate effortful behavior (i.e., instrumental responding) at times when reinforcement is most likely. Because this task inherently involves food intake and learning about food-predictive cues, I hypothesized that neurons that influence feeding behavior may also influence the time-dependent food-seeking observed within this task.

Within the lateral hypothalamic area (LHA), neurons that produce the orexigenic peptide Melanin Concentrating Hormone (MCH) are known to influence learned food intake. In addition, these neurons can influence the timing of instrumental behaviors performed in anticipation of food. For example, in male rats, LHA^{MCH} neurons that project to the hippocampus (HPc) increase early responding for sucrose reinforcement,

an effect that has been described as increased impulsivity (Noble et al., 2019).

However, increased early responding in this task could also indicate an effect of LHAp^{MCH} neurons on time perception whereby rats perceive time as having passed more quickly. For example, an increase in internal clock speed could alternatively account for early lever pressing in this task by causing a rat to perceive the 20s criterion as having already passed faster (e.g., at 18s).

In order to examine whether LHA^{MCH} neurons could influence time perception in this manner, I used chemogenetics to selectively excite LHAp^{MCH} neurons while rats timed a 20s criterion in the PI paradigm. Chemogenetics refers to a class of genetically modified receptors, i.e., Designer Receptors Exclusively Activated by Designer Drugs, or DREADDs, that bind to otherwise inert exogenous chemical ligands like clozapine-Noxide (CNO) to alter cellular excitability (Roth, 2016). These DREADDs can be packaged into adeno-associated viruses (AAVs) and injected into the brain within regions of interest. Control of DREADD expression by a genetic promoter – in this case, the pMCH promoter – allows the DREADDs to be expressed only in cells of a certain type (e.g., those that contain the pMCH promoter and are capable of producing the MCH peptide). In this case, I used a DREADD virus in which the expression of an excitatory, modified human muscarinic receptor (hM3Dq) was controlled by the pMCH promoter.

Previously, I demonstrated that chemogenetic excitation of LHAp^{MCH} neurons reduced peak time, suggesting that rats potentially perceived time as passing more quickly following the excitation of these neurons. In addition, when we plotted responding across time as a proportion of peak rate, females – but not males –

demonstrated a significant effect of CNO on responding across time. In females, the proportion of peak rate responding under CNO was higher than VEH at 18s, but lower than VEH at 24, 29, and 48s. In other words, CNO-treated females displayed a proportional leftward shift in the timing function, such that they responded at a higher proportion of peak rate before the criterion, and lower proportion of peak rate after. These findings suggest that in female rats, LHAp^{MCH} neuronal stimulation accelerated clock speed such that the rats underestimated the criterion duration.

In this previous study, I also examined whether the effects of chemogenetic excitation differed when ovarian hormone levels were relatively high (i.e., during proestrus/ estrus or P/E) or low (i.e., during metestrus/ diestrus or M/D). Although there were no significant effects of LHAp^{MCH} neuronal excitation on the proportion of peak rate responding within M/D or P/E, it is possible that our retrospective approach – which limited the analysis to a small sample size – may have precluded us from observing an effect of chemogenetic excitation based on estrous stage.

While interval timing likely involves a vast network of corticostriatal circuits, a role for the ventral striatum (VS) has been identified in the acquisition of the "stop" function (MacDonald et al., 2012). Thus, effects of chemogenetic excitation of MCH neurons on the "stop" function may occur due to activity of MCH in the VS. Notably, within the VS, the MCH receptor MCH1R is densely expressed in the nucleus accumbens (NAc), which also has an important role in motivated behavior, including MCH-mediated feeding (Berridge, 2004; Floresco, 2015; Georgescu et al., 2005; Kelley, 2004). I thus hypothesized that a portion of these LHA^{MCH} neurons may project to the NAc to influence time-dependent food-seeking.

To address these questions, in this chapter I used a dual-viral, chemogenetic approach to express an excitatory DREADD receptor only in MCH neurons within the LHAp that project to NAc. Similar to previous studies, I injected an AAV containing an excitatory DREADD. However, in this case the expression of the modified hM3Dq receptor depended on both cre recombinase and the pMCH promoter. Thus, the hM3Dq receptor could be expressed only in cells that contain both cre recombinase and pMCH. Therefore, in order to selectively transfect only MCH neurons that project to the NAc, I also injected a retrograde virus containing cre recombinase, which will traffick cre from the NAc to neurons that project to this region, including cells in the LHA. In this manner, I selectively excited LHAp^{MCH} neurons that project to the NAc (LHAp^{MCH}→NAc) during the PI paradigm to investigate their role in time-dependent food seeking across the estrous cycle.

Materials & methods

Subjects

Eight adult female Sprague-Dawley rats (*Envigo*, *Haslett*, *MI*, *USA*; 12-weeks of age at arrival) were pair housed in groups of 2-3 in standard, plexiglass cages with metal tops. Rats were maintained on a standard 12-hr light-dark cycle (lights on 7:00; lights off 19:00), with *ad libitum* access to Teklad diet #8940 and reverse osmosis (RO) water. Rats received ≥7 days of acclimatization to the vivarium before experimental manipulations began. Following this period of habituation, rats were handled daily for 2-3 days before undergoing stereotaxic surgery. Post-op, rats were briefly singly housed while they received daily health monitoring. Rats were pair housed with their original cage mate once postoperative bodyweight recovered (≤7 days) and surgical incisions

appeared healed. Rats continued to be pair-housed throughout all behavioral experiments. All manipulations were conducted in compliance with the Institutional Animal Care and Use Committee, Michigan State University.

Surgical procedures

Stereotaxic Viral Infusion and Cannulation

Under 2-4% isoflurane anesthesia, subjects received bilateral infusions of the retrograde AAV2(retro)-eSYN-EGFP-T2a-icre-WPRE (Addgene, Watertown, MA) and a cre-dependent, excitatory DREADD AAV2-DIO-rMCHp-hM3D(Gq)-mCherry (gift from Dr. Scott Kanoski) to the NAc and to the LHAp, respectively (Table 2.1). A single, 26gauge guide cannula (Plastics1, Roanoke, VA) consisting of an 8 mm plastic pedestal and containing a 2.5 mm projection below the base was placed -1.2 A.P. ±2.25 M.L., -2.5 D.V. This enabled intracerebroventricular (ICV) infusions of the ligand, clozapine-Noxide (CNO; NIDA Drug Supply Program) to the lateral ventricle. Placement of the guide cannula into the left or right lateral ventricle was counterbalanced between animals. The addition of two surgical screws (Fine Science Tools, Foster City, CA), Loctite superglue (Amazon, Seattle, WA), and dental acrylic (Lang Dental, Wheeling, IL) was used to stabilize the base of the cannula and ensure closure of the surgical space. To prolong stable placement of the guide cannula, skin was sutured over the dental acrylic to prevent new skin growth from displacing the cannula. Guide cannulae were protected with a dummy cannula (Plastics1, Roanoke, VA) cut to fit the 2.5 mm guide without a projection. Rats were treated with 2 mg/kg meloxicam prior to surgery and as needed during the following week of post-operative monitoring to manage pain. Rats typically

did not require more than one additional dose of meloxicam. Unfortunately, one rat had an isoflurane reaction and died during surgery.

Table 2.1 Viral approach to selectively target LHAp^{MCH} neurons that project to the NAc.

Virus	Target	Infusion coordinates
AAV2(retro)-eSYN-EGFP-T2a-icre-WPRE 0.3 µl / infusion	NAc Shell	+1.1 A.P., ±0.8 M.L., −7.5 D.V.
AND		
AAV2-DIO-rMCHp-hM3D(Gq)-mCherry 0.3 μl / infusion	LHAp ^{MCH}	-2.6 A.P., ±1.8 M.L., -8.0 D.V. -2.6 A.P., ±1.0 M.L., -8.0 D.V. -2.9 A.P., ±1.1 M.L., -8.8 D.V. -2.9. A.P., ±1.6 M.L., -8.8 D.V.

Behavioral Paradigm

Following recovery from viral infusion and food restriction to 90% baseline weight, rats were trained and tested in the Peak Interval (PI) paradigm. There were three phases of behavioral training and testing, described in detail below. Rats were weighed daily between ~9 – 10 am and when applicable, vaginal lavages were also performed at this time. Behavioral sessions began between 9:30 – 10:30 am (group 1) or 11:30 am – 12:30 pm (group 2) and were run 5-7 days per week throughout training and testing. Days off between behavioral training or testing occurred only when they would provide minimal interruption, i.e., between consecutive days of FI or PI training or between washout days of testing. Due to the length of Peak Interval paradigms, it is typical to run behavioral sessions only 5 days / week and thus these brief interruptions were not expected to influence behavior. Daily chow rations were provided to rats following the completion of the behavioral session.

Phase 1: Pre-training

Sucrose habituation

To reduce neophobia to the 20% w/v sucrose solution used as a reinforcer, rats were given 15 minutes of sucrose pre-exposure in their home cages. Pair-housed rats were separated into clean cages and allowed to rest in their new cages for \geq 30 minutes. Water bottles were removed from the cages, and identical bottles instead filled with \geq 50 ml of a 20% w/v sucrose solution were placed on the opposite side of the wire food hopper. Consumption was observed to ensure that all rats consumed sucrose freely before the session ended. Bottles were weighed before and after consumption to confirm that rats had consumed \geq 10g of the sucrose solution. All rats consumed promptly and met the minimum consumption criteria. After the habituation session, rats were returned to pair housing and fed their daily chow ration.

Magazine training

After sucrose pre-exposure, all behavioral assays were conducted in eight standard operant boxes contained within sound-attenuating cabinets (Med Associates). Boxes were equipped with a recessed food magazine, into which liquid reward solutions could be delivered via automated pumps. Solutions were delivered into a clear acrylic food well located within the recessed food magazine. Infrared (IR) cameras were mounted below the food well to enable consumption to be seen and recorded. In addition, an IR light across the magazine port enabled recording of magazine entries and the overall time spent in the food magazine. Boxes were also equipped with two levers, placed on either side of the food magazine. During magazine training, levers

were recessed. In addition, a house light located in the upper corner of the soundattenuating chamber illuminated the box with red light during magazine training.

During magazine training, rats were provided with 16 presentations of the sucrose reinforcer (20% sucrose solution) on a random time 240s reinforcement schedule; sessions lasted approximately 48 − 60 minutes. A brief click produced by the activation of a solenoid located behind the food magazine occurred simultaneously with pump activation and reinforcer delivery to help orient rats toward the food magazine. Rats were required to meet the criteria of having spent ≥10s in the food magazine during reinforcer delivery in order to move onto lever training. Rats typically met criteria within the first magazine training session; however, all rats were given two magazine training sessions to ensure they met criteria.

Lever training

Rats next received baited lever training in which levers were presented for 25 trials and reinforcement was provided on an FI20 schedule. Levers were baited with a slurry of chow that was made by mashing chow in RO water and then applied to the top and bottom of the extended lever. Baited levers were active and available to rats immediately when rats were placed into the operant box. Lever position relative to the food magazine (left or right) was counterbalanced. The red house light, mounted inside the sound attenuating chamber, was illuminated throughout the lever training session. Rats were required to complete ≥10 of 25 trials during lever training. Rats who failed to meet criteria received additional lever training as needed prior to advancing to the next phase of training. Lever training sessions lasted no longer than 25 minutes; however

most rats quickly acquired the instrumental response and finished lever training in 10-15 minutes.

Phase 2: Peak Interval training

Fixed Interval (FI) Training

After meeting lever training criteria, rats moved to fixed interval (FI) training, where they were taught to time a criterion duration of 20s. At this point, the red house light was replaced with a white light. Sessions were dark except during the FI trials, when light illumination and lever presentation indicated the onset of the trial and the tobe-timed period. During FI trials, only the first lever press that occurred at or after the 20s criterion was reinforced with reinforcer delivery. Early lever responses (i.e., before 20s) were neither reinforced nor punished. Trials ended with simultaneous sucrose delivery, lever retraction, and offset of the light. Rats received 10 sessions of FI training; there were 50 FI trials within each session separated by a variable inter-trial interval (ITI) that averaged 60s. Sessions terminated as rats finished the 50th trial or after 120 minutes had elapsed, whichever came first. As rats acquired the criterion duration, they reliably completed the FI sessions within approximately 70 minutes.

Peak Interval (PI) Training

After FI training, rats received 16 Peak Interval (PI) training sessions. As during FI training sessions, rats also received 50 trials during PI training. However, during PI training 25 probe trials were randomly intermixed with 25 FI trials. Probe trials were identical to FI trials in that they onset with illumination of the house light and presentation of the lever. However, probe trials were unique in that no lever presses were reinforced, regardless of if they occurred at or after the criterion duration. Instead,

probe trials lasted at least 3x the length of the criterion time (i.e., 60s). This enabled examination of responding before, during, and after the criterion had elapsed.

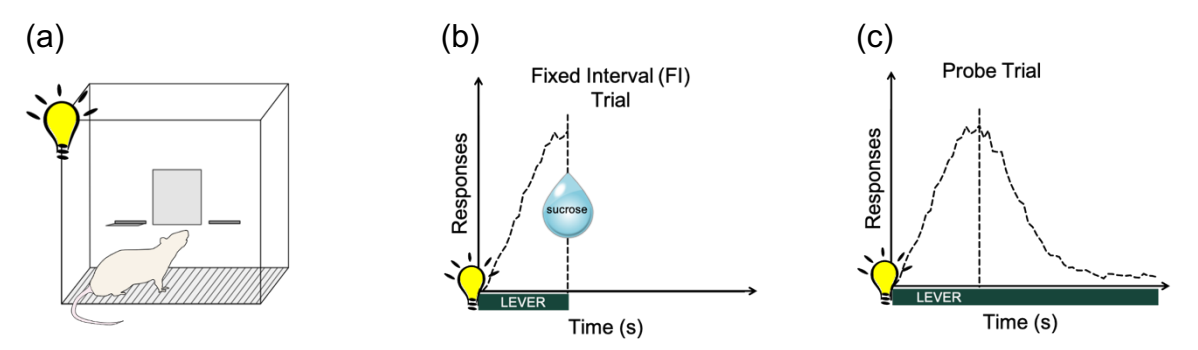


Figure 2.1 The Peak Interval Paradigm. Conducted in standard operant boxes (a), the peak interval paradigm trains rats to time a 20s criterion duration during fixed interval (FI) trials in which the first lever press at or after 20s results in sucrose reinforcement (b). Following FI training, probe trials are randomly intermixed with FI trials in a 1:1 ration. Probe trials onset in the same manner as FI trials, but last at least 3x the length of the criterion duration and differ in that no lever presses are reinforced.

Responses during each trial were time-stamped with centi-second precision, binned within 1s bins, and plotted across time. The total number of responses per bin were normalized as a function of the maximum number of responses that occurred in one bin; this produced the *proportion of peak rate response function*. The time at which maximum responding occurred was labelled *peak time*. PI training was grouped into four blocks (PI session 1-4, 5-8, 9-12, and 13-16). Proportion of peak rate response functions were averaged across training blocks to confirm acquisition of the criterion duration.

Estrous cycle tracking began during PI training; vaginal lavages were performed prior to behavioral training when rats were weighed, as described in *Vaginal Cytology*, below. During the final three PI training sessions (i.e., PI session 14 – 16), subjects

received mock drug delivery in order to habituate them to ICV infusion and intraperitoneal (i.p.) injections. Drugs administration occurred in a separate room located across the hall from the behavioral boxes; beginning with PI session 14, subjects were placed in this room for approximately 15 minutes prior to behavioral sessions regardless of if drugs were administered (i.e., including during washout days). During this period of drug delivery habituation, cannula placement and patency was verified, and rats were assigned to either intracerebroventricular (ICV) infusion or intraperitoneal (i.p.) injection groups. Preference was given to ICV infusion, however at this point cannula had been implanted for a minimum of 35 days and some had sustained damage from chewing by pair-housed rats. At this stage, n=2 rats were assigned to the i.p. injection group; n=5 rats received ICV infusions.

Phase 3: Peak Interval Testing

During the final phase of behavior, subjects continued to receive PI sessions identical to PI training. However, during test sessions, rats received administration of either vehicle (VEH; 0.2M PBS) or clozapine-N-oxide (CNO) prior to the behavioral session. Rats were tested twice each under VEH and CNO in proestrus/ estrus (P/E) and metestrus/ diestrus (M/D). Cycle stage was determined via vaginal cytology prior to daily testing, and drug delivery was determined based on previous test conditions. Efforts were made to counterbalance the order of VEH and CNO administration within P/E and M/D when possible. At least 72 hours and two "washout" PI sessions were given between each drug treatment.

Histology

Vaginal Cytology

Estrous cycle tracking was performed daily at 2 ½ - 4 hours after lights on, i.e. between 9:30 – 11:00 am. Thus, cycle samples were taken ~15-45 minutes prior to behavioral training and testing, which accommodated time for drug administration after vaginal lavages were taken and evaluated. Samples were collected via vaginal lavage, a process which involves gently inserting a P1000 pipet tip into the vaginal canal to flush, and immediately withdraw, 0.9% sterile saline solution. Vaginal samples were placed into a 12-well plate for transport and then imaged wet on an Olympus BX53 microscope. Categorization of vaginal cells into estrus cycle stage was performed based on the proportion of leukocytes, cornified, and epithelial cells. For the purpose of data analyses, estrous cycle stages were grouped into periods when gonadal hormones are generally low (e.g., metestrus, diestrus = M/D) and when gonadal hormones are generally high (e.g., proestrus, estrous=P/E). Once tracking began, estrous cycles were tracked continuously throughout behavioral training and testing.

Perfusion and tissue collection

Euthanasia was performed via fatal overdose of sodium pentobarbital (50mg/kg), followed by transcardial perfusion with 0.9% saline and 4% paraformaldehyde (PFA). Brain tissue was extracted and post-fixed overnight in 4% PFA with 12% w/v sucrose. Tissue was frozen on dry ice and stored at -80°C until slicing on a standard microtome. Five representative tissue series were sliced at 30 µm; the first of five series was mounted immediately upon slicing. The remaining four series were stored in cryoprotectant at -20°C until later processing.

Tissue analysis and immunohistochemistry

Tissue was sliced at 30 µm on a standard sliding microtome into 5 serial sets and stored at -20°C in cryoprotectant. The first representative was mounted in full immediately upon slicing and examined for viral expression of the GFP-cre in the NAc and mCherry-hM3Dq in the LHA. A second series was used for confirmation of DREADD expression in MCH⁺ cells via dual immunofluorescent staining for MCH protein and the mCherry viral tag. Tissue was first rinsed in 6x 8 min washes of 0.1 M phosphate buffered saline (PBS), then incubated in a 0.1 M PBS solution containing 0.03% hydrogen peroxide for 20 min. Next, tissue was washed in 10 min rinses each of 0.1M PBS first containing 0.3% glycine, then containing 0.03% sodium dodecyl sulfide. Tissue was blocked in a blocking solution made of 0.1 M PBS and containing 0.3% normal donkey solution and 0.15% Triton-X. Finally, tissue was incubated overnight in blocking solution with rabbit anti-MCH [1:1000] (Phoenix Pharmaceuticals, Catalog #H-070-47; Burlingame, CA) and goat anti-RFP [1:1000] (Rockland Antibodies, Catalog #200-101-379; Pottstown, Pennsylvania). On the following day, after a series of six 0.1 M PBS rinses, secondary antibody incubation occurred with [1:200] each of AlexaFluor 488 Donkey anti-Rabbit IgG and AlexaFluor 568 Donkey anti-Goat IgG in blocking solution for a period of 2 hours. Finally, tissue was rinsed twice more in 0.1 M PBS. All staining occurred at room temperature.

Following staining, tissue was float-mounted in 0.1M phosphate buffer solution onto gelatin-subbed slides and air dried prior to applying coverslips with Pro-Long Gold Antifade Mountant containing DAPI (Thermofisher). Slices were imaged on an Olympus BX51 epi-fluorescent microscope equipped with DAPI, FITC and CY3 filters and

connected to an IBM-compatible Windows 10 computer with Neurolucida imaging software (MBF Bioscience, Williston, VT).

Statistics

Data transformation

Behavioral data was imported into Microsoft Excel using table profiles built in MedPC2XL (Med Associates). This template sorted data to indicate the start of each of 50 trials, as well as the time of discrete lever presses within a session. From here, data was imported to SPSS where syntax was run to sort lever responses by trial in order to examine when each lever press occurred within each individual trial. For each subject, responses per trial were then totaled into 1s bins across all probe trials (n=25) in a session to determine total responding per 1s bin. The first 1s bin in which peak rate occurred indicated the *peak time* of the session. Peak time indicates the time at which the subject perceives the to-be-timed criterion as having elapsed and reflects the accuracy of temporal perception (Church, 1984; Church & Broadbent, 1991; Meck, 1996; Roberts & Church, 1978). In order to examine responding in the context of peak rate, responding was normalized as a percentage of maximum peak rate, to provide a *proportion of peak rate function*.

To examine the influence of estrous cycle stage, behavioral tests were grouped by periods of the estrous cycle when gonadal hormones are typically low (i.e., metestrus/ diestrus, M/D) or typically high (i.e., proestrus/ estrus, P/E). I first conduced repeated measures analysis of variance (RM ANOVA) with female rats that met the criterion of having been tested under both VEH and CNO during both M/D and P/E (i.e., only rats that were appropriately cycling and had both P/E VEH and CNO as well as

M/D VEH and CNO tests were included). During the 20s PI testing, all rats were cycling regularly and included in this analysis (n=7 ♀). Responding/ bin was totaled across the two sessions in each condition (i.e., 50 trials from two P/E VEH tests) prior to normalization. To procure group normalized functions, individual normalized functions were first averaged and then normalized as a function of group peak rate. In addition, predicted proportion of peak rate response functions were modeled using a multivariate, piecewise growth model (PGM). In this case, responding was normalized within session (i.e., over 25 trials) but the model incorporated two sessions under each drug condition (i.e., two P/E VEH, two M/D VEH, two P/E CNO and two M/D CNO tests). *Analysis*

To examine broad changes in behavior that resulted from the estrous cycle or chemogenetic manipulations, I examined the amount of time spent in the food cup (percent time) as well as the average lever response rate (rate/ min) during a session. I also evaluated whether peak time (i.e., the time at which subjects responded maximally during PI trials) differed as a function of estrous cycle stage or chemogenetic excitation of LHAp^{MCH} NAc neurons. Paired t-tests were performed using GraphPad Prism (Graphstat Technologies, Bangalore, India). Effect sizes were calculated as Cohen's *d* for paired t-tests.

Next, I evaluated how responding differed across time within individual trials by examining whether the proportion of peak rate response function differed as a function of estrous cycle stage (P/E, M/D) or drug treatment (VEH, CNO) within P/E and M/D. The proportion of peak rate response function, which plots response rate across time as a percent of peak rate, was evaluated with repeated measures analysis of variance

(ANOVA). I first examined the effects of estrous cycle stage under baseline (vehicle) conditions before separately examining the effects of drug treatment (VEH, CNO) within each estrous cycle stage. The α level for significance was set to .05. Significant interactions were examined using Bonferroni corrected pairwise comparisons to examine when responding differed between treatment conditions in each of sixty 1s time bins. Analyses of variance were performed using Statistica (Statsoft, Tulsa, OK) and SPSS version 28 (IBM, Armonk, NY).

Finally, I used multilevel piece-wise growth models (PGM) to model the predicted proportion of peak rate responding that would occur before and after peak time under each treatment condition. The peak time was defined as the first instance of the rat's maximal response, and all pre- and post-peak effects were examined relative to each subject's peak time. While the ANOVA examines differences in level or magnitude across time, the PGMs examine differences in magnitude (i.e., intercept) as well as changes in rate (i.e., slope) over time. Each PGM included linear, quadratic, and cubic rates of change across time to predict how the proportion of peak rate response function changed within each treatment condition. These models are particularly sensitive to changes in rate, and could therefore identify subtle differences in the rate of increase or decrease that occurred pre- and post-peak, respectively, due to treatment. The PGMS emphasize the distinction between pre- and post-peak periods of the trial because these periods represent distinct phases of motivated behavior. While the pre-peak period represents an increase in responding in anticipation of reinforcement (i.e., the "start" function), the post-peak period instead represents a decrease in responding following the omission of an expected reward (i.e., the "stop" function). By modeling these preand post-peak periods separately in a piecewise manner, I was able to examine how the rate of responding changed in each period accordingly based on each rat's individual perception of these two qualitatively different aspects of time.

As with the ANOVA, I first examined the effects of estrous cycle stage (M/D vs P/E) under vehicle conditions by modeling the predicted proportion of peak rate responding under M/D and P/E following VEH treatment. Next, I separately modeled drug treatment (VEH vs CNO) within P/E, and then within M/D. Overall, pre-peak effects were examined at the mid-point prior to an animal's peak time, i.e., time was "centered" before the peak. This pre-peak midpoint typically occurred around 10s. Post-peak effects were similarly centered at the midpoint between peak time and 60s, which typically occurred around 40s. The overall PGM thus specifically examines changes in the level and rate of predicted responding at approximately 10s pre-peak and 40s post-peak. A separate interaction model, which predicts estimates of intercepts and slope at these midpoints, was also computed for each PGM analysis. This analysis provided a more refined examination of changes in intercept and slope.

I also separately modeled responding in 5s intervals by centering time at 5, 10, 15, 20, 25, 30, 35 and 40s in order to identify when changes to the intercept or slope occurred during pre- and post-peak periods. As in the overall model, responding was predicted in a piecewise manner with pre- and post-peak effects separately predicted based on each subject's individual peak time. To accomplish this, I coded a new time variable such that time was centered at the interval of interest (e.g., 15s) appropriately before or after the peak for each subject. Thus, for a subject with a peak time of 13s, the 15s timepoint was centered as a post-peak effect, and the pre-peak time was centered

relative to the peak as in the overall model (i.e., 7s). On the other hand, a subject who responded maximally at 17s had 15s centered as a pre-peak effect, with post-peak time centered relative to the peak as in the overall model (i.e., at ~40s). Modeling time in this manner allowed level and rate differences to be estimated at each 5s interval across the trial. This provided more insight into when differences in the level or rate of responding specifically occurred during the pre- and post-peak periods. As in the case of the overall model, I first examined estrous effects under vehicle treatment (vehicle: estrous x time), then examined treatment effects within each estrous cycle stage (P/E: drug x time and M/D: drug x time) for each timepoint. For all analyses, the α level for significance was set to .05. Piecewise growth models were conducted using SPSS version 28 (IBM, Armonk, NY).

Results

Histology

To confirm that intact rats were cycling normally, vaginal cells were collected daily via saline lavage. Samples were roughly categorized by the approximate proportion of cell types (e.g., leukocytes and epithelial cells) visible and at least two representative photomicrographs were taken per sample (Figure 2.2). Rats were immediately categorized into either P/E or M/D in order to assign drug conditions prior to behavioral testing. However, representative images from samples were later reevaluated in context of the preceding and subsequent samples in order to confirm correct assignment of estrous cycle stage on test days. All n=7 rats were cycling appropriately during PI testing and are included in the behavioral results.

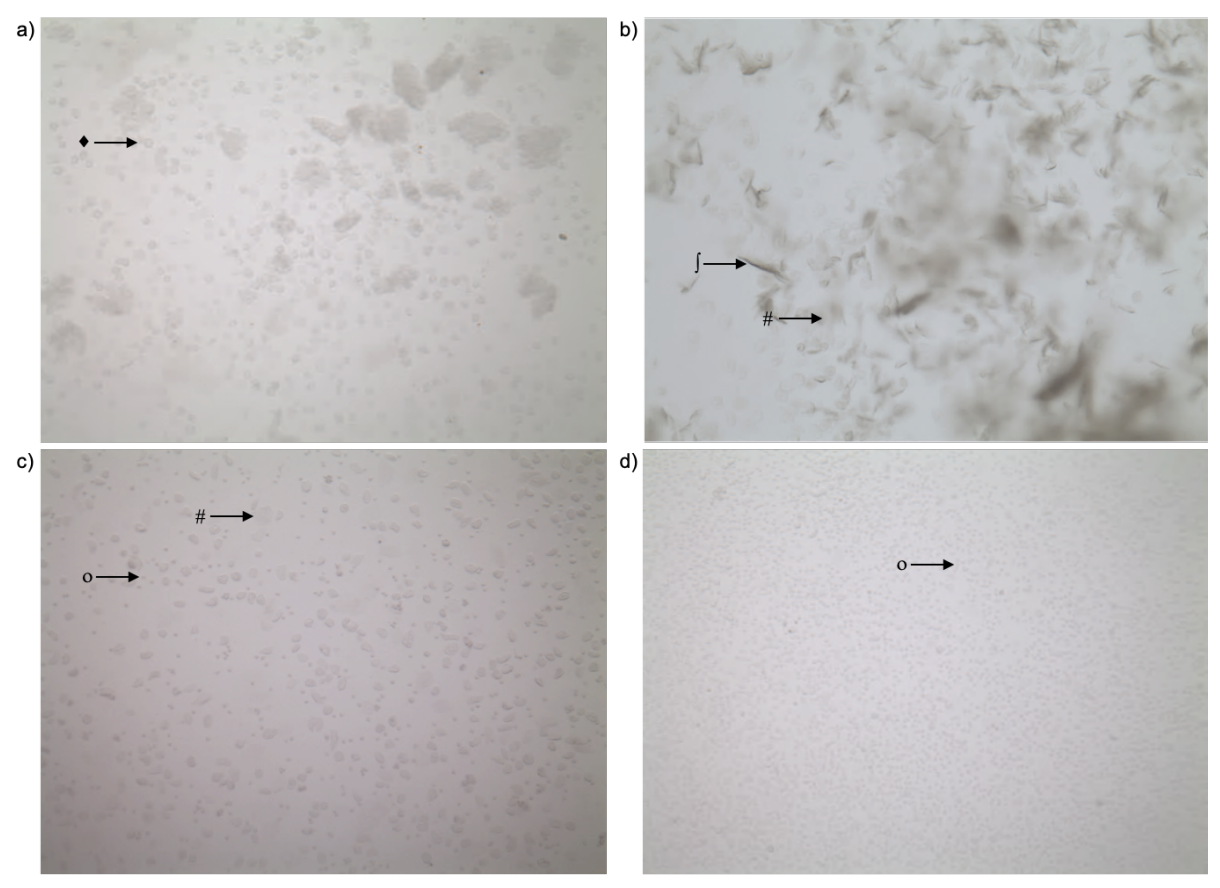


Figure 2.2 Photomicrographs of vaginal epithelial cells indicate the approximate proportion of cells present during the four stages of the rodent estrous cycle. (a) Proestrus vaginal cell samples consist primarily of larger, rounded epithelial (◆) cells. These cells often clump together in groups or strands. (b) During estrus, the cornification of vaginal epithelial cells produces both flat, cornified (#) and thin, needle-like cells that are highly keratinized (ĺ). Large round epithelial cells may also be present. (c) During metestrus, the proportion of leukocytes (o) increases relative to the other cell types. However, large epithelial cells in various stages of cornification persist. (d) Diestrus samples are characterized primarily by the presence of leukocytes. Cycle stages were approximated from the relative proportion of each cell type present on a given day, with consideration for preceding and subsequent days.

Tissue analysis confirmed bilateral expression of the GPF-cre virus in the NAc. Viral expression of the cre-dependent pMCH-HM3D(Gq)-mCherry virus was limited, but in line with previous reports indicating that this approach transfects only ~10% of MCH neurons (Noble et al., 2018; Terrill et al., 2020). Subjects were included as viral hits so long as they had clear GFP-cre expression in the NAc and evidence of the mCherry-HM3D(Gq) virus in the LHA shown through viral tracts, fibers, and a limited number of fluorescent-labeled cells.

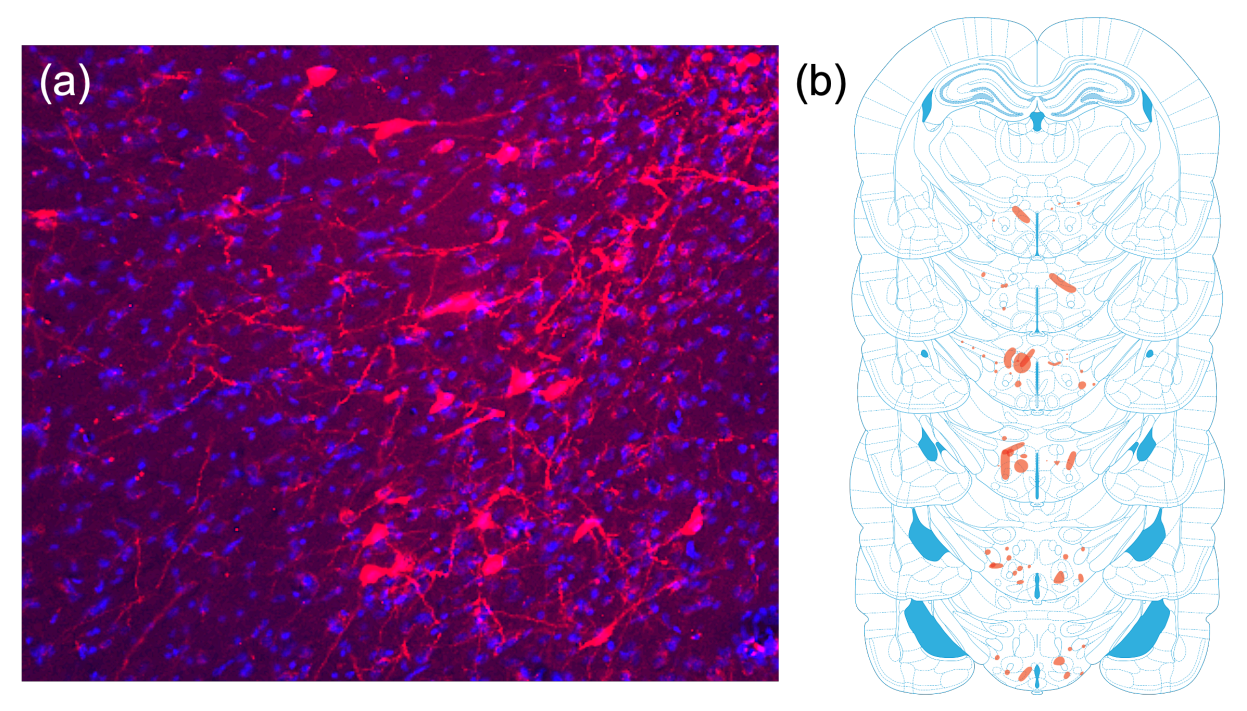


Figure 2.3 DREADD Expression in NAc-projecting LHAp neurons. (a) Representative photomicrograph of mCherry labelled DREADD expression in the LHAp. (b) Heat maps indicate representative DREADD expression (red) throughout the LHAp. Coronal sections modified from Paxinos & Watson 6th edition.

Time-dependent food-seeking across the estrous cycle

Analysis of the overall time spent in the food cup (percent time) or response rate (rate/ min) across the session revealed no baseline effects of estrous cycle stage on

behavior (Figure 2.4 a, b; percent time: t=1.237, df=5, p>.05, d=0.5; response rate: t=0.032, df=5, p>.05, d=.01). The time at which animals responded maximally within trials (i.e., peak time) also did not vary based on estrous cycle stage (Figure 2.4 c, t=0.00, df=5, p>.05, d=0.0).

Analysis of the proportion of peak rate response function revealed only a main effect of time (Figure 2.4, d; F=138.34, df=(59, 295), p<.001, η_p^2 =.97), indicating that regardless of estrous cycle stage, rats significantly altered their response rate across individual trials in expectation of receiving reinforcement at the criterion time.

Similar to the ANOVA, the overall PGM also revealed only effects of time when rats were tested under VEH across the estrous cycle. Before the peak, response rates increased in a primarily linear manner: i.e., there was a significant linear effect of time (F=65.27, df=1325, p<.001) pre-peak. After the peak, response rates declined at a rate that was determined by both linear and quadratic slopes (linear: F=32.69, df=499 p<.001; quadratic: F=14.10, df=637, p<.001). The overall model failed to reveal any estrous cycle effects pre- or post-peak. Results from the overall PGM and the estimates of intercept and slope predicted by the interaction model are reported in Supplemental Table S2.1 and S2.2, respectively.

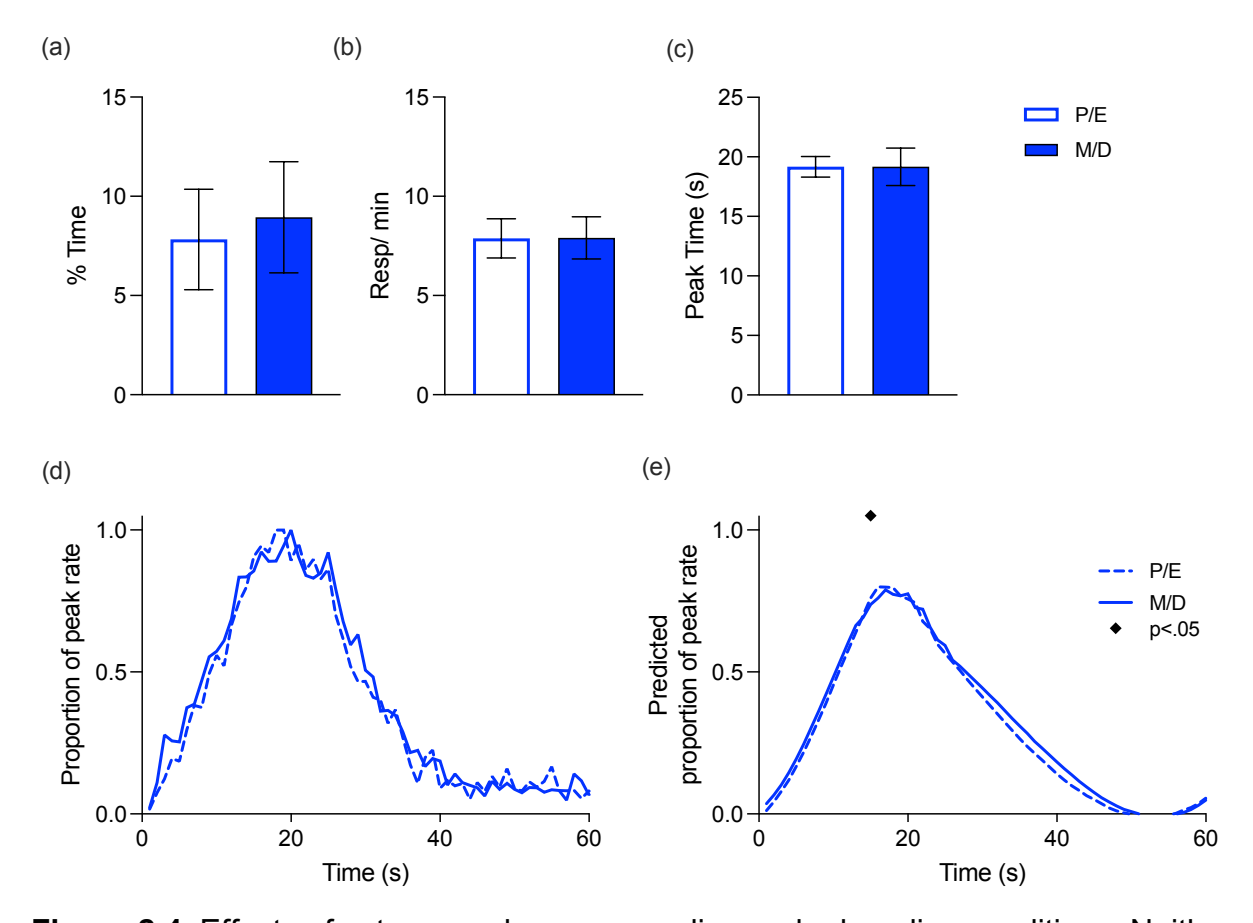


Figure 2.4 Effects of estrous cycle on responding under baseline conditions. Neither the total amount of time spent in the food cup, nor response rate across the session varied based on estrous cycle stage (a, b). Within individual trials, peak time (c) also did not vary between when rats were tested in M/D vs P/E. Finally, estrous cycle stage did not influence the proportion of peak rate responding across time (d), but analyses of predicted proportion of peak rate responding across 5s intervals revealed an effect of estrous cycle stage at 15s (e).

Adopting the refined analysis of responding at 5s intervals (Supplementary tables S2.3 and S2.4) revealed an effect of time as in the ANOVA. In addition, this more sensitive analysis also revealed a main effect of estrous (F=3.89, df=170, p=0.05) and an interaction effect of estrous with the quadratic rate of change over time (F=7.95,

df=733.57, p=.005) at the 15s interval. Note that this is approximately the point in time when the predicted proportion of peak rate responding that occurs during P/E exceeded that predicted during M/D (i.e., where the lines representing predicted responding in each condition cross in Figure 2.4, e). This effect occurs in the post-peak component of the model, implying that it is driven by rats whose peak responding occurs prior to 15s (i.e., rats for whom 15s falls in the post-peak period). This includes data from n=3 M/D and n=2 P/E tests where rats peaked at or before 15s under vehicle treatment. While subtle, this estrous cycle effect suggests that responding may differ near the peak time based on estrous cycle stage. However, given that peak time itself does not vary as a function of estrous cycle, an estrous cycle effect may be limited to influencing the timing of "start" or "stop" functions without altering peak time, *per se*.

Chemogenetic stimulation of LHApMCH → NAc neurons during P/E

Next, I evaluated whether chemogenetic excitation of LHA^{MCH} → NAc neurons influenced responding in the PI task when rats were tested during proestrus/ estrus (P/E). During P/E, there was no difference in the amount of time rats spent in the food cup (t=0.19, df=5, p>.05, d=.08; Figure 2.5 a) nor on the average response rate across the session (t=1.163, df=5, p>.05, d=.23; Figure 2.5 b) under VEH or CNO treatment. Within probe trials, peak time also did not vary following treatment with VEH or CNO (t=0.41, df=5, p>.05, d=.17; Figure 2.5 c).

Likewise, the repeated measure ANOVA which examined the effects of drug and time revealed only a significant main effect of time (F=82.80, df=(59, 295), p<.001, η_p^2 =.94) on the proportion of peak rate response function. As expected, rats changed their response rate during the trial in order to reach a peak rate around the expected time of

reinforcement. However, there was no effect of drug treatment (VEH or CNO) on the proportion of peak rate response function (F=5.48, df=(1, 6), p=.067, η_p^2 =.52). There was also no significant interaction of drug x time (F=0.99, df=(59, 295), p>.05, η_p^2 =.17).

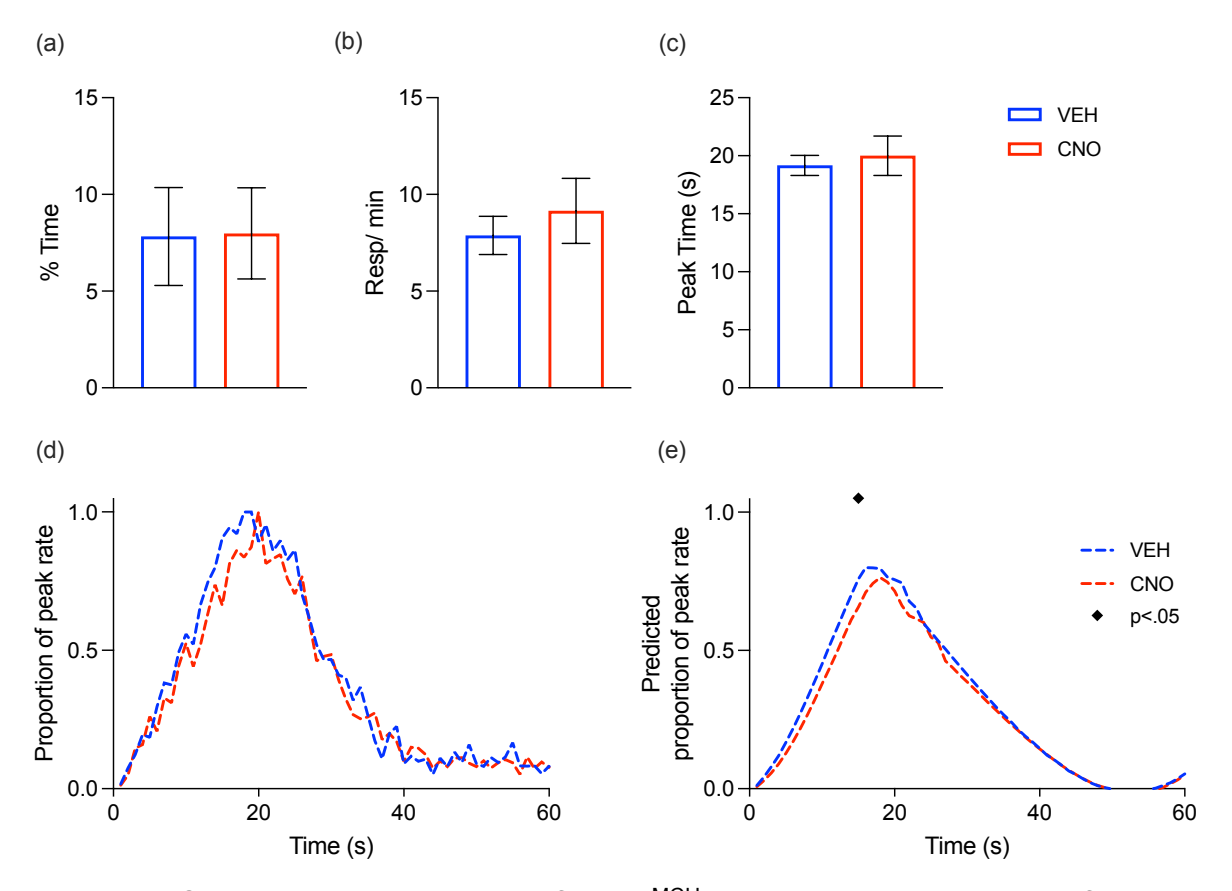


Figure 2.5 Chemogenetic excitation of LHAp^{MCH} \rightarrow NAc neurons does not influence PI responding in P/E. The amount of time spent in the food cup and response rate across the session did not vary as a function of drug treatment when rats were tested during P/E (a, b). There was also no difference in peak time following CNO-mediated excitation of LHA^{MCH} \rightarrow NAc neurons (c). There were also no significant differences in the actual or predicted proportion of peak rate response functions (d, e).

Piece-wise growth modeling of responding under VEH and CNO treatment during P/E also did not reveal any effects of drug treatment on the predicted proportion of peak rate response function. This model revealed only significant effects of time; there was a

significant effect of linear time (F=59.18, df=1365, p<.001) pre-peak and there were significant linear and quadratic effects of time post-peak (F=25.85, df = 536.238, p<.001 and F=14.22, df=688, p<.001, respectively). Results from the piecewise growth model are indicated in supplemental table S2.7; estimates of intercepts and slopes are depicted in S2.8.

Results from the PGM examining the effects of drug treatment at 5s intervals are reported in supplemental tables S2.7 and S2.8. The closer inspection provided by examining data in this manner revealed a drug effect at 15s such that VEH-treated rats displayed a significant difference in the intercept (i.e., level) of responding pre-peak relative to CNO (F=3.99, df=260, p=.047). In addition, the post-peak quadratic rate of change at this timepoint was more negative following CNO administration (F=4.59, df=734, p<.05). This may reflect a slowing down of response rate around the time of the peak, which may drive the lower intercept that occurs at 15s in CNO-treated rats relative to VEH. Because this timepoint occurs just prior to the criterion, it may reflect a particularly sensitive period where subtle differences in motivation or expectation of reward may influence decisions to "start" and "stop" responding. Because the PGMs evaluate changes in linear, quadratic, and cubic slope, they may better capture these subtle changes in response rate that occur around the time of expected reward. Chemogenetic stimulation of LHAp^{MCH} → NAc neurons during M/D

Rats tested during M/D also did not differ in the amount of time they spent in the food cup (t=.76, df=5, p>.05, d=.15), their rate of responding (t=1.49, df=5, p>.05, d=.20) or peak time (t=0.37, df=5, p>.05, d=.17) (Figure 2.6).

Analysis of the proportion of peak rate response function under each drug condition (VEH, CNO) also failed to reveal any significant effects of CNO on responding across time (Drug: F=0.026, df=(1, 5), p=.88, η_p^2 =.00; Drug x time: F=0.73, df=(59, 295), p=.93, η_p^2 =.13).

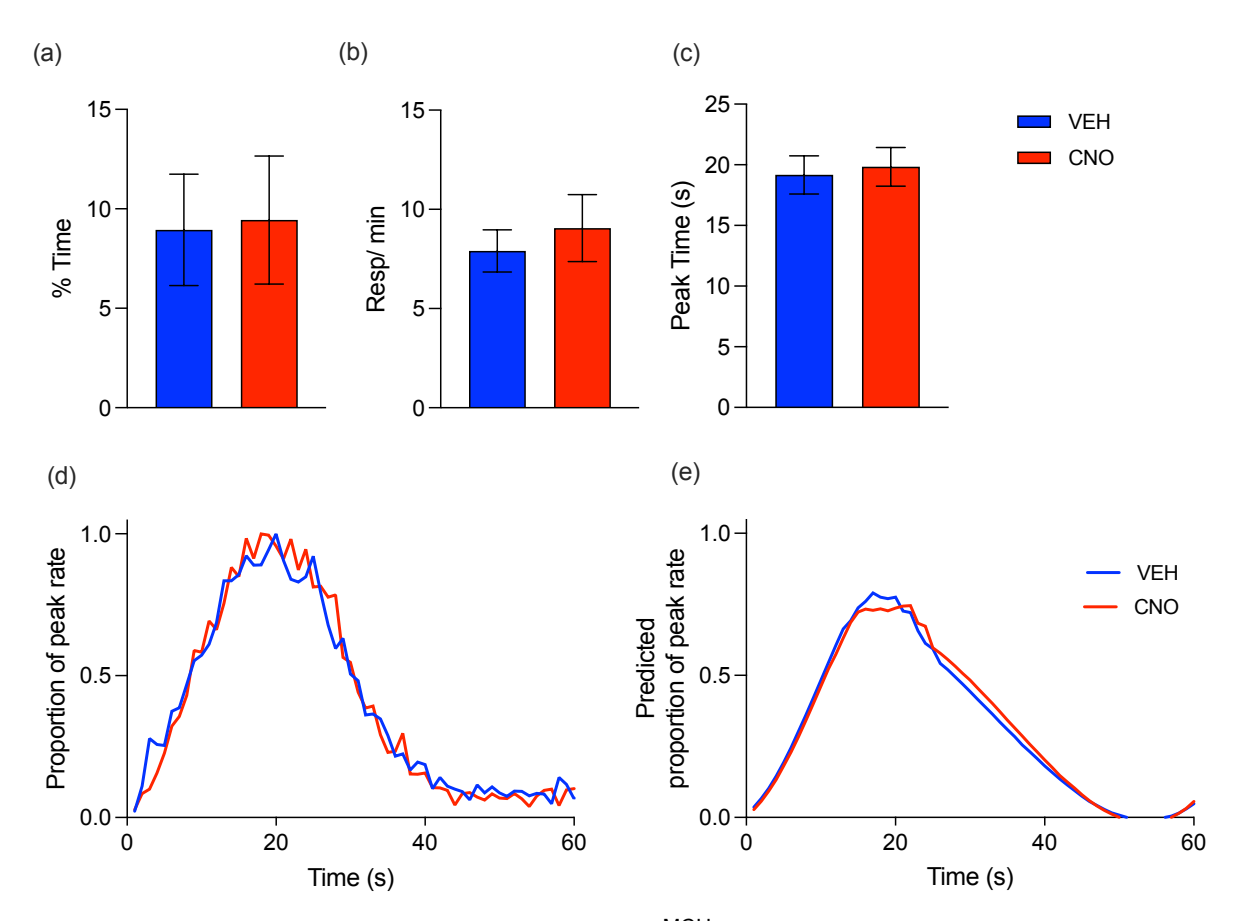


Figure 2.6 Chemogenetic excitation of LHAp^{MCH}→NAc neurons during M/D. There were no significant differences in response rate, time spent in the food cup, or peak time (a-c) when rats were treated with VEH or CNO. The actual and predicted proportion of peak rate response functions (d, e) also did not differ following CNO-mediated excitation of LHAp^{MCH}→NAc neurons.

Modeling the predicted proportion of peak rate revealed no differences in the level of responding following CNO treatment in rats tested during M/D (see

supplemental table S2.9 and S2.10). Moreover, there were no differences in response rate or magnitude as revealed by the overall PGM and analyses at 5s intervals (Table S2.11 and S2.12). Interestingly, the lack of an effect at 15s is in contrast to subtle baseline (vehicle) estrous effects and to effects of chemogenetic excitation of LHAp^{MCH} NAc neurons in rats tested during P/E.

Discussion

Summary of results

There were no significant effects of chemogenetic excitation of LHAp^{MCH}→NAc neuronal excitation on interval timing, *per se,* in female rats. Excitation of LHAp^{MCH}→NAc neurons did not influence peak time or the proportion of peak rate response function in a manner indicative of a change in clock speed. Thus, in line with our expectations, LHAp^{MCH}→NAc neurons did not influence time perception in the peak interval task, suggesting that if LHAp^{MCH} neurons are indeed capable of influencing interval timing, they do so through an alternative target. This LHAp^{MCH}→NAc projection is not capable of influencing interval timing.

Although there were no effects of LHAp^{MCH} →NAc neuronal excitation on interval timing, *per se*, there was a subtle effect of estrous cycle stage on responding during the PI task under baseline conditions. Specifically, when the predicted proportion of peak rate response function was modeled in a piecewise manner to examine the influence of estrous cycle on behavior at 5s intervals, estrous cycle selectively influenced responding in the 5s interval just prior to the criterion time (i.e., at 15s). Under baseline conditions, rats accelerated responding more quickly at 15s during P/E relative to M/D (i.e., there was a significant effect of estrous cycle on the quadratic slope). This resulted

in a higher level of responding under P/E than M/D at 15s, although the magnitude of this difference was not significant. This effect was also transient, as there were no significant differences in magnitude or slope at the next 5s interval at 20s. Rats thus differed in their pre-peak responding immediately prior to the criterion time depending on estrous cycle stage but exhibited no differences in the magnitude or rate of responding at the criterion itself. In line with this, there was also no difference in peak time when rats were tested in M/D compared to P/E. Altogether, these findings suggest that there may be subtle differences in the rate of PI responding based on estrous cycle stage, but that these effects are not driven by a change in time perception.

To my knowledge, only one other study to date has examined estrous cycle effects on timing performance in intact female rats (Panfil et al., 2023), and has reported mixed effects of cycle stage on timed performance. However, accumulating evidence from studies examining the effects of exogenous estradiol (EB) replacement in gonadectomized rats suggests that there may be multiple mechanisms of EB on timing (Pleil et al., 2011; Ross & Santi, 2000; Sandstrom, 2007), including both acute and phasic effects. Evidence indicating that long-term estradiol treatment does not influence time perception (Ross & Santi, 2000), suggests that any baseline effect of fluctuating gonadal hormones on PI performance may be subtle, especially in well-trained rats who have repetitively experienced the task in all phases of the estrous cycle. Thus, while acute estradiol replacement in OVX rats accelerates clock speed (Sandstrom, 2007), these effects are transient and may not be representative of the effects of endogenous fluctuations of estrogen in intact rats. For example, Ross and Santi (2000) reported that two weeks of EB replacement decreased discrimination accuracy but did not influence

time perception in a duration discrimination task. Likewise, Pleil et al. (2011) found that cyclic EB replacement in OVX rats produced a clock speed effect only during the first hormone cycle. These authors attribute this effect to previous experience of the task following EB pretreatment and/or the extensive training rats received between testing cycles (Pleil et al., 2011). Given that rats in the present experiment had ample experience performing the task during both M/D and P/E, they may have learned to rapidly and flexibly adjust responding to compensate for any hormone-induced changes in clock speed.

In fact, that an effect of estrous cycle on PI responding at 15s was captured by the refined PGM analysis examining responding in 5s intervals speaks to the sensitivity of this analysis. This analysis was able to identify transient behavioral effects not revealed by the ANOVA or overall PGM because it separately examines pre- and post-peak effects at 5s intervals, rather than across the entire trial, or entire pre- vs post-peak period. This estrous effect was constrained to the period immediately preceding the peak, and occurred just prior to the criterion time, which is a behaviorally distinct period during the trial that coincides with the highest probability of reinforcement delivery. Thus, during this period the expectation of reward is highest and rats may be most motivated to respond for reinforcement. Thus, this refined analysis may capture transient changes in motivation that occur within a trial.

In addition, the more sensitive, PGM analysis across 5s intervals also revealed an effect of chemogenetic excitation of LHAp $^{\text{MCH}} \rightarrow \text{NAc}$ neurons at 15s when rats were tested during P/E. In this case, CNO-mediated excitation of LHAp $^{\text{MCH}} \rightarrow \text{NAc}$ neurons altered both the level and rate of responding at 15s. Responding at 15s was significantly

greater in VEH-treated than in CNO-treated P/E rats pre-peak. Post-peak (i.e., for rats that had already peaked responding prior to 15s), the quadratic rate of decrease was steeper in CNO-treated rats. Thus, CNO-treated rats that had already reached a peak rate prior to 15s attenuated responding more quickly than VEH-treated rats at 15s. This suggests that chemogenetic excitation of LHAp^{MCH} → NAc neurons may subtly accelerate the "stop" function, as CNO-treated P/E rats "stop" responding more quickly at this time.

As was the case with the baseline estrous cycle effect, chemogenetic excitation of LHApMCH -> NAc neurons also only influenced responding in a manner that was both subtle and transient: neither the ANOVA nor the overall PGM revealed effects of drug treatment during P/E, and effects were only observed at 15s. Thus, the effect once again coincided with the period when rats perceived reinforcement delivery as being most likely and thus had high expectations of reward delivery. As motivated responding reaches a peak at this time, effects of LHAp^{MCH} →NAc neuronal excitation on motivation may be more easily revealed. Differences in responding that occur immediately before and after the peak indicate finite changes in motivated behavior coordinated around time of expectation – and subsequent omission – of reward delivery. Interestingly, in this case the effect of LHAp^{MCH} →NAc neuronal excitation on the magnitude of responding occurred pre-peak, whereas effects on the rate of responding occurred postpeak. This is possible because some rats had already reached a peak time at 15s, whereas other rats had not (i.e., for some rats 15s is pre-peak, whereas for others it is post-peak). Thus, In this case, chemogenetic excitation of LHApMCH->NAc neuronal excitation appears to modestly increase the level of pre-peak responding, while also

reducing the rate of response decay post-peak, resulting in a higher level of responding that rapidly decays. Although these effects are centered around 15s, they are subtle, and occur without influencing the peak time. Thus, they are not clearly indicative of an effect on time perception, but may reveal a subtle decrease in motivation. That these LHAp^{MCH} →NAc neurons may be capable of influencing motivated responding during P/E is unexpected given the inhibitory effect of estrogen on MCH. However, the subtle nature of the effect is in line with the idea that the effects of the neurons may be attenuated during P/E.

Surprisingly, however, there were no effects of LHAp^{MCH}→NAc neuronal excitation on motivated responding in rats tested during M/D. This is unexpected not only because effects – albeit modest and transient – were observed in P/E, but also because the inhibitory influence of estradiol is absent during M/D. In other words, although there was a subtle effect of LHAp^{MCH}→NAc neuronal excitation on post-peak response rate during P/E, there was no effect of the same excitation during M/D. This suggests provides additional evidence for estrous cycle effects on PI performance in intact female rats and further indicates that LHA^{MCH} neurons that project to the NAc interact with circulating ovarian hormones.

Limitations

Despite the subtle effects captured by the refined PGM analysis in this study, which indicated potential estrous cycle and chemogenetic effects of LHAp^{MCH}→NAc neuronal excitation at 15s, there was little evidence of a role for these neurons in influencing PI responding. Regardless, this general lack of effect should be interpreted with caution, as only a small proportion of LHAp neurons expressed the mCherry

fluorophore indicative of successful DREADD expression in the LHA. While a limited number of mCherry-labelled cells were present in the expected LHAp regions (see Figure 2.3), mCherry-labelled fibers were more apparent than cell bodies. Poor expression of the mCherry fluorophore persisted even after amplification using immunohistochemistry, which limited the extent of histological analyses included. These issues also made it difficult to examine MCH protein expression in mCherry, DREADD-expressing neurons. Regardless, that there is no overall effect of CNO administration in these rats, particularly during M/D, indicates that even if an insufficient number of cells expressed the DREADD for a behavioral effect, there were also no off-target effects of CNO.

Conclusion

In conclusion, chemogenetic excitation of LHAp^{MCH}→NAc neurons failed to influence timing in the PI paradigm, indicating that this projection is not capable of altering time perception. In addition, there were no effects of LHAp^{MCH}→NAc neuronal excitation on motivated responding during M/D. There were subtle effects of chemogenetic excitation of LHAp^{MCH}→NAc neurons on the rate of responding around 15s when rats were tested during P/E, potentially indicating an acceleration of the "stop" function during P/E. There was also a baseline effect of estrous cycle stage at 15s such that P/E rats attenuated high rate responding more quickly (i.e., the "stop" occurred more abruptly). In both cases, these subtle effects are not indicative of a change in time perception, but may reveal a slight attenuation in motivation to food seek during P/E.

CHAPTER 3: MCH Neurons in the anterior LHA interact with estrous cycle stage to influence motivation in a time-dependent manner

Abstract

In order to appropriately coordinate motivated behavior, an individual must decide when to start or stop behavior using information from the local environment. Temporal information, which allows an individual to understand predictive relationships between stimuli and outcomes, is particularly important for learning and decision making. Previously, I demonstrated that chemogenetic excitation of cells that produce the appetite-stimulating neuropeptide Melanin Concentrating Hormone (MCH) could influence time-dependent responding in female rats tested in the Peak Interval (PI) paradigm. Specifically, chemogenetic excitation of MCH neurons delayed when female rats stopped responding after the omission of an expected reward during probe trials. In other words, MCH neurons prolonged high rate responding in female rats, indicating an increase in motivation to continue working for reinforcement. This influence of MCH neurons on motivated behavior may reflect a role for MCH in the nucleus accumbens (NAc), a region important for both motivated behavior and the decision to "stop" responding in interval timing tasks (Floresco, 2015; Kelley, 2004; MacDonald et al., 2012). Thus, in this chapter I examined whether MCH neurons that project to the NAc would likewise prolong motivated responding in the PI paradigm. To examine the influence of these cells on motivation, I used chemogenetics to selectively excite NAcprojecting MCH neurons while female rats were tested in both the PI paradigm, as well as a more typical task used to study broad features of motivation: the progressive ratio (PR) task. Rats were tested during periods of both low (i.e., metestrus/ diestrus, M/D)

and high (i.e., proestrus/ estrus, P/E) circulating gonadal hormones. I hypothesized that chemogenetic excitation of NAc-projecting MCH neurons would prolong high rate responding in the PI paradigm, reflecting an increase in motivation. Furthermore, because estradiol inhibits the activity of MCH and because chemogenetic excitation of MCH neurons previously prolonged high rate responding predominantly during M/D, I hypothesized that projection-specific excitation of these neurons would also selectively produce effects when rats were tested during M/D. In line with my hypotheses, excitation of NAc-projecting MCH neurons influenced motivation in the PI task by altering post-peak responding, and this effect occurred in M/D. However, contrary to my initial hypothesis, excitation of NAc-projecting MCH neurons decreased post-peak responding, reflecting a decrease in motivation to work for an omitted food reward. Interestingly, these effects were limited to the post-peak period (i.e., they were temporally selective) and did not influence responding in the PI task overall. In line with this, there was no effect of LHAa > NAc neuronal excitation on PR responding, indicating that these effects are selective to the timing – rather than overall rate – of motivated responding. The activation of LHAa^{MCH} neurons appears to alter the decision of when to "stop" responding for a sucrose reward. In contrast to my previous studies, in which activation of all LHAaMCH neurons prolonged high rate responding, activation of only those LHAaMCH neurons that project to the NAc instead decreased high rate responding. In both cases, these effects were limited to the post-criterion period, and occurred selectively when cells were activated during M/D. Altogether, these results indicate that LHAa^{MCH}→NAc neurons interact with the estrous cycle to influence

decisions about how to respond for food within a temporal context that predicts food availability.

Introduction

Previously, I demonstrated that LHAa^{MCH} neurons could delay the "stop" function in female – but not male - rats. Using a chemogenetic approach, I selectively excited MCH neurons in the anterior LHA (LHAa) in male and female rats tested in the Peak Interval (PI) paradigm. The excitation of these neurons had no influence on peak time, indicating that these neurons did not influence time perception, *per se.* However, chemogenetic excitation of LHAa^{MCH} neurons selectively prolonged high rate responding after the criterion in female rats. Moreover, this effect occurred only during metestrus/diestrus (M/D), when circulating levels of ovarian hormones are typically lower than during proestrus/ estrus (P/E). In addition, neither peak time nor responding prior to the criterion time were affected, indicating an intact "start" function and accurate time perception. These findings not only indicate that LHAa^{MCH} neurons interact with the estrous cycle, but also suggested a role for the nucleus accumbens (NAc), a ventral striatal region important in both motivated behavior and the "stop" function of interval timing (Floresco, 2015; MacDonald et al., 2012).

Within interval timing procedures, the "start" and "stop" functions are described as dissociable decision processes wherein a rat begins to respond at a high rate prior to the expectation of reward and then stops high rate responding after the reward has been omitted, as occurs in PI probe trials (Balcı, 2014; Church et al., 1994; Church & Broadbent, 1991; Gallistel & Gibbon, 2000; Gibbon, 1977; MacDonald et al., 2012). The "stop" function relies on an intact ventral striatum (MacDonald et al., 2012), which is also an area instrumental in motivated behavior and food intake (Floresco, 2015; Kelley, 2004; Kelley et al., 1996, 2005; Stratford & Kelley, 1997). Indeed, the a delay in the

"stop" function can be interpreted as an increase in motivation to continue responding for an omitted food reward, and changes in reward magnitude can separately influence the "start" and "stop" functions without influencing time perception (Galtress & Kirkpatrick, 2009; Roberts, 1981). For instance, decreasing reward value by devaluing the food reinforcer used in timing tasks generally delays the "start" function (Galtress & Kirkpatrick, 2009; Roberts, 1981). This delay would be interpreted as a decreased motivation to respond for the devalued reinforcer and occurs without influencing time perception itself. On the other hand, continued high rate responding after the omission of an expected reward, as observed following chemogenetic excitation of LHAaMCH neurons during M/D, would be interpreted as an increase in motivation to continue responding for the omitted food reinforcer. This type of perseverative, unproductive reward seeking has also been associated with activity in the NAc (Ambroggi et al., 2011; Floresco, 2015; Lafferty et al., 2020). Furthermore, the inhibitory tone produced by median spiny neurons (MSNs) in the NAc is thought to be differentially modulated via GABA- and glutamatergic inputs (Lafferty et al., 2020), which may include afferents from LHA^{MCH} neurons.

Indeed, LHA^{MCH} neurons densely innervate the NAc, and the MCH receptor (MCH1R) is particularly strongly expressed within the NAc shell (Georgescu et al., 2005; Haemmerle et al., 2015; O'Connor et al., 2015). Thus, LHAa^{MCH} neurons may project to the NAc to modulate motivated behavior, including the "stop" function of PI responding. Thus, I hypothesized that LHAa^{MCH} neurons that project to the NAc (LHAa^{MCH} → NAc neurons) could increase motivation and delay the PI "stop" function. In this chapter, I used a dual virus approach to selectively transfect LHAa^{MCH} → NAc

neurons with an excitatory DREADD. To examine the influence of these cells on motivation, rats were tested in both the progressive ratio (PR) and peak interval (PI) paradigm. While the PI paradigm specifically examines the "stop" decision within the temporal context of probe trials, the PR task more generally examines motivation by requiring progressively more instrumental responding for reinforcement.

Previously, chemogenetic excitation of LHA^{MCH} neurons delayed the "stop" function during PI responding, without influencing overall response rates in the PI task.

This suggests that excitation of LHA^{MCH} → NAc neurons may similarly influence the "stop" function in PI responding without affecting PR performance. In addition, given that LHA^{MCH} neurons influenced motivated food-seeking only during M/D, I expect that LHA^{MCH} → NAc neurons will also influence responding selectively during this period of the estrous cycle.

The lack of effect of chemogenetic excitation of LHA^{MCH} neurons on responding during P/E suggests that high levels of circulating ovarian hormones may block the action of these neurons. Given that the MCH system is generally inhibited by estradiol (Messina et al., 2006; Santollo & Eckel, 2008, 2013; Terrill et al., 2020), it is possible that high levels of estradiol during P/E block the effects of LHA^{MCH} neuronal excitation. Thus, the lack of effect of chemogenetic excitation of LHA^{MCH} neurons during P/E may represent a protective role of estradiol. In contrast, relatively low levels of estradiol circulating during M/D may create a vulnerability for LHA^{MCH} neuronal excitation to influence behavior beyond the level observed in P/E when high levels of estradiol act as a "brake" on the MCH system. This "brake" could prevent chemogenetic excitation of

LHA^{MCH} neurons from influencing the "stop" function during P/E, whereas the release of the brake in M/D enables these cells to influence behavior.

Given that the striatum is highly sexually dimorphic (Becker, 1990a, 1990b; Becker & Ramirez, 1981) and contains a dense colocalization of MCH1R and the estrogen receptor- α (ER- α) (Terrill et al., 2020), estrogen may mediate MCH activity via the NAc. In line with this notion, Terrill et al. (2020) report sex differences in feeding behavior following infusion of MCH to the NAc, and that MCH peptide infusion to the NAc increased feeding in oil-treated – but not estrogen-treated – ovariectomized (OVX) females. Thus, the projections from LHAaMCH neurons to the NAc may both influence the "stop" function and underlie the estrous cycle effects observed in the PI paradigm. Thus, in this chapter I will examine the influence of chemogenetic excitation of LHAa^{MCH} NAc neurons on PI responding across the estrous cycle (i.e., in both P/E and M/D) to determine whether this projection can recapitulate the motivated phenotype observed following LHAa^{MCH} neuronal excitation in M/D females. I will also separately examine the effects of this projection more broadly on motivated behavior in a PR task. I hypothesize that LHAaMCH > NAc neuronal excitation will selectively prolong high rate responding after the criterion duration during M/D, but not when rats are tested in P/E. Furthermore I expect that this excitation will not influence overall response rates in the PR task.

Materials & methods

Subjects

Eight adult female Sprague-Dawley rats (*Envigo, Haslett, MI, USA*; 12-weeks of age at arrival) were housed as described in Chapter 2.

Surgical procedures

Stereotaxic Viral Infusion and Cannulation

Rats underwent stereotaxic viral infusion and cannulation as described in Chapter 2, except that infusions of the cre-dependent excitatory DREADD was selectively targeted to the anterior LHA (Table 3.1).

Table 3.1 Viral approach to selectively target LHAa^{MCH} neurons that project to the NAc.

Dual Virus Approach			
Virus	Target	Infusion coordinates	
AAV2(retro)-eSYN-EGFP-T2a-icre-WPRE 0.3 μl / infusion	NAc Shell	+1.1 A.P., ±0.8 M.L., −7.5 D.V.	
AND			
AAV2-DIO-rMCHp-hM3D(Gq)-mCherry 0.5 μl / infusion	LHAa-MCH	-2.12 A.P., ±2.1 M.L., -8.4 D.V.	

Behavioral Paradigms

Rats were first trained and tested in the Peak Interval paradigm (Experiment 3a), as described in Chapter 2. After completing PI training and testing, rats were also tested in a Progressive Ratio task (Experiment 3b).

Peak Interval Paradigm

All training and testing procedures during Phase 1 and Phase 2 were identical to those described in Chapter 2, as behavioral assays in these chapters were performed simultaneously.

Progressive Ratio Task

Following completion of the PI paradigm, rats were next tested in a Progressive Ratio (PR) task. The PR task provides a classic assessment of how hard an animal is willing to work in order to earn a reward. In this task, rats must make progressively more

instrumental responses in order to receive reinforcement. The task ends when a rat fails to make an instrumental response within the timeout period (i.e., 15 min) or after 5 hours, whichever comes first. Notably, unlike the PI paradigm, there is no temporal component involved in the PR paradigm except that animals must respond at least once every 15 min.

Autoshaping

Given that rats had been extensively trained to lever press in the PI paradigm, rats were shifted to a nosepoke instrumental response in order to help distinguish this task from prior experience in the PI paradigm. Nosepoke ports, which consist of small, recessed openings containing an IR beam across the opening, were placed into the operant box on either side of the food magazine, thus taking the former position of the levers. Rats first underwent two sessions of FI20 nosepoke training to acquire the instrumental response. Then, rats were shifted to a progressive ratio (PR) schedule of reinforcement in which they needed to make progressively more nosepokes to obtain the same amount of sucrose reinforcement. The number of responses required to obtain a single reward increased following a variable schedule (i.e., PR1, 2, 4, 9, 12, 15, 20, 25, 32, 40, 50, 62, 77, 95, 118, 145, 178, 219, 268, 328, 402, 492, 603, 737, 901, 1102, 1347, 1647, 2012). PR sessions ended when rats failed to make at least one nosepoke over a 900 s (15 min) period or after five hours, whichever came first. Rats received 12 consecutive days of PR training before moving onto testing with VEH and CNO.

Progressive Ratio Testing

PR tests sessions were identical to PR training sessions except that rats received an *i.p.* dose of either vehicle (0.2 M PBS) or clozapine-N-oxide (CNO; 0.3mg/kg) 15 min prior to beginning the behavioral session. Rats were tested under each drug once in P/E and once in M/D; sessions in which drugs were administered were separated by at least a 72-hour washout period. Between tests sessions, animals performed ordinary PR sessions. Efforts were made to counterbalance the order of VEH and CNO administration between subjects, with consideration of the estrous cycle stage. In order to capture all phases of the estrous cycle, some rats received additional washout days between test sessions; all rats completed PR testing in 10-14 sessions. Histology

Vaginal cytology, perfusion, tissue collection, and analysis were performed as described in Chapter 2.

Statistics

Data transformation

Behavioral data from both the PI and PR tasks were imported into Microsoft Excel using table profiles built in MedPC2XL (Med Associates). Data from the Peak Interval task was sorted and normalized as described in Chapter 2.

Statistics

Data from the Peak Interval paradigm were analyzed as described in Chapter 2.

Data from the Progressive Ratio task were first examined for differences in PR responding across the estrous cycle, and then as a result of chemogenetic excitation of LHAa^{MCH}→NAc neurons separately in P/E and M/D. Using paired t-tests, I first

examined whether there were differences in session time or response rate between P/E and M/D rats tested under vehicle conditions. Next, I examined whether these measures differed based on drug treatment (VEH, CNO) when rats were tested in P/E or M/D. Finally, I used a Mantel-Cox, log-rank survival analysis to determine whether there were any differences in the probability of survival of (1) P/E vs M/D rats tested under VEH, (2) VEH vs CNO treatment in P/E, and (3) VEH vs CNO treatment in M/D.

Results

Tissue Analysis

DREADD expression was confirmed by examining LHA sections from approximately - 1.20 mm to -3.90 mm posterior to bregma. In these subjects, DREADD expression extended from approximately -2.04 mm to -3.48 mm posterior to bregma. Expression was sparse, with few mCherry-labelled cells identified within each subject. Fibers and processes were slightly more apparent, suggesting successful DREADD targeting in spite of the low number of mCherry-labelled cell bodies. Expression was primarily concentrated in the more anterior and dorsolateral aspects of the LHA and entirely absent in slices beyond -3.48 mm posterior to bregma (Figure 3.1).

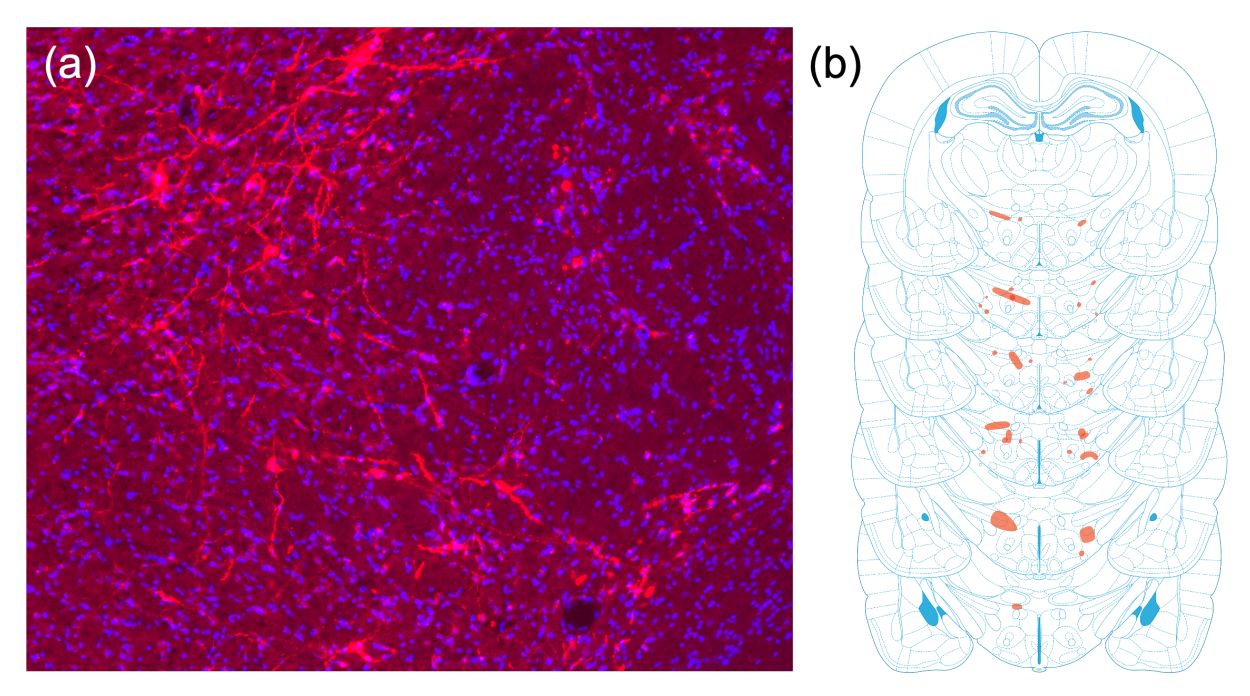


Figure 3.1 DREADD Expression in NAc-projecting LHAa neurons. (a) Representative photomicrograph of mCherry labelled DREADD expression in the LHAa. (b) Heat maps indicate representative DREADD expression (red) throughout the LHAa. Coronal sections modified from Paxinos & Watson 6th edition.

Estrous cycle influences time-dependent food seeking

To determine whether baseline differences in responding occurred due to fluctuating levels of circulating gonadal hormones, we first examined whether responding differed between rats tested in P/E and M/D under VEH treatment. There were no differences in the amount of time rats spent in the food cup (Figure 3.2 a; t=0.090, d=7, p>.05, d=.03) or the overall response rate during the behavioral session (Figure 3.2 b; t=1.08, d=7, p>.05, d=.38). Although rats tested in P/E may appear to respond at a peak rate earlier, there was also no significant difference in peak time between rats tested in P/E and M/D under VEH (Figure 3.2 c; t=1.93, t=7, t=1.95, t=1.98). The repeated measures ANOVA evaluating proportion of peak rate responding

across time revealed both a main effect of time (F=128.51, df=(59, 413), p<.001, η_p^2 =0.95) and a significant interaction of estrous cycle stage and time (F=2.12, df=(59, 413) p<.001, η_p^2 =0.23). Planned comparisons evaluating whether responding differed in M/D and P/E in 1s bins revealed that responding was higher under M/D at 20, 27, 32, 35 and 50s. This suggests that M/D rats continued to respond at a higher level longer than P/E rats after the omission of an expected reward.

Next, I used piecewise growth modeling (PGM) to model the predicted proportion of peak rate responding across time during P/E and M/D. The effects of estrous cycle stage were examined at the mid-point of the pre- and post-peak periods in the overall model. This analysis revealed only significant effects of time on the predicted proportion of peak rate response functions (see supplemental tables S3.1 and S3.2). The overall model, which estimates rate and intercept at the mid-point pre- and post-peak, did not reveal any overall effects of estrous cycle stage.

Although the overall model did not capture estrous cycle effects, modeling the data separately in 5s intervals revealed effects of estrous cycle on the predicted proportion of peak rate responding at 25s, 30s, and 35s. Specifically, after the peak, there was a significant difference in the quadratic rate of change over time (i.e., quadratic slope) based on estrous cycle stage. At each time, the quadratic slope was more negative during M/D compared to P/E. This indicates a significant difference in the rate at which the slope changes over time. The overall slope is also influenced by the linear and cubic slopes, but a difference in the quadratic rate of change can influence how steeply responding decreases post-peak. In this case, M/D animals initially decay high rate responding less quickly than P/E animals, resulting in higher level of

responding lasting longer than in P/E animals. However, as time passes the rate of decrease in M/D accelerates, resulting in a steeper negative slope than in P/E animals (Figure 3.2 e). Because M/D rats are predicted to initially delay decreasing post-peak responding, the level of responding predicted under M/D continued to exceed the level predicted under P/E during this period. This suggests that the predicted response rate in M/D animals may be decreasing more quickly later in the trial in order to "catch up" or normalize back down to the level of responding observed in P/E animals. Altogether, these differences in the rate of change indicate that P/E animals attenuate high rate responding more quickly after the peak than M/D animals, who delay attenuating high rate responding post-peak. These effects agree with the results of the ANOVA, which revealed differences in the magnitude of responding under P/E and M/D selectively after the criterion duration. Together, the piecewise growth model and ANOVA suggest that post-criterion responding is higher under M/D as rats attenuated high level responding post-peak more slowly. In other words, the "stop" function is delayed in M/D rats. Notably, this finding is in line with the general idea of estrogen as an anorexigenic feeding signal (Eckel, 2011). Higher levels of circulating estrogen during P/E may attenuate the motivation of an animal to continue food-seeking after the criterion duration has elapsed.

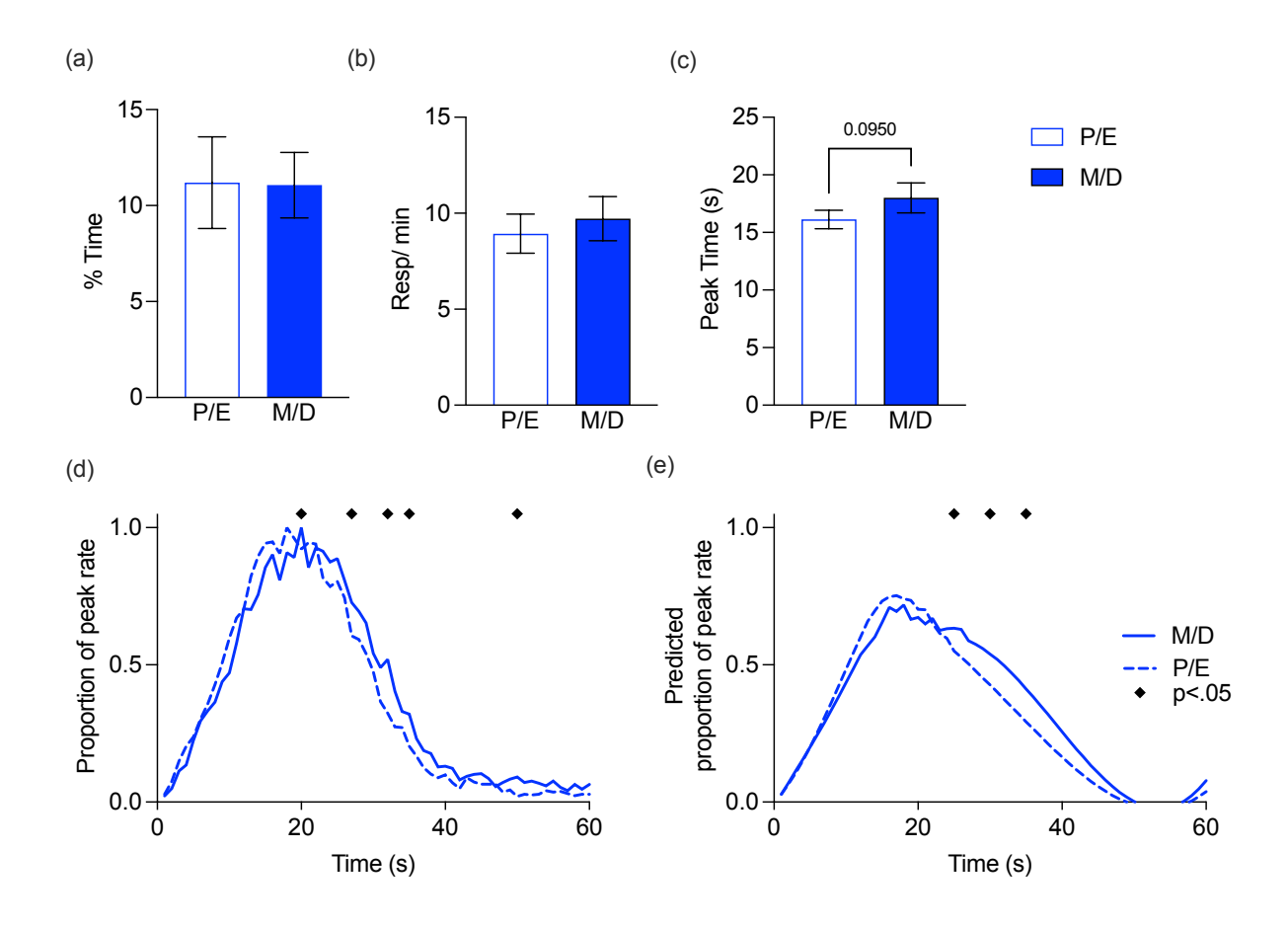


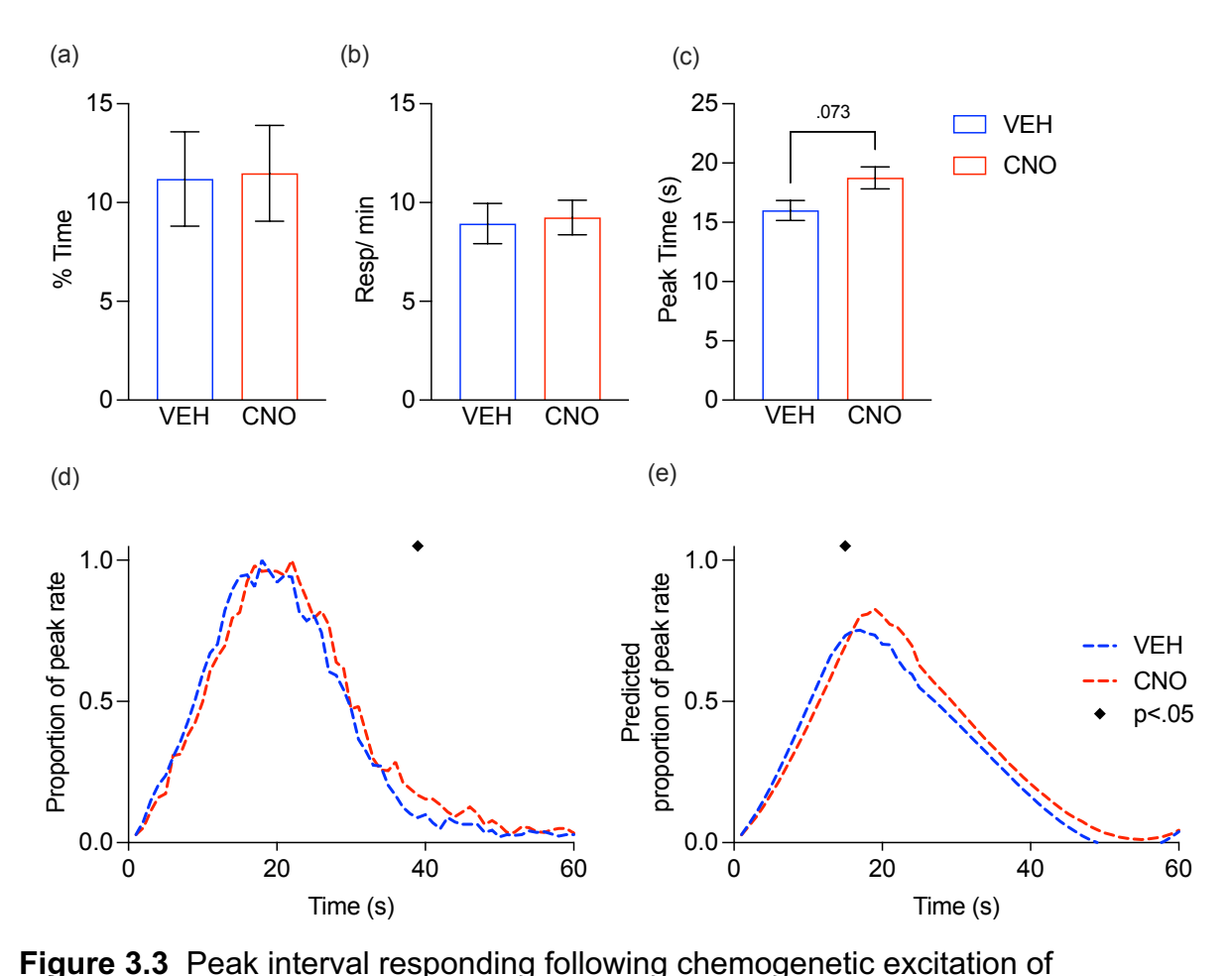
Figure 3.2 Responding in the Peak Interval paradigm across the estrous cycle. (a) The amount of time rats spent in the food cup did not differ based on estrous cycle stage. (b) Rats responded at comparable rates in P/E and M/D. (c) P/E rats respond slightly earlier than M/D rats, but this effect did not reach significance. (d) M/D rats respond at a higher proportion of peak rate than P/E rats after the criterion duration. (e) Piecewise growth modeling indicates that the predicted proportion of peak rate responding is higher post-peak in M/D rats than in P/E rats.

Proestrus/ estrus rats are not sensitive to LHAa^{MCH} →NAc excitation

Due to the higher levels of estrogen present during proestrus and estrus (P/E), I hypothesized that LHAa^{MCH}→NAc neuronal excitation would fail to produce effects on PI responding when rats were tested during P/E. Indeed, there was no effect of CNO-

mediated excitation of LHAa^{MCH} \rightarrow NAc neurons on the amount of time rats spent in the food cup (Figure 3.3; t=.27, df=7, p>.05, d= .10) nor on their response rate across the session (t=.50, df=7, p=.63, d=.18). While rats tended to reach their peak response rate at a later time (i.e., peak time) under CNO, this effect did not reach significance (t=2.11, df=7, p=.073, d=.74).

A repeated measures ANOVA was used to evaluate whether the proportion of peak rate response function differed following VEH or CNO treatment revealed an interaction of drug X time (F=1.65, df=(59, 413, p<.05, η_p^2 =.19), indicating that CNO-mediated excitation of LHAa^{MCH} \rightarrow NAc neurons influenced the timing of motivated responding in the PI task. However, pairwise comparisons revealed that the effect was modest given that the level of responding that occurred was greater under CNO than VEH only at 39s.



LHAa^{MCH}→NAc neurons during P/E. (a) Chemogenetic excitation of LHAa^{MCH}→NAc neurons did not influence the amount of time P/E rats spent in the food cup or (b) response rate during the session. (c) While there was a trend toward a later peak time following chemogenetic excitation of LHAa^{MCH}→NAc neurons in P/E rats, this effect did not reach significance. (d) CNO-treated rats responded at a higher proportion of peak rate after the peak, an effect that was significant only at 39s. (e) Piecewise growth modeling revealed an effect of drug treatment at 15s, where predicted proportion of peak rate responding continued to increase in CNO-treated rats while leveling off in VEH-treated rats.

The predicted proportion of peak rate responding indicated by the overall PGM did not reveal any treatment effects at the pre- and post-peak midpoints (supplemental tables S3.5 and S3.6). However, the 5s analyses revealed a post-peak treatment effect at 15s. At this time, there was a significant interaction of drug treatment (VEH, CNO) and the quadratic rate of change over time. As seen in Figure 3.3 e, the predicted proportion of peak rate responding in CNO-treated continues to increase at this time while the predicted proportion of peak rate responding in VEH-treated rats begins to decay. However, there is no significant effect on the intercept (i.e., level of magnitude) of predicted proportion of peak rate responding, indicating that although the slopes differ, the overall level of responding is not significantly changed by CNO-treatment. Indeed, any effects of CNO treatment are brief, as treatment effects are not revealed at any other time points.

Chemogenetic excitation of LHAa →NAc MCH neurons reduced motivated food-seeking post-peak during M/D

Chemogenetic excitation of LHA^{MCH}→NAc neurons did not influence the amount of time rats spent in the food cup (t=.26, df=7, p>.05, *d*=.09), response rate (t=.55, df=7, p>.05, *d*=.20), or peak time (t=1.136, df=7, p>.05, *d*=.40). The ANOVA evaluating differences in the proportion of peak rate response function following drug treatment revealed a significant interaction of drug x time (F=1.40, df=(59, 413), p<.05, η_p²=.17), indicating that the effect of drug treatment varied as a function of time within the trial. Pairwise comparisons revealed significant effects of drug treatment in six 1s bins, at 17, 20, 25, 28, 29, and 32s (p's<.05). While responding was significantly higher under CNO than VEH at 17s, responding was significantly lower under CNO than VEH at 20, 25, 28,

29, and 32s. Notably, these latter times all occurred after the mean peak time in both VEH and CNO-treated rats (18 and 19.125s, respectively). In other words, post-peak responding was significantly reduced following CNO-mediated excitation of LHAa^{MCH} → NAc neurons when rats were tested during M/D.

Notably, the overall PGM analyzing the predicted proportion of peak rate response function also revealed a post-peak effect of treatment in M/D rats. Specifically, drug treatment interacted with the post-peak cubic rate of change over time at the post-peak mid-point (~40s). In addition, the 5s analyses also revealed post-peak treatment effects in M/D animals. There was a significant interaction of treatment x the quadratic rate of change at 30 and 35s (p's <.05). In addition, there was a significant interaction of treatment x the cubic rate of change at 35 and 40s (p's <.05). Initially, post-peak predicted responding decreases at a faster rate in CNO than in VEH-treated rats. However, the rate of decrease in VEH-treated rats accelerates as the trial continues, resulting in comparable responding predicted under VEH and CNO at the end of the trial.

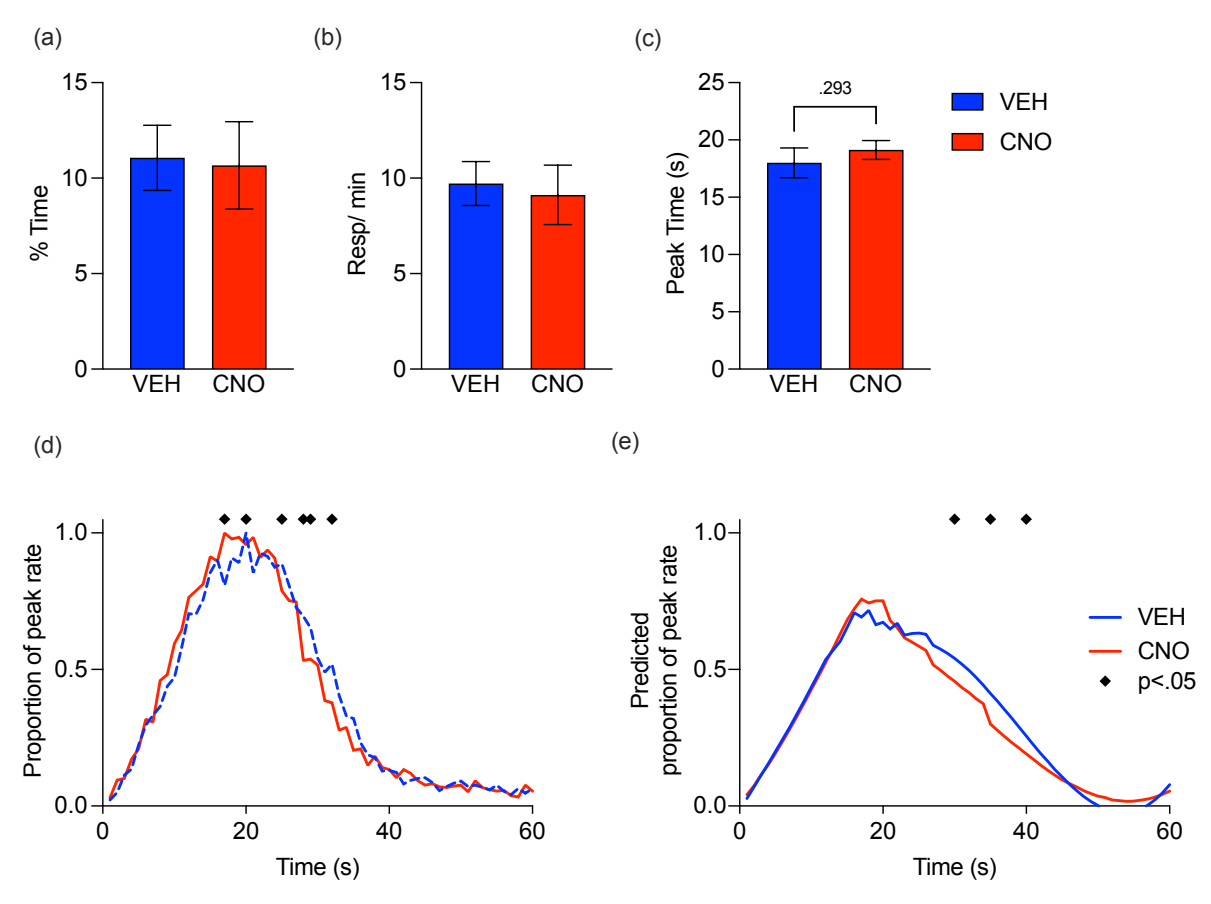


Figure 3.4 Peak interval responding following chemogenetic excitation of

LHAa^{MCH}→NAc neurons during M/D. Chemogenetic excitation of LHAa^{MCH}→NAc neurons did not influence the amount of time M/D rats spent in the food cup or (b) response rate during the session. (c) There was no effect of chemogenetic excitation of LHAa^{MCH}→NAc neurons on peak time in M/D rats. (d) CNO-treated rats responded at a higher proportion of peak rate pre-peak at 17s, and a lower proportion of peak rate after the peak, at 20, 25, 28, 29 and 32s. (e) Piecewise growth modeling revealed an effect of drug treatment at 30, 35, and 40s.

Progressive ratio responding is unaffected by LHAa^{MCH} → NAc neuronal excitation

To further evaluate the effects of LHAa^{MCH} → NAc neuronal excitation on motivation, I also evaluated the influence of these cells on motivated responding in a

progressive ratio task. Unlike the PI paradigm, in which time-dependent effects of LHAa^{MCH} → NAc neuronal excitation were revealed in the post-peak period, there were no effects of LHAa^{MCH} → NAc neuronal excitation on PR responding. PR sessions continued for 5 hours or until a rat failed to make a response for 15 minutes, whichever came first.

First, I examined whether PR responding differed based on estrous cycle under baseline, vehicle conditions. Estrous cycle did not affect how long vehicle-treated rats spent in a session before timing out (t=.06, df=4, p>.05, d=.03) or how many nosepokes they made during the session (t=.23, df=4, p>.05, d=.11). As in the PI task, there were also no effects of chemogenetic excitation of LHAa^{MCH} \rightarrow NAc neurons on PR responding. P/E rats did not differ in the length of sessions (t=.16, df=4, p>.05, d=.07) nor in the number of responses they made (t=.32, df=4, p>.05, d=.14) during a session. There was also no effect of drug on PR responding in M/D rats: these rats also did not differ in session time (t=.37, df=4, p>.05, d=.16) or number of nosepokes (t=.40, df=4, p>.05, d=.18). There were also no effects of estrous cycle or drug treatment on the probability of survival in the task (χ^2 =.13, df=3, p>.05). Thus, there were no effects of chemogenetic excitation of LHAa^{MCH} \rightarrow NAc neurons on progressive ratio responding.

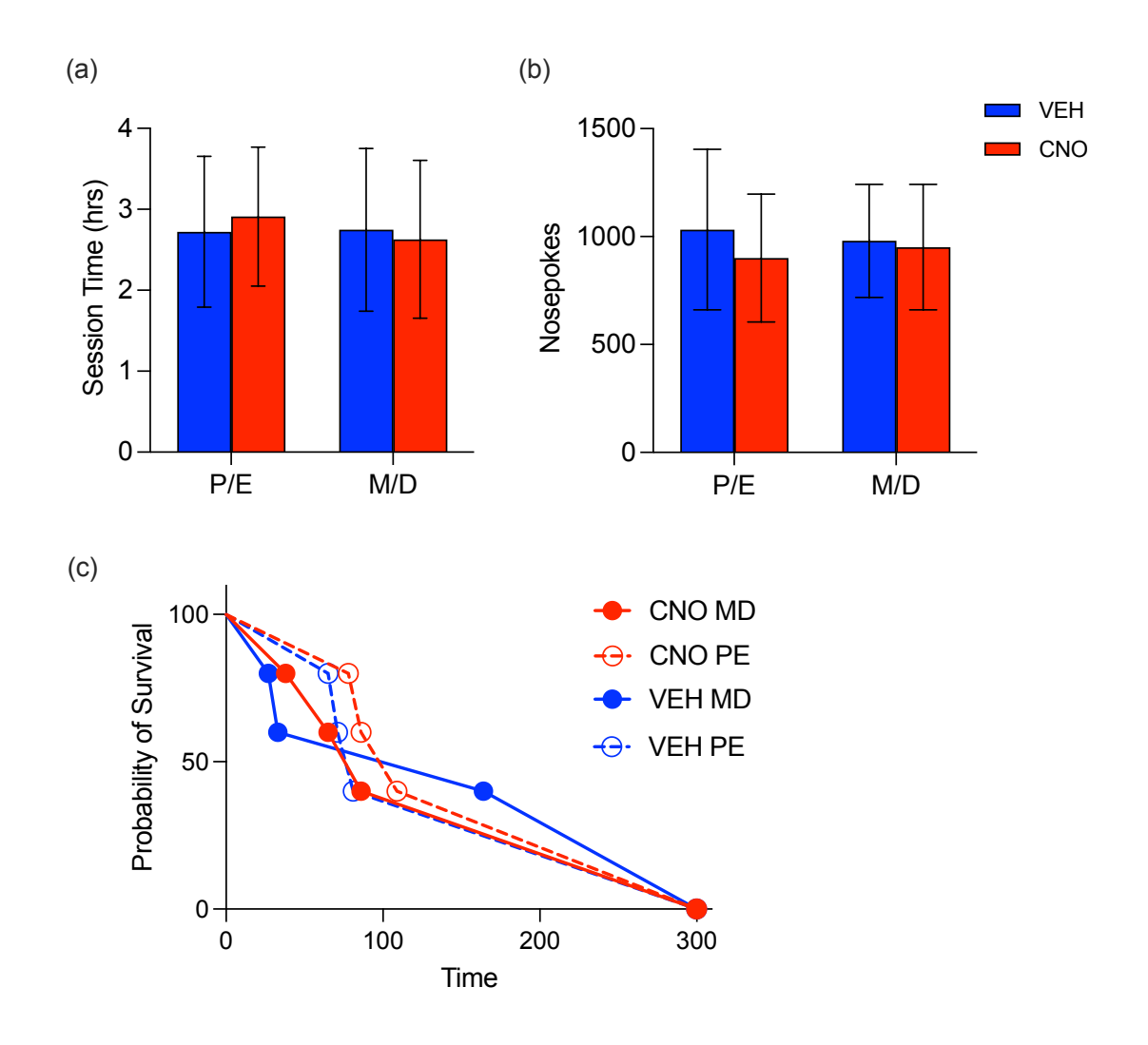


Figure 3.5 Progressive ratio responding following CNO-mediated excitation of NAc-projecting LHAa^{MCH} neurons. (a) There were no differences in session time (hours) following VEH or CNO treatment in M/D and P/E. (b) There was also no effect of estrous cycle stage or drug treatment on the number of nosepokes rats made during sessions. (c) The probability of survival in the task was also unaffected by estrous cycle stage or drug treatment.

Discussion

Summary of results

In this chapter, I examined whether projections from LHAaMCH neurons to the NAc could influence motivated responding in the peak interval (PI) task, specifically through alterations of the "stop" function. Given that little is known about estrous cycle effects on interval timing, I also examined baseline effects of the estrous cycle on PI responding. Indeed, even at baseline, estrous cycle stage influenced peak interval responding: rats attenuated high rate responding more abruptly after the criterion duration when tested under vehicle (VEH) during P/E compared to M/D. However, there was no significant effect of estrous cycle stage on peak time, indicating that post-criterion responding was altered without affecting time perception, per se. This decrease in post-criterion responding indicates a decrease in motivation to continue seeking an omitted food reward during P/E, when circulating levels of estrogen are highest. This effect is thus in line with the general anorexigenic effect of estradiol, which is marked by decreased food consumption driven by a decrease in meal size (Eckel, 2011). Despite this, rats reached a peak response rate at comparable times during P/E and M/D, and their overall amount of responding did not differ based on estrous cycle stage. This suggests that estrous cycle influences the timing of motivated behavior within a trial, without necessarily affecting time perception or the overall response rate. Likewise, estrous cycle stage did not influence responding in the progressive ratio (PR) task. Taken together, these findings suggest that estrous cycle may subtly modulates the timing of motivated behavior without influencing willingness to respond.

While estrogen has been reported to increase clock speed in OVX rats, these effects are acute and transient, indicating that any clock speed effects are quickly compensated for by an updating reference memory system (Pleil et al., 2011; Sandstrom, 2007). Indeed, prolonged estrogen administration in OVX rats failed to produce a change in time perception (Ross & Santi, 2000), although it did reduce discrimination accuracy in OVX females. In contrast to the effects of estrogen on time perception, effects of EB on motivation may be able to more robustly and persistently influence the timing of responding. Thus, estrous cycle effects captured across multiple tests – as in the case of the present study – may more readily reveal motivational rather than timing effects. That the "stop" function is influenced by circulating gonadal hormones in the present study may thus reflect an estrogen-mediated influence on motivation to continue responding after the omission of an expected sucrose reward.

In line with this, Gur et al. (2019) suggest that sex differences in interval timing may arise from differences in incentive motivation between males and females rather than time perception, *per se* (Gür et al., 2019). Although this group observed no differences in time perception in mice tested in the PI paradigm, they report that female mice began high rate responding later than male mice, indicating a delayed "start" function. Thus, the "start" function was selectively modified by sex, with females displaying lower motivation to initiate high rate responding than males (Gür et al., 2019). Similarly, Pleil et al. (2011) also report that male rats respond earlier than females under baseline conditions. However, in this case the effects of sex are interpreted as true timing effects, with the delay in females attributed to a prolonged reference memory for time (Pleil et al., 2011). This is consistent with reports from the human literature, in

which women tend to overestimate durations (Block et al., 2000; Morita et al., 2005; Williams, 2011). Altogether these findings indicate that ovarian hormones may influence the timing of motivated behavior through multiple mechanisms (Pleil et al., 2011).

Interestingly, when LHAa^{MCH} NAc neurons were excited during P/E, the opposite effect was observed: rats tended to respond later under CNO, resulting in a subtle increase in responding post-criterion. Although this effect was limited, it perhaps suggests an ability of MCH neurons to increase motivated food intake when motivation for food is otherwise low (i.e., during P/E). However, given that estradiol inhibits the actions of MCH, any effect of MCH during P/E is likely blunted by high levels of this ovarian hormone.

On the other hand, when LHAa^{MCH}→NAc neurons were excited during M/D, post-criterion responding was consistently decreased, an effect that is similar to our previous findings which revealed a role for LHA^{MCH} neurons in determining post-criterion responding during M/D. Recall that non-projection-specific excitation of LHAa^{MCH} neurons prolonged high rate responding after the omission of an expected sucrose reward, suggesting an increase in motivation and delay in the "stop" function. I thus hypothesized that excitation of LHAa^{MCH}→NAc neurons during M/D would replicate this finding and prolong high rate responding after the omission of sucrose. However, in contrast to my hypothesis, projection-specific chemogenetic excitation of LHAa^{MCH}→NAc neurons decreased post-criterion responding by accelerating the "stop" function. This indicates a decrease in motivation to continue working for an omitted food reward, and suggests an inhibitory action of these neurons on food-seeking.

Although I initially hypothesized that this projection-specific manipulation would increase motivation and result in increased responding post-peak, the observed decrease in responding is not altogether surprising. For example, the NAc is also important for behavioral inhibition, which includes the inhibition or attenuation of ongoing motivated behaviors (Ambroggi et al., 2011; Lafferty et al., 2020; Zamorano et al., 2014). Although the PI paradigm is not typically described in terms of behavioral inhibition, it inherently involves the inhibition of high rate responding based on the temporal context of the task. Animals typically inhibit high rate responding prior to the period of time when reinforcement is most likely, respond at a high rate around the criterion time when reinforcement might occur, and then inhibit responding again after they perceive that too much time has elapsed for reinforcement to occur. Thus, the "break-run-break" pattern of responding observed during probe trials could instead be described as an "inhibit- allow- inhibit" pattern of behavioral control informed by the temporal constraints of the task. From this perspective, the "start" and "stop" function of interval timing would reflect a release from inhibition (the "start") and return to inhibition (the "stop"). In the present study, LHAa^{MCH}→NAc neuronal excitation resulted in an altered "stop" function by rapidly decreasing post-peak responding, perhaps by increasing inhibition of post-peak responding.

These results suggest that NAc-projecting LHAa^{MCH} neurons may guide behavioral state transitions, an effect which is in line with the role of the LHA as an integrative relay station and the NAc as an important region involved in action selection (Berthoud & Münzberg, 2011; Floresco, 2015; Stuber & Wise, 2016). LHAa^{MCH} neurons may contact the NAc to coordinate food-related behaviors. Indeed, the "stop" function

may represent an inhibition of high rate responding mediated by the action of GABAergic median spiny neurons (MSNs) in the NAc (Ambroggi et al., 2011; Floresco, 2015; Lafferty et al., 2020). A delay in the "stop" function could thus be mediated by inputs onto these MSNs, which could originate from MCH neurons in the LHAa neurons. Given that more general excitation of LHAa^{MCH} neurons delayed the "stop" function consistent with a decrease in behavioral inhibition, it is possible that additional LHAa^{MCH} neurons not captured in this projection-specific approach instead promote prolonged responding. This could be accomplished either by indirectly modulating the inhibitory control of the NAc or through actions in another target region. Regardless, these data indicate that LHAa^{MCH} neurons modulate the "stop" function to prolong or attenuate motivated behavior. While this phenotype was expressed in a time-dependent food-seeking paradigm, the general effect of altering the duration of feeding related behaviors – like burst or meal size – is in line with the typical mechanism through which MCH promotes feeding (Baird et al., 2006; Messina et al., 2006; Sherwood et al., 2015).

Consistent with our previous findings, excitation of NAc-projecting LHAa^{MCH} neurons also influenced motivated responding predominantly during M/D. While the direction of this effect was opposite to that observed following non-projection-specific excitation of LHAa^{MCH} neurons, the estrous cycle phase is consistent: neuronal excitation of LHAa^{MCH} neurons produces motivational effects only when rats are tested during M/D. As described previously, this likely reflects a vulnerability produced by comparably low levels of estrogen than what are present during P/E, when the effects of these neurons appear to be attenuated. The influence of estradiol on LHAa^{MCH}→NAc neuronal excitation during PI responding is examined in Chapter 4.

Limitations

As in chapter 2, mCherry labelling of DREADD expression in the LHAa was limited to small number of neurons and primarily visible through evidence of mCherry-labelled fibers of passage. Again, it was difficult to perform detailed histological analyses on tissue in which the mCherry fluorophore was difficult to visualize, even after amplification. However, unlike the previous study, behavioral effects were clearly apparent following CNO treatment in these animals. This suggests that the CNO-mediated excitation of this limited number of LHAa neurons was sufficient to influence the "stop" function. In addition, the effect of this neuronal excitation was consistent with previous findings indicating that LHAa^{MCH} neurons influence that the "stop" function only during M/D.

Conclusion

CNO-mediated excitation of LHAa^{MCH}→NAc neurons accelerates the "stop" function during M/D. This finding is consistent with previous work in our lab, which indicated that non-projection specific excitation of LHAa^{MCH} neurons also influence the "stop" function during M/D. However, excitation of LHAa^{MCH} neurons prolonged high rate responding during M/D by delaying the "stop" function, excitation of only the NAc-projecting neurons within this population instead accelerates the "stop" function. This indicates that LHAa^{MCH} neurons may bidirectionally influence motivational processes influencing the decision when to "stop" motivated behaviors. While a small subset of these neurons that project to the NAc decrease motivated responding after the omission of an expected reward, LHAa^{MCH} that do not project directly to the NAc may instead increase motivated responding. Altogether, this data supports a role for LHAa^{MCH}

neurons in gating motivated behavior, particularly after the omission of an expected reward after a criterion duration. Thus, these neurons may be incorporating temporal cues to guide motivated behavior.

CHAPTER 4: Estrogen is necessary for LHAa^{MCH}→NAc neuronal effects on postcriterion responding

Abstract

Previously, I demonstrated that Nucleus Accumbens (NAc) projecting Melanin Concentrating Hormone (MCH) neurons in the anterior Lateral Hypothalamic Area (LHAa) decrease time-dependent motivated responding in the PI task during periods of the estrous cycle when estrogen levels are typically lower. Specifically, chemogenetic excitation of LHAa^{MCH} → NAc neurons attenuated responding during the "stop" function in rats tested during metestrus/ diestrus (M/D). In contrast, when rats were tested when ovarian hormone levels peak during proestrus and estrus (P/E), chemogenetic excitation of LHAa^{MCH} \rightarrow NAc neurons did not influence the "stop" function. This suggests that circulating ovarian hormones interfere with the excitation of LHAaMCH > NAc neurons to blunt their effects. Although multiple hormones fluctuate across the estrous cycle, estrogen is known to influence both interval timing and MCH-mediated feeding behaviors (Eckel, 2011; Panfil et al., 2023; Ross & Santi, 2000; Sandstrom, 2007; Santollo & Eckel, 2008, 2013). Estradiol attenuates the orexigenic effects of MCH, which suggests that higher concentrations of circulating estrogen during P/E might interfere with the effects of LHAa $^{MCH} \rightarrow NAc$ neuronal excitation. In the present study, I ovariectomized adult female rats to remove the primary source of endogenous estrogen. I then tested OVX rats in the PI paradigm with and without estrogen (17-Bestradiol benzoate; EB) replacement before chemogenetically exciting LHAaMCH -> NAc neurons. In OVX rats, estradiol replacement delayed the "start" of high rate responding in the PI task, without influencing the "stop" function or peak time. This suggests that EB alone reduced motivation to respond for a sucrose reward and delayed when rats initiated high rate responding. Interestingly, in OVX rats that were pretreated with oil, chemogenetic excitation of LHAa^{MCH} → NAc neurons did not influence PI responding. Instead, in contrast to my hypothesis, chemogenetic excitation of LHAa^{MCH} → NAc neurons decreased motivated food-seeking only in EB pretreated rats. This suggests that EB is necessary for LHAa^{MCH} → NAc neurons to influence post-criterion responding, but that the timing or source of estradiol (i.e., high levels of endogenous estrogens in P/E or following administration of exogenous EB) can influence how these systems interact. Additionally, EB may act in concert with other ovarian hormones to modulate the influence of LHA^{MCH} neurons in intact, cycling rats.

Introduction

LHAa^{MCH} neurons alter the "stop" function when rats are tested in the peak interval (PI) task during metestrus/ diestrus (M/D). In the previous chapter, I revealed that projection-specific excitation of LHAa^{MCH} → NAc neurons accelerated the "stop" function selectively when rats were tested during M/D. While circulating levels of ovarian hormones – including luteinizing hormone (LH), follicle stimulating hormone (FSH), progesterone (P) and estrogen (EB) – are typically highest during proestrus and early estrus (P/E), M/D is characterized by relatively low levels of these fluctuating hormones (Goldman et al., 2007). Estrogen, in particular, is of interest because of its inhibitory influence over MCH (Messina et al., 2006; Mystkowski et al., 2000; Santollo & Eckel, 2008, 2013). Thus, the absence of high levels of estrogen during M/D may create a vulnerability for LHAa^{MCH} → NAc neurons to influence motivated behavior beyond the level typically observed during P/E. Thus, in order to isolate the effects of estrogen, in this chapter I ovariectomized (OVX) adult female rats prior to training and testing in the PI paradigm. Rats were then tested with and without estrogen replacement to examine both baseline effects of estrogen on PI responding as well as its influence on the chemogenetic excitation of LHAa^{MCH} → NAc neurons.

Although sex differences in interval timing procedures are apparent (M. Buhusi et al., 2017; Gür et al., 2019; Williams, 2011), few studies have directly examined the influence of ovarian hormones (Morita et al., 2005; Morofushi et al., 2001; Panfil et al., 2023), or estradiol on time perception (Pleil et al., 2011; Ross & Santi, 2000; Sandstrom, 2007). In interval timing tasks, acute estrogen replacement via 17-β-estradiol (EB) in OVX rats shifts the proportion of peak rate response function to the left,

consistent with an increase in clock speed (Pleil et al., 2011; Sandstrom, 2007). This effect occurs rapidly and acutely. As such, it suggests an abrupt increase in the accumulation rate of striatal DA which in turn increases clock speed (Meck, 1996; Sandstrom, 2007). Indeed, like DA agonists, EB treatment appears to produce transient effects on clock speed, prior to the formation of an updated internal reference memory for time under this altered clock speed (Pleil et al., 2011). Similarly, when EB is administered only once prior to PI testing, effects dissipate by 72 hours later (Sandstrom, 2007). These rapid effects of EB suggest that they are mediated by nongenomic mechanisms of EB in the striatum (Becker, 1990b; Grove-Strawser et al., 2010; Micevych & Mermelstein, 2008).

In contrast to the rapid effects of estrogen on interval timing, effects of EB on food intake can occur over multiple timeframes, including in both a tonic and phasic manner (Eckel, 2004, 2011; Varma et al., 1999). The phasic effects of estrogen can be observed in cycling rats who display a decrease in food intake during estrus, after the periovulatory release of estrogen has peaked and fallen following proestrus (Eckel, 2004, 2011). Thus, this phasic decrease in food intake actually occurs during a period of the estrous cycle when circulating estrogens are lower (Eckel, 2004, 2011). Both phasic and tonic effects of EB can be observed in OVX rats treated with exogenous EB as part of a hormone replacement regimen (Asarian & Geary, 2002; Geary & Asarian, 1999). However, the anorexigenic effects of estradiol on food intake primarily occur after a delay of 36 – 40 hours, indicating a phasic effect (Eckel, 2011).

Estrogen exerts its influence on food intake indirectly, primarily by influencing signals that control meal size (Butera, 2010; Eckel, 2004, 2011). Thus, as an orexigenic

neuropeptide that promotes consumption by increasing meal size, MCH is a candidate peptide to mediate the effects estrogen on food intake. Indeed, others have examined interactions between MCH and estrogen in both intact and OVX rats (Murray et al., 2000; Santollo & Eckel, 2008, 2013) and reported that circulating estrogen modulates the MCH system. While mRNA of the pMCH promoter is detected in comparable levels during proestrus and diestrus in intact rats (Murray et al., 2000), both MCH and MCH1R protein are decreased during proestrus (Santollo & Eckel, 2013). In OVX rats, exogenous EB reduces both pMCH mRNA as well as the MCH and MCH1R protein (Murray et al., 2000; Santollo & Eckel, 2013), indicating that estrogen typically inhibits the MCH system. Notably, the behavioral effects of EB on MCH occur through phasic effects: when EB is replaced on a four day, cyclic regimen of two days of EB injection followed by two days of washout, the orexigenic effects of MCH are attenuated on the fourth day of this cycle (Santollo & Eckel, 2008). Likewise, the orexigenic effects of intra-NAc infusion of MCH are attenuated on the fourth day of EB replacement in this cycle (Terrill et al., 2020). Although this does not exclude rapid, nongenomic effects of EB on MCH, these findings indicate that at least some of the effects of EB on MCH occur in a phasic manner, likely due to genomic effects.

In keeping with cyclic hormone regimens that replace estrogen rhythmically across four to five days, I administered EB 30 minutes prior to the behavioral session on two consecutive days, followed by a two day washout period. In order to increase the probability that EB replacement would influence MCH signaling in the PI task, I chose to time the chemogenetic excitation of LHAa^{MCH}→NAc neurons with the second day of EB administration. This would enable the test to capture both slower-acting genomic effects

from the previous day of EB priming, as well as any acute, nongenomic effects of EB administration. Furthermore, to enable within subjects testing but ensure that no phasic or lingering effects of estrogen were present during oil tests, all rats received oil pretreatment tests prior to EB testing.

Given that EB has been reported to increase clock speed and shift the proportion of peak rate response function to the left, I hypothesized that EB treatment would produce effects on PI responding under baseline, vehicle conditions, perhaps by initially shifting the response function leftward before renormalizing following repeated testing. In addition, because the effects of LHAa^{MCH} →NAc neuronal excitation were pronounced during M/D but not P/E, I hypothesized that LHAa^{MCH} →NAc neuronal excitation would influence post-criterion food-seeking in oil-treated OVX – but not EB-treated OVX – rats. In line with the inhibitory effects of EB on MCH, I expected that EB pretreatment would attenuate or block the effects of LHAa^{MCH} → NAc neuronal excitation.

Materials & methods

Subjects

Eight adult female Sprague-Dawley rats (*Envigo, Haslett, MI, USA*; 12-weeks of age at arrival) were pair housed in groups of 2-3 in standard, plexiglass cages with metal tops. Rats were maintained on a standard 12-hr light-dark cycle (lights on 7:00; lights off 19:00), with *ad libitum* access to Teklad diet #8912. Rats received ≥7 days of acclimatization to the vivarium before experimental manipulations began. Following the period of habituation, rats were handled daily for 2-3 days before undergoing surgical procedures. Post-op, rats were briefly singly housed while they received daily health monitoring. Rats were pair housed with their original cage mate once postoperative

bodyweight recovered and surgical incisions appeared healed (≤7 days). Rats continued to be pair-housed throughout all behavioral experiments. All manipulations were conducted in compliance with the Institutional Animal Care and Use Committee, Michigan State University.

Surgical procedures

Stereotaxic Viral Infusion and Cannulation

Under isoflurane anesthesia, subjects received bilateral infusions of the retrograde AAV2(retro)-eSYN-EGFP-T2a-icre-WPRE and a cre-dependent, excitatory DREADD AAV2-DIO-rMCHp-hM3D(Gq)-mCherry to the NAc and to the LHAa, respectively as described in Table 4.1. In contrast to surgical procedures described in Chapter 3, rats received an additional infusion of 0.25 µl of the cre-dependent, excitatory DREADD virus into the LHAa to increase the probability of successful DREADD expression.

Table 4.1 Viral approach to selectively target LHAa^{MCH} neurons that project to the NAc in OVX rats.

Dual Virus Approach			
Virus	Target	Infusion coordinates	
AAV2(retro)-eSYN-EGFP-T2a-icre-WPRE 0.3 μl / infusion	NAc Shell	+1.1 A.P., ±0.8 M.L., −7.5 D.V.	
AND			
AAV2-DIO-rMCHp-hM3D(Gq)-mCherry 0.5 μl / infusion #1 0.25 μl / infusion #2	LHAa-MCH	#1: -2.12 A.P., ±2.1 M.L., -8.4 D.V. And #2: -2.40 A.P., ±2.1 M.L., -8.4 D.V.	

Ovariectomy & Hormone Replacement

Immediately following completion of the viral infusion surgery, rats were moved from the stereotaxic set-up to a standard nosecone to maintain anesthesia under

isoflurane gas. Flanks were shaved and sterilized. Bilateral incisions were made, and the fat pad and ovary were identified and moved out of the body cavity. Fallopian tubes were clamped, and the ovary was removed via cauterization. Muscle incisions were closed with interrupted absorbable sutures; skin was closed with surgical staples and covered with triple antibiotic cream. Rats were treated with 2 mg/ kg meloxicam to reduce post-operative pain. To confirm complete ovariectomy, estrous cycle tracking was performed as previously described, beginning during PI sessions. Unfortunately, one rat continued to display evidence of cyclicity and was excluded.

OVX rats were trained in the absence of hormone replacement. During behavioral testing, rats received hormone (17- β -estradiol benzoate, EB; 5 μ g/ 0.1ml sesame oil) or control (sesame oil, 0.1 ml) treatment via subcutaneous (s.c.) injections 30 minutes prior to the behavioral session. Oil or EB was administered in four-day cycles: two consecutive days of oil or EB pretreatment, followed by a two-day washout period. Tests sessions, in which animals also received either vehicle (0.2M PBS) or clozapine-N-oxide (CNO; 0.3 mg/ kg) prior to the behavioral session, occurred during the second day of hormone/ oil treatment during each four-day cycle. Oil tests (2x VEH, 2x CNO) were performed first.

Behavioral Paradigm

Following recovery from viral infusion and food restriction to 90% baseline weight, subjects received training in the Peak Interval (PI) paradigm, as described in Chapter 2. All training and testing procedures during Phase 1 and Phase 2 were identical to those described in Chapter 2. Training occurred in the absence of hormone replacement. Beginning on the sixteenth session of PI training, rats began receiving the

first of four oil treatment cycles, in which rats were primed with oil (0.1ml sesame oil) 30 min prior to the behavioral session for two consecutive days, then allowed two days of washout. The same cyclic regimen was followed for 17-β-estradiol (EB; 5 μg EB/ 0.1ml sesame oil) replacement. Chemogenetic excitation of LHAa^{MCH} neurons occurred during the second day of oil or hormone replacement (i.e., 24 hours after the first dose and 30 minutes after second does). Although the order of drug treatment (VEH or CNO) was counterbalanced, all rats received oil tests prior to EB tests to avoid unintended effects of EB on subsequent oil tests.

Histology

Vaginal cytology was performed in ovariectomized rats to confirm cessation of the estrous cycle. Cytology was performed as described in Chapter 2. Although rats were not cycling, sample collection continued throughout behavior to ensure that rats were handled in a consistent manner regardless of whether they were OVX or intact. Perfusion, tissue collection, and analysis were performed as described in Chapter 2.

Results

Histology

Complete ovariectomy was confirmed by performing vaginal lavages in OVX rats and verifying a lack of round or cornified epithelial cells present within the sample over a period of at least four consecutive days. While the lack of estrous cycles was quickly confirmed, daily lavages continued throughout testing to ensure that rats were handled in a manner consistent with previous cohorts of intact, cycling animals. Interestingly, cyclic replacement of EB produced changes in vaginal epithelial cells even after rats had lacked changes in these cells for a period of several weeks. While EB replacement

alone is not sufficient to fully recapitulate the profile of fluctuating ovarian hormones in intact animals, this treatment has been reported to alter vaginal epithelial cells in OVX rats (Montes & Luque, 1988) and in the present study led to a qualitative increase in the proportion of round epithelial cells, particularly after multiple cycles of EB replacement.

Bilateral DREADD expression was confirmed in each of n=7 adult OVX females. In this group, the addition of a second LHA infusion of the cre-dependent pMCH driven DREADD resulted in robust expression from approximately -1.92 to -3.72 mm posterior to Bregma.

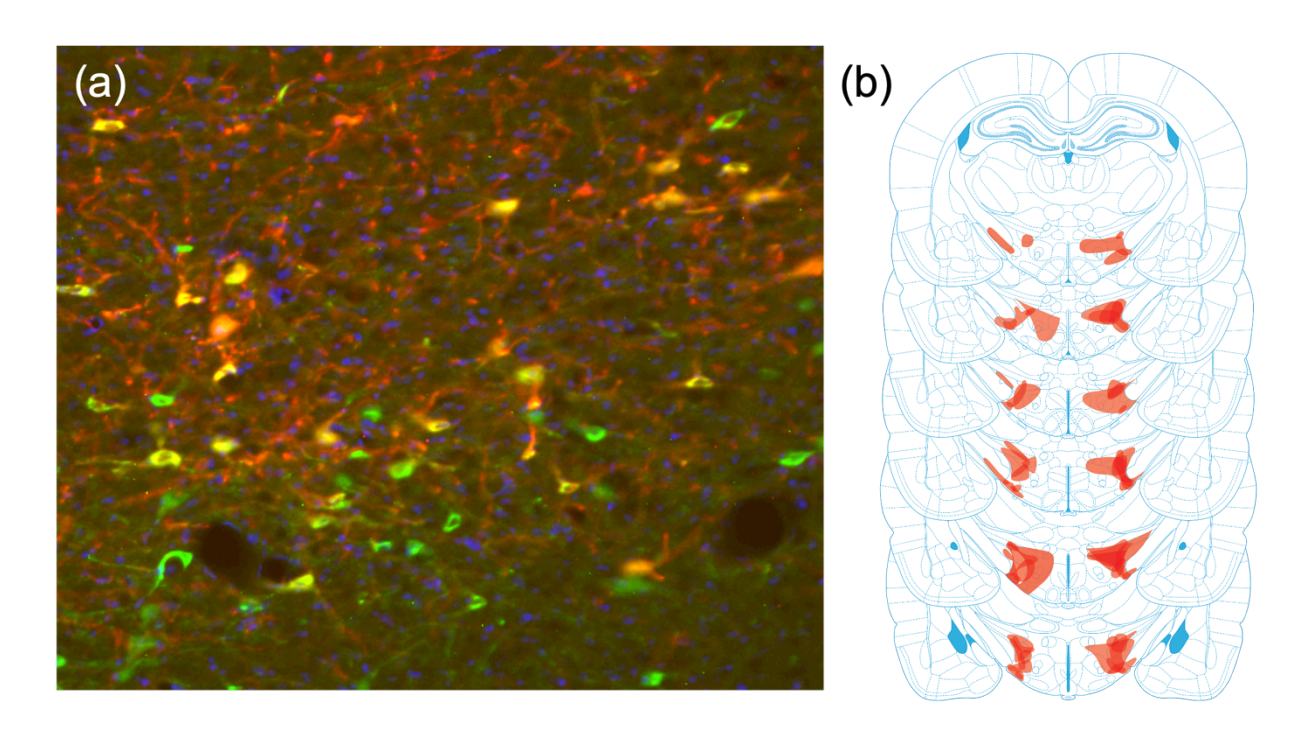


Figure 4.1 DREADD Expression in NAc-projecting LHAa neurons of OVX animals. (a) Representative photomicrograph of mCherry labelled DREADD expression in the LHAa (red) and cells expressing the MCH protein (green); colocalization is indicated in yellow/ orange. (b) Heat maps indicate representative DREADD expression (red) throughout the LHAa. Coronal sections modified from Paxinos & Watson 6th edition.

Peak Interval responding is influenced by estradiol

To determine whether estradiol influenced PI responding in ovariectomized (OVX) rats, I first examined whether responding differed when OVX rats were tested under control vehicle (0.2M PBS) conditions following oil (0.1 ml sesame oil) or estradiol (5 μ g/ 0.1 ml oil) pretreatment. There were no significant effects of hormone replacement on the amount of time rats spent in the food cup (t=2.2, df=6, p=.07, d=.84), response rate (t=.60, df=6, p>.05, d=.23) or peak time (t=.81, df=6, p>.05, d=0.31). Despite not affecting these overall measures of responding or the accuracy of time perception, hormone replacement in adult OVX rats delayed the "start" function by significantly reducing the proportion of peak rate responding that occurred pre-peak following EB pretreatment. In addition to a main effect of time (F=156, df=(59, 354), p<.001, η p²=.96), there was also a trend toward a main effect of estrous in these rats (F=5.45, df=(1, 6), p=.058, η p²=.48).

In addition, there was a significant interaction of estrous cycle stage and time (F=2.74, df=(59, 354), p<.001, η_p^2 =.31), indicating that time and estrous cycle stage interact to guide responding. Pairwise comparisons using a Bonferroni correction were computed at each of sixty 1s time bins to identify when responding significantly differed between oil and EB-treated rats. Responding significantly differed at: 4-12, 15, 18, 22 and 59s (p's <.05). Notably, responding was significantly lower following EB pretreatment before the criterion (i.e., at 4-12, 15, and 18s) but significantly higher following EB pretreatment after the criterion at 22s.

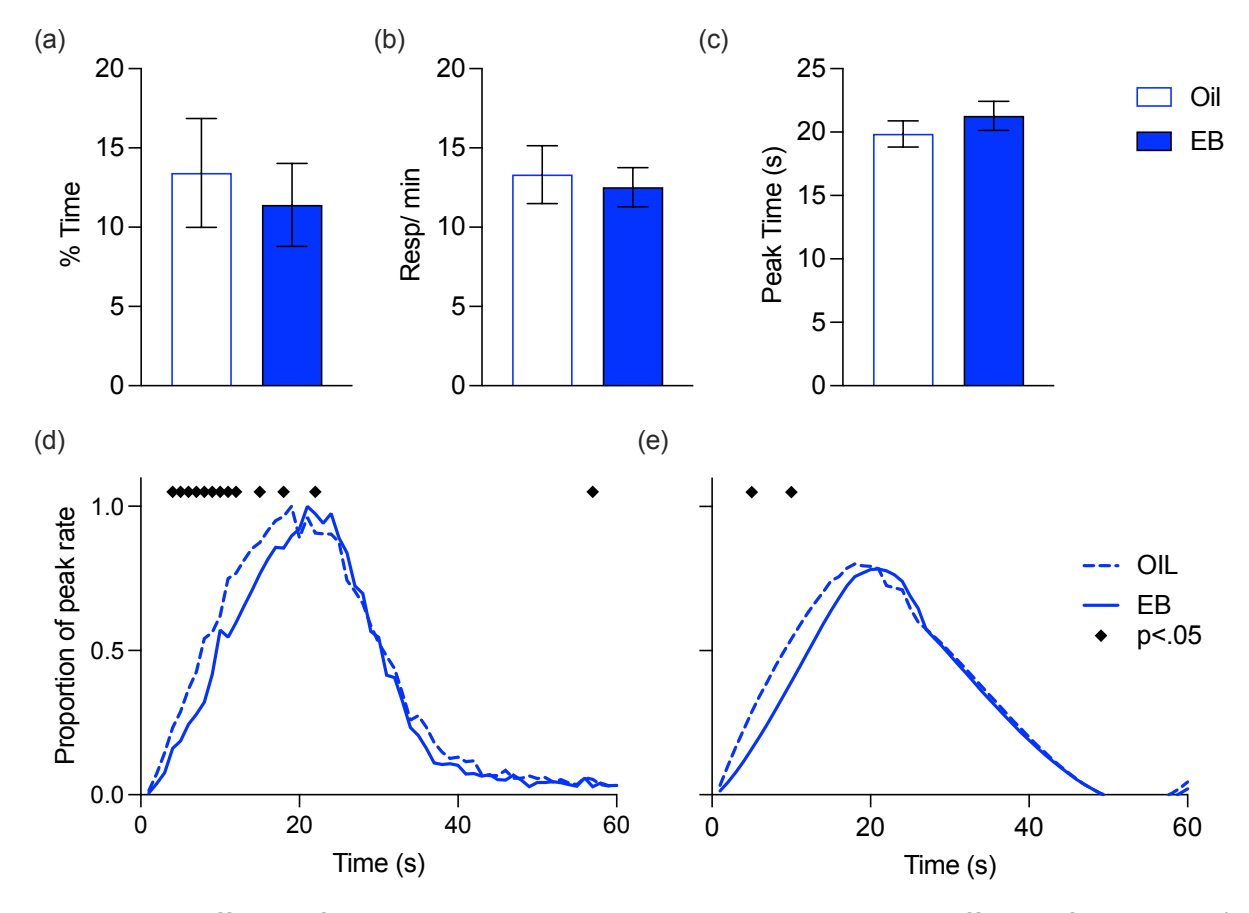


Figure 4.2 Effects of hormone on PI responding. There were no effects of hormone (oil control or estradiol, EB, replacement) in adult OVX rats on overall measures of responding during the behavioral session, including (a) amount of time spent in the food cup or (b) response rate. (c) EB replacement in adult OVX rats also did not significantly change peak time. (d) The "start" of the proportion of peak rate response function was shifted rightward in EB-treated rats relative to oil-treated controls. (e) Piecewise growth models of the predicted proportion of peak rate response function following oil or EB pretreatment confirm that the "start" function is delayed in EB treated rats.

In contrast to this pattern, responding was higher following oil pretreatment at 59s. However, because response rates were so low and the proportion of peak rate response was near zero at 59s, this effect may be an artifact. These results suggest

that EB-treated rats delay the "start" function relative to oil-treated rats. However, this delay in start function does not significantly affect peak time (no significant change). In addition, the effects of EB on the "start" function do not coincide with an effect of EB on the "stop" function.

While the overall multilevel PGM centered at the pre- and post-peak mid-points did not reveal any effects of hormone pretreatment (supplemental tables S4.1 and S4.2), the 5s analysis revealed pre-peak effects of hormone at 5 and 10s (p's<.05; supplemental tables S4.3 and S4.4). There were significant interaction effects of hormone with the quadratic and cubic rate of change at both 5 and 10s (p's<.05; see supplemental tale S4.3 and S4.4). While the difference in magnitude was not significant, oil pretreated rats initially responded at a higher level and increase their response rate more abruptly than EB-treated rats. The predicted proportion of peak rate increased in both groups pre-peak as the criterion neared, but the oil-treated rats accelerated their response rate more quickly than EB-treated rats at 5 and 10s, indicating that EB-treated rats delay the "start" of high rate responding relative to oil controls. As the criterion nears and both groups approach peak rate, these differences in rate of change dissipate (i.e., there are no significant differences in slope after 10s). Notably, all EB pretreatment exclusively influences the "start" function, leaving peak time and the "stop" function unaffected.

LHAa^{MCH}→ NAc excitation in oil pretreated rats does not influence the "stop" function

As in previous studies, chemogenetic excitation of LHAa^{MCH}→ NAc neurons did not influence overall measures of responding during the PI task in oil pretreated rats.

There was no effect of LHAa^{MCH}→ NAc neuronal excitation on the amount of time rats

spent in the food cup (t=.67, df=6, p>.05, d=.25) or their overall response rate during the session (t=.57, df=6, p>.05, d=.22). As was the case in intact animals, there was also no effect of LHAa^{MCH} \rightarrow NAc neuronal excitation on peak time in oil pretreated rats (F=1.27, df=6, p>.05, d=.48).

Contrary to my hypothesis, there was also no effect of LHAa^{MCH} \rightarrow NAc neuronal excitation on the proportion of peak rate response function in oil pretreated rats. The ANOVA revealed a main effect of time (F=161.35, df=(59, 354), p<.001, η_p^2 =.31) but no effect of drug (F=.05, df=(1, 6), p>.05, η_p^2 =.01) or interaction effect of drug x time (F=.70, df=(59, 354), p>.05, η_p^2 =.10).

The overall PGM also failed to reveal any effect of chemogenetic excitation of LHAa^{MCH} NAc neurons in oil pretreated rats at the pre- or post-peak mid-points (see supplemental tables S4.5 and S4.6). This is not surprising given that the predicted proportion of peak rate response functions under VEH and CNO are nearly superimposed in oil pretreated rats. However, the refined PGM analysis that examined responding in 5s intervals did capture an effect of CNO on responding at 15s. At this time, there was a significant interaction of drug treatment (VEH, CNO) and the pre-peak quadratic rate of change in oil-treated rats. Consistent with previous transient effects observed around 15s in Chapters 2 and 3, this effect also dissipated by the 20s interval. Thus, CNO briefly accelerated the rate at which responding decreased at 15s in oil-treated rats. Notably, this subtle effect is in contrast to the robust post-peak reduction observed in intact, M/D rats.

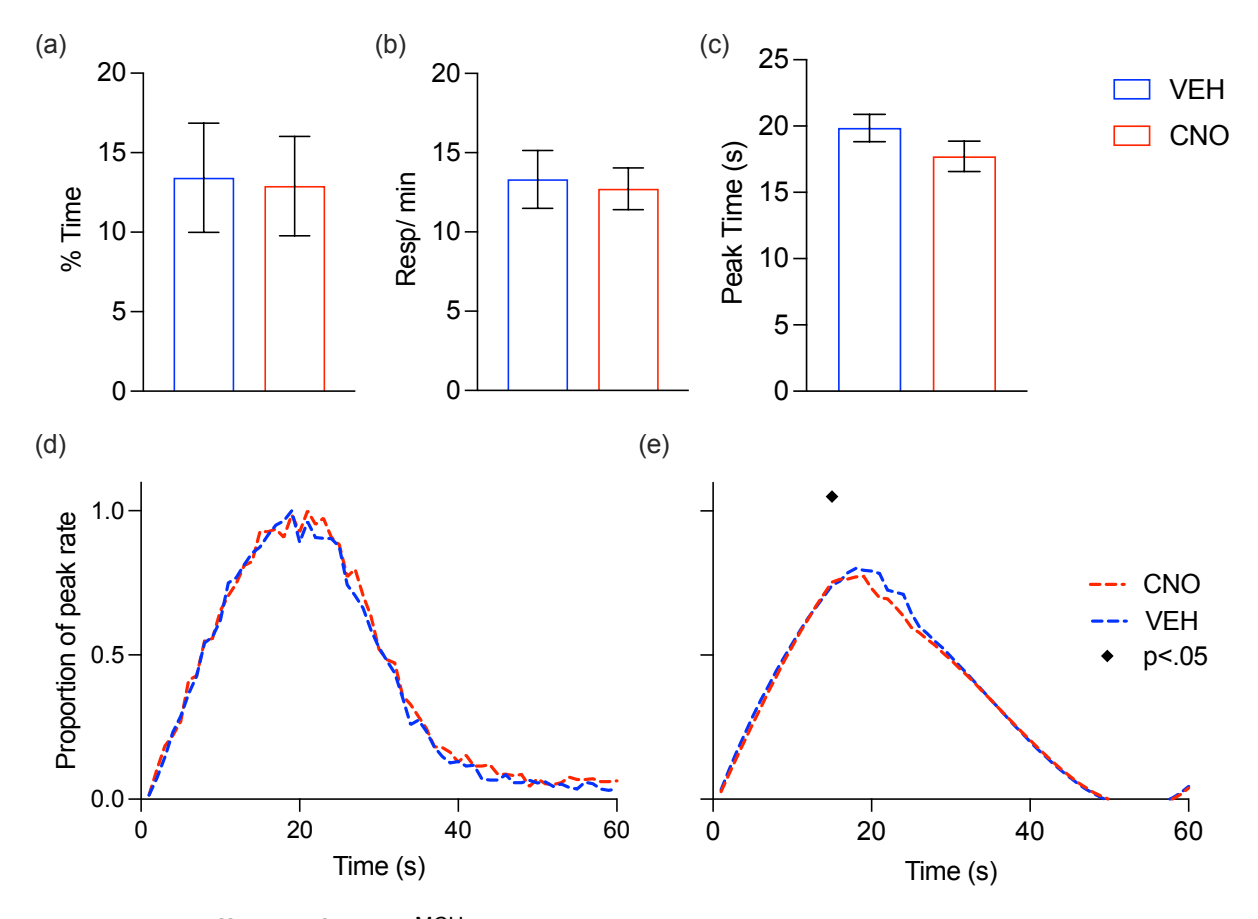


Figure 4.3 Effects of LHAa^{MCH} → NAc excitation on PI responding in oil-treated rats.

(a) There were no differences in the amount of time rats spent in the food magazine during PI sessions following treatment with VEH or CNO. (b) There was also no influence on the overall response rate during the interval timing task. (c) While peak time was reduced following CNO mediated excitation of LHAa^{MCH}→ NAc neurons in oil pretreated rats, this effect did not reach significance.

Estradiol pretreatment enables post-peak effects of LHAaMCH→ NAc neuronal excitation on the "stop" function

As in previous studies, there were no effects of chemogenetic excitation of LHAa^{MCH} \rightarrow NAc neurons on overall measures of behavior from the session, including the time spent in the food magazine (t=.70, df=6, p>.05, d=.26) or response rate (t=1.07, df=6, p>.05, d=.4). In contrast to previous studies, however, chemogenetic excitation of LHAa^{MCH} \rightarrow NAc neurons significantly reduced peak time in EB pretreated rats (t=2.45, df=6, p<.05, d=.93). This reduction in peak time indicates that CNO-mediated excitation of LHAa^{MCH} \rightarrow NAc neurons in EB-treated rats results in earlier responding, an effect that was not evident in oil-treated rats.

In addition to the effects on peak time, chemogenetic excitation of LHAa^{MCH}→
NAc neurons also influenced the proportion of peak rate response function. The ANOVA
evaluating the proportion of peak rate responding (Figure 4.4c) revealed a main effect of
time (F=101.22, df=(59, 354), p<.001, η_p²=.94). While there was no main effect of drug
(F=2.26, df=(1,6), p>.05, η_p²=.27), there was a significant interaction effect of drug x
time (F=2.56, df=59, 354, p>.05, η_p²=.30). Pairwise comparisons evaluating where
responding significantly differed under VEH and CNO in 1s bins revealed significant
differences at 25, 26, 30, 31 and 35s − all times that occur after the criterion duration,
and typically after peak time. Importantly, at each of these time points, responding was
greater under VEH than CNO, indicating that CNO-treated rats respond at a lower level
post-peak than their VEH-treated counterparts.

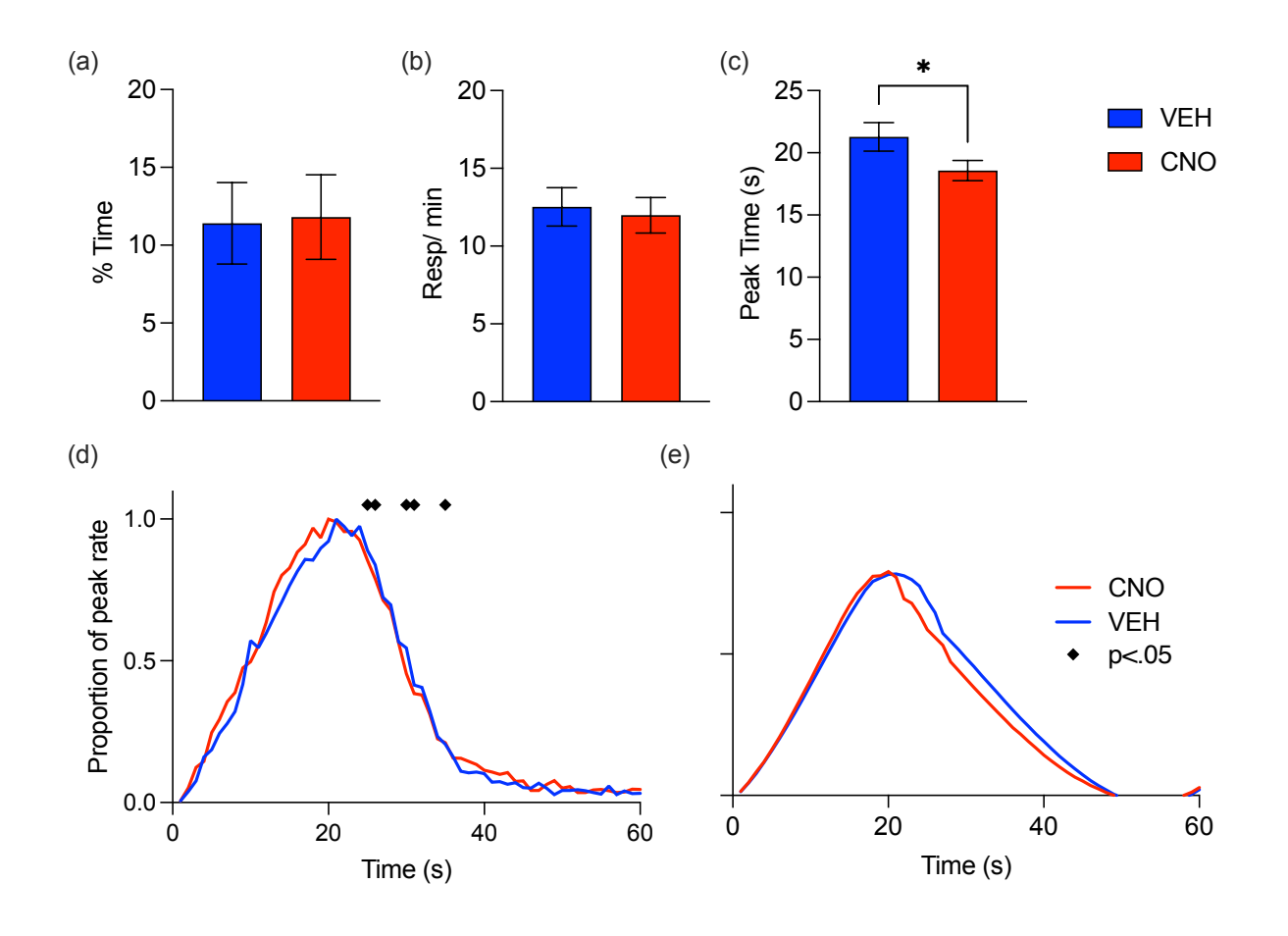


Figure 4.4 Effects of LHAa^{MCH} → NAc excitation on PI responding in EB-treated rats. There were no effects on overall measures of responding during the behavioral session, including (a) amount of time in the food cup or (b) response rate. (c) Chemogenetic excitation of LHAa^{MCH} → NAc neurons reduced peak time in rats pretreated with EB. (d) Proportion of peak rate responding was reduced in EB pretreated rats following CNO-mediated excitation of LHAa^{MCH} → NAc neurons. (e) Modeling the predicted proportion of peak rate response functions did not reveal any differences in the predicted responding under VEH and CNO in EB pretreated rats.

Interestingly, neither the overall PGM nor the refined analyses at 5s intervals revealed effects of CNO in EB pretreated rats. This suggests that while there are differences in the actual magnitude of responding – as revealed by the ANOVA – the

predicted magnitude and the rate of change is similar regardless of CNO treatment.

These differences may be attributable to methodological approaches: while the ANOVA collapses data from two VEH tests and two CNO tests together, the PGM is capable of treating each test independently due to its multivariate structure.

Discussion

Summary of results

In this chapter, I examined the influence of estrogen on NAc-projecting MCH neurons from the anterior LHA. In the previous chapter, I demonstrated that excitation of these LHAa^{MCH} NAc neurons decreased post-peak responding in the peak interval (PI) task in a manner that suggests a change in the "stop" function. In intact, cycling rats excitation of these neurons produced behavioral effects only when rats were tested during metestrus/ diestrus, when circulating levels of estrogen are typically lower. In the present study, I directly modulated the level of plasma estradiol (EB) by removing the primary source of endogenous estrogen through ovariectomy (OVX). Adult female rats were OVX prior to undergoing behavioral training in the PI paradigm and testing with and without estrogen replacement. Chemogenetic excitation of LHAa^{MCH} NAc neurons first occurred in rats pretreated with oil; rats were tested under both oil + vehicle (VEH) and oil + clozapine-N-oxide (CNO) conditions. Next, rats were pretreated with EB before repeating PI testing with VEH and CNO.

To separately examine the influence of estrogen on this task, I first examined the influence of EB on PI responding under baseline (i.e., VEH) conditions. Following EB pretreatment, rats delayed high rate responding pre-peak compared to when they received oil pretreatment. This indicated a delay in the "start" function; EB delays the

start of high rate motivated responding. This effect occurred without significantly altering peak time or producing any effects on the stop function. That EB shifts the response function to the right is consistent with reports suggesting that females respond later than males in interval timing tasks (Gür et al., 2019; Pleil et al., 2011). The delayed "start" suggests that EB reduces motivation to begin high rate responding (i.e., begin exerting high levels of effort) for potential sucrose reinforcement. In addition, given that the peak time and the "stop" function were unaffected, it appears that this motivational effect of EB occurs without influencing the perception of time, *per se*. This delay in the "start" function is consistent with reports of delays in the "start" of motivated responding following reinforcer devaluation (Galtress & Kirkpatrick, 2010; Roberts, 1981). Thus, EB pretreatment decreased motivation to engage in effortful lever pressing until the time when reinforcement was more likely (i.e., around the criterion duration).

Interestingly, this effect is in contrast to reports from the literature suggesting that EB increases clock speed, perhaps by increasing striatal dopamine (DA) release (Sandstrom, 2007). However, our paradigm differs from Sandstrom et al. in that rats were administered EB on two consecutive days and received two separate VEH tests intermixed with CNO testing. Thus, rats in our study had received PI training under EB at least once prior to their first VEH test, and across at least three cycles prior to their second VEH test. Thus, in our case clock speed effects of EB may be masked by new learning that has occurred during the previous days of PI training under EB. In other words, the reference memory for time may have updated to reflect the new clock speed induced by EB pretreatment. However, while clock speed effects are transient and dependent on an outdated reference memory for time, the motivational effects of EB

occur independently of these clock and memory effects. Thus, a persistent delay in high rate responding following EB pretreatment suggests that EB decreases motivation to respond for potential sucrose reinforcement in the PI task, regardless of the capacity of rats to accurately time the criterion.

In contrast to my hypothesis, chemogenetic excitation of LHAa^{MCH} NAc neurons in OVX rats failed to influence the "stop" function in the absence of EB pretreatment. While CNO treatment briefly influenced the quadratic rate of change at 15s by accelerating the rate of response attenuation, there was no other influence of this treatment on responding in the PI task. Given that the accelerated "stop" function was observed following LHAa^{MCH} NAc neuronal excitation during M/D, but not P/E, I expected that removal of circulating gonadal hormones would facilitate these effects. Instead, chemogenetic excitation of LHAa^{MCH} NAc neurons following oil pretreatment failed to influence post-peak responding. This suggests that the removal of ovarian hormones in adulthood reduced the ability of these neurons to influence motivated responding via alterations in the "stop" decision. In other words, removal of ovarian hormones reduced the susceptibility of female rats to the action of these neurons. Thus, without fluctuating ovarian hormones, adult female rats may be protected against the influence of LHAa^{MCH} NAc neurons on time-dependent motivated responding.

Although this finding is surprising, it is perhaps in line with evidence from my initial studies including both males and females. In these studies, females – but not males – were vulnerable to the influence of LHAa^{MCH} neurons on motivated responding post-peak. Thus, males are somehow protected against the effects of LHAa^{MCH} neuronal excitation. Although OVX females are not male-like, *per se*, the absence of

fluctuating ovarian hormones may be similarly protective against the influence of LHAa^{MCH} NAc neurons on PI responding.

In line with the idea that estrogen may create a vulnerability to the effects of LHAa^{MCH} NAc neurons on time-dependent motivated responding, LHAa^{MCH} NAc neuronal excitation unexpectedly accelerated the "stop" function in EB pretreated rats. EB-pretreated rats attenuate high rate responding more quickly under CNO than VEH. They also reached a peak significantly earlier than VEH-treated rats (i.e., peak time is reduced), an effect which may be driven by an abrupt "stop" function rather than change in time perception, *per se*.

While these effects are in contrast to my hypothesis that EB pretreatment would attenuate the effects of LHAa^{MCH} → NAc neuronal excitation, the post-peak effect closely resembles the phenotype observed in M/D females that I thought would occur in oil pretreated rats. Thus, the presence – rather than absences – of EB may be necessary to enable LHAa^{MCH} → NAc neurons to influence motivated responding. However, that this effect occurs following acute administration of EB 30 minutes prior to testing is unexpected, given that EB generally inhibits the actions of MCH. Importantly, however, the reported inhibitory effects of EB on MCH occur through phasic rather than tonic mechanisms. When EB is replaced in a four day, cyclic regimen, the effects of EB on MCH occur on the fourth day – i.e.,, 36-72 hours after administration, during the washout period (Messina et al., 2006; Santollo & Eckel, 2013; Terrill et al., 2020). Thus, rather than reflect an interaction of EB with the chemogenetic excitation of LHAa^{MCH} → NAc neurons, I may instead be capturing a phasic effect. The inability to separate acute and phasic effects of estradiol is one limitation of this study, discussed below.

Limitations

While I also replaced EB in a four day regiment, I intentionally tested rats on the second day of EB replacement in order to capture both slower, genomic and rapid, acute effects of EB on PI performance. I expected that the level of estradiol present on the second day of EB replacement would resemble that observed in early estrus, when estrogen levels still remain high after rising steadily during the preceding day of proestrus (Asarian & Geary, 2002; Geary & Asarian, 1999; Goldman et al., 2007; Hu et al., 2004). After testing with VEH or CNO, rats received two days of PI sessions without hormone or drug delivery during a 48 h washout period before the cycle of hormone administration and chemogenetic testing was repeated. However, this procedure limits the ability to identify whether effects of EB are driven by rapid or genomic effects, and also complicates the interpretation of these results in context of data from intact, cycling animals presented in Chapter 3. It would be interesting to examine whether the influence of EB on LHAa^{MCH}→ NAc neuronal excitation is an effect of the initial dose of EB 24 hours prior to testing, the acute EB administered 30 min prior, or both. If the behavioral effects of EB on LHAa^{MCH}→ NAc neuronal excitation are reproduced after only administering one dose of EB 24 hours prior to testing, this phenotype may be comparable to that observed during metestrus, when hormone levels are relatively low after peaking ~24 hours previously. It would also be beneficial to examine whether EB modulates behavior when chemogenetic excitation of LHAa^{MCH}→ NAc neurons is applied 36-72 hours after EB pretreatment. This is a timeframe more in line with when effects of EB on MCH are typically reported (Messina et al., 2006; Santollo & Eckel, 2008; Terrill et al., 2020), and would indicate that the rise and then subsequent fall –

rather than current plasma EB level – is important for modulation of the effects of LHAa^{MCH}→ NAc neuronal excitation.

In contrast to previous studies, DREADD viral expression in these animals was robust and easily visualized. Given that expression patterns were poor in the previous cohort, I had adapted the DREADD infusion protocol to include an additional 0.25 µl infusion, bilaterally, to the LHAa. These animals thus received an additional 0.5 µl of virus compared to the LHAa infusion performed in intact, cycling animals in Chapter 3. Animals were also sacrificed much earlier than in previous cohorts, within three months after viral infusion rather than after 8-9 months. Tissue collected from these subjects generally appeared healthier, with DREADD expression clearly visualized by the mCherry label in neuronal cell bodies as well as fibers.

While this modified infusion protocol resulted in ample DREADD expression in LHAa^{MCH} neurons, DREADD expression also extended into more posterior aspects of the LHA than in previous LHAa groups. Thus, the cells targeted may have overlapped to a greater extent with LHAp neurons targeted in Chapter 2. However, this infusion was still less than the total volume of DREADD infused to LHAp targets (1.5 µl vs 2.4 µl / rat). It is thus especially interesting that such robust DREADD expression was observed in these animals, but not in the LHAp group. While the LHAp animals were euthanized much later after DREADD expression (i.e., after 8-9 months), expression of the DREADD receptor and mCherry label should remain intact across this timeframe. However, DREADD expression depended on the presence of the pMCH promoter in LHAa neurons. Therefore, the amount of DREADD expression observed in OVX animals may arise from differences in the relative expression of pMCH in the LHA.

Given that estrogen inhibits pMCH expression (Messina et al., 2006; Murray et al., 2000; Santollo & Eckel, 2013), simultaneous OVX in these subjects may have permitted more robust pMCH expression by facilitating a rapid drop in plasma estrogens. This release from inhibition by estrogen would facilitate greater pMCH expression, in turn facilitating more robust DREADD expression in these OVX subjects. This potential effect could be examined by altering the timing of DREADD infusion and OVX, or by comparing DREADD expression in OVX animals receiving immediate post-operative EB vs oil treatment.

Conclusion

Despite these challenges, this study adds to a limited body of work examining the influence of estradiol on timing (Panfil et al., 2023; Pleil et al., 2011; Ross & Santi, 2000; Sandstrom, 2007; Williams, 2011) and provides the first direct evidence that estrogen interacts with LHAa^{MCH} neurons to influence the timing of motivated behavior.

Consistent with work examining the influence of LHAa^{MCH} → NAc neurons on PI responding in intact rats, effects of LHAa^{MCH} → NAc neuronal excitation also produced effects primarily on the "stop" function during the interval timing task. In addition, although a greater number of LHAa^{MCH} → NAc DREADD-expressing neurons were identified, the behavioral phenotype observed – an accelerated "stop" function post criterion – was similar. Thus, these neurons are robustly capable of altering the "stop" function, even when only a few neuronal cell bodies are recruited.

Shockingly, the effects of LHAa^{MCH} → NAc neuronal excitation were only observed in EB-pretreated rats, suggesting that estrogen is necessary for the effects of this manipulation. It remains unclear whether effects of EB pretreatment are driven by

one or both doses of EB administered 24 h and 30 min prior to testing, respectively. Thus, while effects of LHAa^{MCH} → NAc neuronal excitation appear to require EB, the mechanism of this effect (i.e., a tonic or phasic effect driven by membrane-bound or genomic ERs, respectively) remains unclear. The accelerated "stop" function observed in EB-pretreated rats resembles the behavioral phenotype observed following chemogenetic excitation of LHAa^{MCH} → NAc neurons in M/D females. This suggests that effects of EB on LHAa^{MCH} neurons may differ based on the source of estrogen (exogenous vs endogenous) and/ or occur through multiple mechanisms. Regardless, the present study confirms that estrogen interacts with LHAa-MCH → NAc neurons to mediate their effects on motivated behavior. In fact, the presence of estrogen in adult females appears to be necessary to observe any effects of this neuronal manipulation.

In addition, this study also indicated an influence of cyclic EB replacement on the "start" function of adult OVX rats. This is consistent with sex differences reported in female mice, who generally delay the "start" function relative to males (Gür et al., 2019) and provide more insight into a potential role for endogenous estrogen on time perception than studies in which estrogen is replaced only acutely.

In contrast to the baseline effects of EB, which selectively influenced the "start" function, chemogenetic excitation of LHAa^{MCH} → NAc neurons selectively influenced the "stop" function, which is consistent effects reported in intact, cycling animals. This indicates that these neurons are capable of affecting the decision to "stop" engaging in motivated behavior, and suggests these neurons can guide food-related decision making within a temporal context that predicts food availability.

CHAPTER 5: Overall Discussion

Summary of key findings

Previously, I demonstrated that chemogenetic excitation of MCH neurons is capable of producing distinct phenotypes in the Peak Interval (PI) paradigm in female depending on the location of MCH neurons within the LHA. Excitation of MCH neurons in the LHAp reduced peak time in female rats, indicating a potential change in time perception. In contrast, LHAaMCH neuronal excitation prolonged high rate responding without affecting time perception, indicating a motivational effect on the "stop" decision process. Importantly, this effect was observed only when rats were tested during metestrus/ diestrus (M/D), when levels of circulating ovarian hormones are relatively low. This suggests that LHA^{MCH} neurons may be capable of modulating time perception and/ or motivation in the PI task, and do so in a manner that depends on estrous cycle stage. The Nucleus Accumbens (NAc) is implicated in both timing and motivated behavior (Floresco, 2015; Kelley et al., 2005; MacDonald et al., 2012; Meck, 1996; Meck et al., 2008), is modulated by estrogen in females (Becker, 1990a; Becker & Ramirez, 1981; Robinson et al., 1980), and is a site of MCH action (Georgescu et al., 2005; Haemmerle et al., 2015; Karlsson et al., 2016; Terrill et al., 2020). Therefore, in this dissertation, I examined whether projections to the NAc from MCH neurons in the LHAp (Chapter 2) and LHAa (Chapters 3 & 4) could account for these effects.

In Chapters 2 and 3, I first examined whether excitation of NAc-projecting LHAp and LHAa MCH neurons, respectively, could influence PI responding in intact, cycling female rats. Given that little is known about the effects of estrous cycle on PI responding (Gür et al., 2019; Panfil et al., 2023; Pleil et al., 2011; Ross & Santi, 2000;

Sandstrom, 2007; Williams, 2011), I first examined whether or not the estrous cycle influenced task performance at baseline. I then examined the influence of LHA^{MCH} > NAc neuronal excitation separately while rats were in proestrus/ estrus (P/E) and metestrus/ diestrus (M/D).

In Chapter 2, chemogenetic excitation of with LHAp^{MCH} → NAc neurons did not influence time perception in the PI paradigm, indicating that this projection is not capable of accelerating clock speed to increase early responding. Although there was potentially a subtle effect of CNO on the rate at which responding changed at 15s when rats were tested during P/E, this effect occurred without any other changes in responding (i.e., a change in peak time, proportional changes to the "start" and "stop" function) and likely does not indicate a change in time perception itself. In addition, there was also a baseline effect of estrous cycle stage on responding at 15s, indicating that multiple factors may contribute to subtle effects at this timepoint. As such, the potential effect of LHAp^{MCH} → NAc neuronal excitation on responding at 15s during P/E should be interpreted with caution. Thus, altogether, this chapter revealed that LHAp^{MCH} → NAc neurons have little to no influence on responding in the PI task, regardless of estrous cycle stage.

In contrast, in Chapter 3, chemogenetic excitation of LHAa^{MCH} → NAc neurons robustly influenced post-peak responding when rats were tested during M/D. This effect occurred with influencing the "start" function or peak time, indicating that it is a selective modulation of the decision to "stop" motivated responding after the omission of an expected reward. Thus, these neurons integrate temporal information to guide decision making and attenuate effortful responding during periods when reinforcement is not

likely (i.e., after the criterion). That this effect occurred only when rats were tested during M/D is in line with our previous findings in which LHAa^{MCH} neuronal excitation also influenced post peak responding. However, previously, I demonstrated that LHAa^{MCH} neuronal excitation prolonged – rather than attenuated! – high rate responding after the omission of an expected reward. Thus, while LHAa^{MCH} neurons overall delay the "stop" function, a subset of these neurons that project to the NAc instead accelerate the "stop" function. Interestingly, this is in line with the role of the NAc in behavioral inhibition, which posits that motivated behaviors are controlled via an inhibitory influence of the NAc (Ambroggi et al., 2011; Floresco, 2015; Lafferty et al., 2020). Thus, NAcprojecting LHAa^{MCH} neurons may modulate activity within the NAc to inhibit high rate responding after the criterion duration has elapsed and reinforcement is perceived as being unlikely.

Changes to the "stop" function in interval timing procedures are often interpreted in terms of motivation because they represent a form of perseverative responding that occurs in the absence of reinforcer delivery, even as the animal correctly perceives the criterion time as having elapsed. Thus, given that LHAa^{MCH} → NAc neurons influenced a form of motivated responding in the PI task, I also examined whether they could more broadly modulate motivated behavior in task that measures motivated responding more directly: the progressive ratio (PR) task. Despite having altered how quickly rats give up high rate responding after the criterion duration in the PI task, LHAa^{MCH} → NAc neuronal excitation failed to influence when rats gave up in the PR task. That is, rats responded comparably regardless of LHAa^{MCH} → NAc neuronal excitation. In addition, there were no estrous cycle effects on responding in the PR task, which is in line with previous

findings suggesting estrous cycle influences PR responding only during early training (Quigley et al., 2021). That there were no effects of DREADD manipulation on PR responding coincide with the lack of effect observed on overall response rates in the PI task. That is, chemogenetic excitation of LHAa^{MCH} → NAc neurons also did not influence overall response rate or magnitude during the PI task, but rather selectively modulated the profile of responding across time within trials. Thus, the influence of LHAa^{MCH} → NAc neurons on behavior is time-dependent, indicating an ability of these neurons to incorporate information from food predictive cues to determine when reinforcer is likely to become available. Rather than modulate the amount of effort extended over a behavioral session, these neurons modulate *how* that effort is extended (i.e., by coordinating responding around the time of expected reinforcer delivery).

Because these effects of LHAa^{MCH} → NAc neuronal excitation on the "stop" function were observed only when rats were tested during M/D, in Chapter 4 I ovariectomized rats to isolate the effect of estradiol (EB) on DREADD-mediated PI responding. Shockingly, chemogenetic excitation of LHAa^{MCH} → NAc neurons in adult OVX rats failed to influence PI performance! Because LHAa^{MCH} → NAc neurons influence motivated behavior selectively during M/D, when plasma estrogen is relatively low, I hypothesized that chemogenetic excitation of these neurons in oil pretreated rats would produce robust effects on the "stop" function. In addition, evidence suggests that sex differences in striatal circuits underlying interval timing are regulated by genetic or prenatal organization and these differences cannot be reversed by hormones in adulthood (Pleil et al., 2011). Thus, I expected that an absence of EB during adulthood

would simply enable LHAa^{MCH} neurons to influence behavior without being inhibited by endogenous estrogens.

Perhaps even more shockingly, when adult OVX rats were treated with EB, chemogenetic excitation of LHAa^{MCH} → NAc neurons attenuated post peak responding, consistent with an effect on the "stop" function. Although the absence of high levels of circulating estrogen was associated with DREADD effects in intact animals, EB priming was necessary for DREADD effects in OVX animals! Thus, estrogen is necessary in some capacity to sensitize the system to the effects of LHAa^{MCH} → NAc neuronal excitation. In addition, although the hormonal condition at test (relatively low vs high [EB]) differed, the direction of the effect was consistent: chemogenetic excitation of LHAa^{MCH} → NAc neurons reduced high rate after the peak, indicating an acceleration of the "stop" function. In addition, in OVX rats this change in "stop" function was also sufficient to influence peak time, as CNO treatment resulted in a decreased peak time in EB pretreated rats, without proportionally altering the "start" function.

Altogether, results from this dissertation indicate that MCH neurons in the LHAa – but not the LHAp – control motivated behavior through the "stop" function. In addition, these effects are modulated by estrous cycle stage and EB, perhaps requiring fluctuations in EB for the expression of a behavioral phenotype. Given that both MCH and estrogen influence feeding behavior through meal size, they may interact to determine the "stop" function to determine when bouts of feeding are terminated. Limitations

While these studies clearly indicate a role for NAc-projecting MCH neurons in the LHAa, but not LHAp, clarity regarding how these populations of neurons differ is limited.

Furthermore, limited DREADD expression in both the LHAa and LHAp of intact, cycling animals relative to OVX animals suggests that DREADD expression itself – which is controlled by the pMCH promoter – may be influenced by OVX and circulating estrogen. This is not surprising, given that the pMCH promoter is downregulated by EB replacement in OVX rats (Messina et al., 2006), but suggests a need for examining this interaction more directly.

A second limitation of the present studies is that while DREADD expression was selectively targeted to neurons expressing the pMCH promoter, these cells are capable of producing other peptides and neurotransmitters, which may be released in addition to, or in lieu of, the MCH peptide (Bonnavion et al., 2016; Mickelsen et al., 2017, 2019). Without the coadministration of an MCH1R antagonist, it is not possible to isolate behavioral effects of this DREADD manipulation to the MCH peptide. For example, it is also possible that these LHAMCH neurons corelease glutamate, which could also modulate the activity of MSNs in the NAc to alter motivated responding. Future studies could address this shortcoming by administering an MCH1R antagonist (e.g., H6408) with CNO. Although I intended to complete these studies via ICV infusion of H6408 prior to CNO infusion, issues with cannula patency prevented me from reaching a sufficient sample size to make any meaningful conclusions. There is limited data to suggest that H6408 is capable of crossing the blood brain barrier in rats, but preliminary data from a subset of rats (n=2) suggests that i.p. administration of this ligand may be capable of MCH1R binding in the CNS. Regardless, with a limited sample size and knowledge of the pharmacokinetics, this data is also not included. Future work should include pharmacological antagonism of the MCH1R receptor in conjunction with chemogenetic

manipulations, or directly examine the influence of intra-NAc MCH on PI performance to isolate a role for the MCH peptide.

Conclusions

In conclusion, this body of work provides evidence for a role of LHA^{MCH} neurons on the timing of motivated behavior, particularly within the context of when to "stop" effortful responding. In particular, MCH neurons in the anterior LHA are important for modulating the "stop" function. Previously, I demonstrated that non-projection-specific excitation of LHAa^{MCH} neurons prolonged high rate responding by delaying the "stop" function. Here, I demonstrated that projections from these LHAa^{MCH} neurons to the NAc do not underlie this effect. Instead, LHAa^{MCH} → NAc neurons attenuate post peak responding by accelerating the "stop" function. This indicates a bidirectional control of the "stop" by LHAa^{MCH} neurons, depending in part on their afferents. Critically, these effects were observed only in females tested during M/D, indicating that these neurons are modulated by the estrous cycle in intact, cycling females. Furthermore, an influence of estradiol was isolated through OVX and selective EB replacement. This manipulation indicated that EB is necessary to observe behavioral effects of LHAa^{MCH} → NAc neuronal excitation, as there was no effect of DREADD manipulations in oil-treated rats.

Given that both MCH and estrogen modulate food intake via changes in meal size (Baird et al., 2006; Eckel, 2011; Messina et al., 2006), their effects may occur through changes to the "stop" decision that determines when to stop consuming.

Although the present studies do not directly examine consumption patterns, and the "stop" function is specifically modulated in the absence of an expected food reinforcer, they still provide evidence for the behavioral control of inhibition by MCH and estrogen.

Specifically, the PI paradigm provides unique insight into the control of the "stop" decision by examining how motivated responding changes within a trial based on the expectation of reinforcer delivery, which is informed by the passage of time. Thus, these neurons integrate temporal information to guide effortful behavior. Changes to the decision of when to "stop" high rate responding reflect control of these neurons over motivated responding in real time. That these effects are time-dependent, and occur only in the post-peak period after the omission of an expected reward, further indicates the subtle control of these LHAa^{MCH} on decision processes affecting motivated behavior.

Altogether, these data suggest that MCH and estrogen interact to influence the "stop" decision in motivated food-seeking. Typically, estrogen decreases food intake by reducing meal size, while MCH promotes food intake by increasing meal size – in both cases, these effects may also occur through changes in the decision processes that guide when to "stop" feeding. The present study demonstrates that MCH neurons in the anterior LHA interact with estrogen to modulate the "stop" decision in an interval timing task. This provides a potential mechanism through which estrogen and MCH may interact to influence the "stop" decision process in feeding-related behaviors, especially those that include a temporal component. Thus, these neurons could influence a variety of learned and motivated feeding behaviors, providing a potential mechanism to explore in maladaptive feeding behaviors.

BIBLIOGRAPHY

- Almey, A., Milner, T. A., & Brake, W. G. (2015). Estrogen receptors in the central nervous system and their Implication for Dopamine-Dependent Cognition in Females. *Hormones and Behavior*, 74, 125–138. https://doi.org/10.1016/j.yhbeh.2015.06.010.Estrogen
- Ambroggi, F., Ghazizadeh, A., Nicola, S. M., & Fields, H. L. (2011). Roles of Nucleus Accumbens Core and Shell in Incentive-Cue Responding and Behavioral Inhibition. *Journal of Neuroscience*, 31(18), 6820–6830. https://doi.org/10.1523/JNEUROSCI.6491-10.2011
- Arrigoni, E., Chee, M. J. S., & Fuller, P. M. (2019). To eat or to sleep: That is a lateral hypothalamic question. *Neuropharmacology*, *154*(August 2018), 34–49. https://doi.org/10.1016/j.neuropharm.2018.11.017
- Asarian, L., & Geary, N. (2002). Cyclic estradiol treatment normalizes body weight and restores physiological patterns of spontaneous feeding and sexual receptivity in ovariectomized rats. *Hormones and Behavior*, *42*(4), 461–471. https://doi.org/10.1006/hbeh.2002.1835
- Bäckberg, M., Ultenius, C., Fritschy, J. M., & Meister, B. (2004). Cellular localization of GABAA receptor α subunit immunoreactivity in the rat hypothalamus: Relationship with neurones containing orexigenic or anorexigenic peptides. *Journal of Neuroendocrinology*, *16*(7), 589–604. https://doi.org/10.1111/j.1365-2826.2004.01207.x
- Baird, J., Rios, C., Gray, N. E., Walsh, C. E., Fischer, S. G., Pecora, A. L., Rios, C., Gray, N. E., Walsh, E., & Fischer, S. G. (2006). Effects of melanin-concentrating hormone on licking microstructure and brief-access taste responses. *American Journal of Physiology Regulatory Integrative and Comparative Physiology*, 291(5), 1265–1274. https://doi.org/10.1152/ajpregu.00143.2006.
- Balcı, F. (2014). Interval Timing, Dopamine, and Motivation. *Timing & Time Perception*, 2(3), 379–410. https://doi.org/10.1163/22134468-00002035
- Balcı, F., & Freestone, D. (2020). The Peak Interval Procedure in Rodents: A Tool for Studying the Neurobiological Basis of Interval Timing and Its Alterations in Models of Human Disease. *Bio-Protocol*, *10*(17), 1–20. https://doi.org/10.21769/bioprotoc.3735
- Balsam, P., Drew, M., & Gallistel, C. (2010). Time and Associative Learning. *Comparative Cognition & Behavior Reviews*, 5, 1–22. https://doi.org/10.3819/ccbr.2010.50001
- Balsam, P., Sanchez-Castillo, H., Taylor, K., Van Volkinburg, H., & Ward, R. D. (2009).

- Timing and anticipation: Conceptual and methodological approaches. *European Journal of Neuroscience*, *30*(9), 1749–1755. https://doi.org/10.1111/j.1460-9568.2009.06967.x
- Bass, J., & Takahashi, J. S. (2010). Circadian Integration of Metabolism and Energetics. *Science*, *330*(6009), 1349–1354.
- Bayer, J., Rusch, T., Zhang, L., Gläscher, J., & Sommer, T. (2020). Dose-dependent effects of estrogen on prediction error related neural activity in the nucleus accumbens of healthy young women. *Psychopharmacology*, 237(3), 745–755. https://doi.org/10.1007/s00213-019-05409-7
- Becker, J. B. (1990a). Direct effect of 17β-estradiol on striatum: Sex differences in dopamine release. *Synapse*, *5*(2), 157–164. https://doi.org/10.1002/syn.890050211
- Becker, J. B. (1990b). Estrogen rapidly potentiates amphetamine-induced striatal dopamine release and rotational behavior during microdialysis. *Neuroscience Letters*, *118*(2), 169–171. https://doi.org/10.1016/0304-3940(90)90618-J
- Becker, J. B., & Ramirez, V. D. (1981). (Accepted June 26th, 1980). *Water*, 204, 361–372.
- Berridge, K. C. (2004). Motivation concepts in behavioral neuroscience. *Physiology and Behavior*, *81*(2), 179–209. https://doi.org/10.1016/j.physbeh.2004.02.004
- Berridge, K. C., & Valenstein, E. S. (1991). What Psychological Process Mediates Feeding Evoked by Electrical Stimulation of the Lateral Hypothalamus? *Behavioral Neuroscience*, *105*(1), 3–14. https://doi.org/10.1037/0735-7044.105.1.3
- Berthoud, H. R., & Münzberg, H. (2011). The lateral hypothalamus as integrator of metabolic and environmental needs: From electrical self-stimulation to optogenetics. *Physiology and Behavior*, *104*(1), 29–39. https://doi.org/10.1016/j.physbeh.2011.04.051
- Bittencourt, J., Presse, F., Arias, C., Peto, C., Vaughan, J., Nahon, J., Vale, W., & Sawchenko, P. (1992). The melanin concentrating hormone system of the rat brain An immuno and hybridisation histochemical characterisation.pdf. *The Journal of Comparative Neurology*, 319, 218–245. https://doi.org/10.1002/cne.903190204
- Blaustein, J. D., & Wade, G. N. (1976). Ovarian influences on the meal patterns of female rats. *Physiology and Behavior*, *17*(2), 201–208. https://doi.org/10.1016/0031-9384(76)90064-0
- Block, R. A., Hancock, P. A., & Zakay, D. (2000). Sex differences in duration judgments: A meta-analytic review. *Memory and Cognition*, *28*(8), 1333–1346. https://doi.org/10.3758/BF03211834

- Blouin, A. M., Fried, I., Wilson, C. L., Staba, R. J., Behnke, E. J., Lam, H. A., Maidment, N. T., Karlsson, K. Æ., Lapierre, J. L., & Siegel, J. M. (2013). Human hypocretin and melanin-concentrating hormone levels are linked to emotion and social interaction. *Nature Communications, May 2012*. https://doi.org/10.1038/ncomms2461
- Bonnavion, P., Mickelsen, L. E., Fujita, A., de Lecea, L., & Jackson, A. C. (2016). Hubs and spokes of the lateral hypothalamus: cell types, circuits and behaviour. *Journal of Physiology*, *594*(22), 6443–6462. https://doi.org/10.1113/JP271946
- Boulware, M. I., Weick, J. P., Becklund, B. R., Kuo, S. P., Groth, R. D., & Mermelstein, P. G. (2005). Estradiol Activates Group I and II Metabotropic Glutamate Receptor Signaling, Leading to Opposing Influences on cAMP Response Element-Binding Protein. *The Journal of Neuroscience*, *25*(20), 5066–5078. https://doi.org/10.1523/JNEUROSCI.1427-05.2005
- Broberger, C., De Lecea, L., Sutcliffe, J. G., & Hökfelt, T. (1998). Hypocretin/orexin- and melanin-concentrating hormone-expressing cells form distinct populations in the rodent lateral hypothalamus: relationship to the neuropeptide y and agouti generelated protein systems. *Journal of Comparative Neurology*, 402(4), 460–474. https://doi.org/10.1002/(sici)1096-9861(19981228)402:4<460::aid-cne3>3.0.co;2-s
- Brown, J. A., Woodworth, H. L., & Leinninger, G. M. (2015). To ingest or rest? Specialized roles of lateral hypothalamic area neurons in coordinating energy balance. *Frontiers in Systems Neuroscience*, 9(FEB), 1–25. https://doi.org/10.3389/fnsys.2015.00009
- Buhusi, M., Bartlett, M. J., & Buhusi, C. V. (2017). Sex differences in interval timing and attention to time in C57Bl/6J mice. *Behavioural Brain Research*, *324*, 96–99. https://doi.org/10.1016/j.bbr.2017.02.023
- Buhusi, C. V., & Meck, W. H. (2002). Differential effects of methamphetamine and haloperidol on the control of an internal clock. *Behavioral Neuroscience*, *116*(2), 291–297. https://doi.org/10.1037/0735-7044.116.2.291
- Buhusi, C. V., & Meck, W. H. (2005). What makes us tick? Functional and neural mechanisms of interval timing. *Nature Reviews Neuroscience*, *6*(10), 755–765. https://doi.org/10.1038/nrn1764
- Buhusi, C. V., & Meck, W. H. (2006). Time sharing in rats: A peak-interval procedure with gaps and distracters. *Behavioural Processes*, 71(2–3), 107–115. https://doi.org/10.1016/j.beproc.2005.11.017
- Buhusi, C. V., & Meck, W. H. (2009). Relative time sharing: New findings and an extension of the resource allocation model of temporal processing. *Philosophical Transactions of the Royal Society B: Biological Sciences*, *364*(1525), 1875–1885.

- https://doi.org/10.1098/rstb.2009.0022
- Butera, P. C. (2010). Estradiol and the control of food intake. *Physiology & Behavior*, 99(2), 175–180. https://doi.org/10.1016/j.physbeh.2009.06.010
- Caggiula, A. R., & Hoebel, B. (1966). "Copulation-Reward Site" in the Posterior Hypothalamus Author. *Science*, *153*(3741), 1284–1285.
- Challet, E. (2019). The circadian regulation of food intake. *Nature Reviews Endocrinology*, *15*(7), 393–405. https://doi.org/10.1038/s41574-019-0210-x
- Chambers, J., Ames, R. S., Bergsma, D., Muir, A., Fitzgerald, L. R., Hervieu, G., Dytko, G. M., Foley, J. J., Martin, J., Liu, W. S., Park, J., Ellis, C., Ganguly, S., Konchar, S., Cluderay, J., Leslie, R., Wilson, S., & Sarau, H. M. (1999). Melanin-concentrating hormone is the cognate ligand for the orphan G- protein-coupled receptor SLC-1. *Nature*, *400*(6741), 261–265. https://doi.org/10.1038/22313
- Chee, M. J. S., Arrigoni, E., & Maratos-Flier, E. (2015). Melanin-concentrating hormone neurons release glutamate for feedforward inhibition of the lateral septum. *Journal of Neuroscience*, *35*(8), 3644–3651. https://doi.org/10.1523/JNEUROSCI.4187-14.2015
- Church, R. M. (1984). Properties of the Internal Clock. In J. Gibbon & A. Lorraine (Eds.), *Time and Time Perception* (pp. 566–582). Annals of the New York Academy of Sciences.
- Church, R. M., & Broadbent, H. A. (1991). A connectionist model of timing. In M. L. Commons, S. Grossberg, & J. E. R. Staddon (Eds.), *Quantitative Models of Behavior: Neural Networks and Conditioning.* Lawrence Erlbaum Associates, Inc. https://books.google.com/books?hl=en&lr=&id=oeYcDQAAQBAJ&oi=fnd&pg=PT24 0&dq=A+connectionist+model+of+timing&ots=eWUT5DUVv-&sig=e4J03AdA5H4oWtcE_qLChnlyxRY
- Church, R. M., Meck, W. H., & Gibbon, J. (1994). Application of Scalar Timing Theory to Individual Trials. *Journal of Experimental Psychology: Animal Behavior Processes*, 20(2), 135–155. https://doi.org/10.1037/0097-7403.20.2.135
- Couse, J. F., Lindzey, J., Grandien, K. A. J., Gustafsson, J.-åke, & Korach, K. S. (1997). Tissue Distribution and Quantitative Analysis of Estrogen Receptor- a (ER a) and Estrogen Receptor-b (ERb) Messenger Ribonucleic Acid in the Wild-Type and ER a -Knockout Mouse. *Endocrinology*, 138(11).
- Davis, J. D., & Smith, G. P. (1988). Analysis of lick rate measures the positive and negative feedback effects of carbohydrates on eating. *Appetite*, *11*(3), 229–238.
- Davis, J. D., & Smith, G. P. (1992). Analysis of the Microstructure of the Rhythmic

- Tongue Movements of Rats Ingesting Maltose and Sucrose Solutions. *Behavioral Neuroscience*, *106*(1), 217–228. https://doi.org/10.1037/0735-7044.106.1.217
- Della-Zuana, O., Presse, F., Ortola, C., Duhault, J., Nahon, J. L., & Levens, N. (2002). Acute and chronic administration of melanin- concentrating hormone enhances food intake and body weight in Wistar and Sprague Dawley rats. *International Journal of Obesity*, *26*, 1289–1295.
- Dilsiz, P., Aklan, I., Sayar Atasoy, N., Yavuz, Y., Filiz, G., Koksalar, F., Ates, T., Oncul, M., Coban, I., Ates Oz, E., Cebecioglu, U., Alp, M. I., Yilmaz, B., & Atasoy, D. (2020). MCH Neuron Activity Is Sufficient for Reward and Reinforces Feeding. Neuroendocrinology, 110(3–4), 258–270. https://doi.org/10.1159/000501234
- Diniz, G. B., & Bittencourt, J. C. (2017). The melanin-concentrating hormone as an integrative peptide driving motivated behaviors. *Frontiers in Systems Neuroscience*, 11(May), 1–26. https://doi.org/10.3389/fnsys.2017.00032
- Eckel, L. A. (2004). Estradiol: A rhythmic, inhibitory, indirect control of meal size. *Physiology and Behavior*, *82*(1), 35–41. https://doi.org/10.1016/j.physbeh.2004.04.023
- Eckel, L. A. (2011). The ovarian hormone estradiol plays a crucial role in the control of food intake in females. *Physiology and Behavior*, *104*(4), 517–524. https://doi.org/10.1016/j.physbeh.2011.04.014
- Fiorillo, C. D., Tobler, P. N., & Schultz, W. (2003). Discrete coding of reward probability and uncertainty by dopamine neurons. *Science*, 299(5614), 1898–1902. https://doi.org/10.1126/science.1077349
- Floresco, S. B. (2015). The nucleus accumbens: An interface between cognition, emotion, and action. *Annual Review of Psychology*, *66*, 25–32. https://doi.org/10.1146/annurev-psych-010213-115159
- Gallardo, M. G. P., Chiocchio, S. R., & Tramezzani, J. H. (2004). Changes of melanin-concentrating hormone related to LHRH release in the median eminence of rats. *Brain Research*, 1030(1), 152–158. https://doi.org/10.1016/j.brainres.2004.10.005
- Gallistel, C. R., & Gibbon, J. (2000). Time, Rate, and Conditioning. *Psychological Review*, 107(2), 289–344.
- Galtress, T., & Kirkpatrick, K. (2009). Reward value effects on timing in the peak procedure. *Learning and Motivation*, *40*(2), 109–131. https://doi.org/10.1016/j.lmot.2008.05.004
- Galtress, T., & Kirkpatrick, K. (2010). Reward magnitude effects on temporal discrimination. *Learning and Motivation*, *41*(2), 108–124.

- https://doi.org/10.1016/j.lmot.2010.01.002
- Geary, N., & Asarian, L. (1999). Cyclic estradiol treatment normalizes body weight and test meal size in ovariectomized rats. *Physiology and Behavior*, 67(1), 141–147. https://doi.org/10.1016/S0031-9384(99)00060-8
- Georgescu, D., Sears, R. M., Hommel, J. D., Barrot, M., Bolaños, C. A., Marsh, D. J., Bednarek, M. A., Bibb, J. A., Maratos-Flier, E., Nestler, E. J., & DiLeone, R. J. (2005). The hypothalamic neuropeptide melanin-concentrating hormone acts in the nucleus accumbens to modulate feeding behavior and forced-swim performance. *Journal of Neuroscience*, *25*(11), 2933–2940. https://doi.org/10.1523/JNEUROSCI.1714-04.2005
- Gibbon, J. (1977). Scalar expectancy theory and Weber's law in animal timing. *Psychological Review*, *84*(3), 279–325. https://doi.org/10.1037/0033-295X.84.3.279
- Goldman, J. M., Murr, A. S., & Cooper, R. L. (2007). The Rodent Estrous Cycle. *Birth Defects Research*, *80*(2), 83–97.
- Gomori, A., Ishihara, A., Ito, M., Mashiko, S., Ishihara, A., Ito, M., Matsushita, H., Yumoto, M., Ito, M., Tanaka, T., & Tokita, S. (2023). *Chronic intracerebroventricular infusion of MCH causes obesity in mice*. 583–588.
- Goodless-Sanchez, N., Moore, R. Y., & Morin, L. P. (1991). Lateral hypothalamic regulation of circadian rhythm phase. *Physiology and Behavior*, *49*(3), 533–537. https://doi.org/10.1016/0031-9384(91)90276-T
- Grove-Strawser, D., Boulware, M. I., & Mermelstein, P. G. (2010). Membrane estrogen receptors activate the metabotropic glutamate receptors mGluR5 and mGluR3 to bidirectionally regulate CREB phosphorylation in female rat striatal neurons. *Neuroscience*, *170*(4), 1045–1055. https://doi.org/10.1016/j.neuroscience.2010.08.012
- Gür, E., Fertan, E., Kosel, F., Wong, A. A., Balcı, F., & Brown, R. E. (2019). Sex differences in the timing behavior performance of 3xTg-AD and wild-type mice in the peak interval procedure. *Behavioural Brain Research*, *360*(September 2018), 235–243. https://doi.org/10.1016/j.bbr.2018.11.047
- Haemmerle, C. A. S., Campos, A. M. P., & Bittencourt, J. C. (2015). Melanin-concentrating hormone inputs to the nucleus accumbens originate from distinct hypothalamic sources and are apposed to GABAergic and cholinergic cells in the Long-Evans rat brain. *Neuroscience*, 289, 392–405. https://doi.org/10.1016/j.neuroscience.2015.01.014
- Hahn, J. D., & Swanson, L. W. (2010). Distinct patterns of neuronal inputs and outputs of the juxtaparaventricular and suprafornical regions of the lateral hypothalamic

- area in the male rat. *Brain Research Reviews*, 64(1), 14–103. https://doi.org/10.1016/j.brainresrev.2010.02.002
- Hahn, J. D., & Swanson, L. W. (2015). Connections of the juxtaventromedial region of the lateral hypothalamic area in the male rat. *Frontiers in Systems Neuroscience*, 9(MAY), 1–53. https://doi.org/10.3389/fnsys.2015.00066
- Harthoorn, L. F., Sañé, A., Nethe, M., & Van Heerikhuize, J. J. (2005). Multi-transcriptional profiling of melanin-concentrating hormone and orexin-containing neurons. *Cellular and Molecular Neurobiology*, 25(8), 1209–1223. https://doi.org/10.1007/s10571-005-8184-8
- Hassani, O. K., Lee, M. G., & Jones, B. E. (2009). Melanin-concentrating hormone neurons discharge in a reciprocal manner to orexin neurons across the sleep-wake cycle. *Proceedings of the National Academy of Sciences*, *106*(7), 2418–2422. https://doi.org/10.1073/pnas.0811400106
- Hawes, B. E., Erin, K. I. L., Green, B., O'Neill, K. I. M., Fried, S., & Graziano, M. P. (2000). The melanin-concentrating hormone receptor couples to multiple G proteins to activate diverse intracellular signaling pathways. *Endocrinology*, *141*(12), 4524–4532. https://doi.org/10.1210/endo.141.12.7833
- Hervieu, G. J., Cluderay, J. E., Harrison, D., Meakin, J., Maycox, P., Nasir, S., & Leslie, R. A. (2000). The distribution of the mRNA and protein products of the melanin-concentrating hormone (MCH) receptor gene, slc-1, in the central nervous system of the ratt. *European Journal of Neuroscience*, *12*(4), 1194–1216. https://doi.org/10.1046/j.1460-9568.2000.00008.x
- Hinton, S. C., & Meck, W. H. (2004). Frontal-striatal circuitry activated by human peak-interval timing in the supra-seconds range. *Cognitive Brain Research*, 21(2), 171–182. https://doi.org/10.1016/j.cogbrainres.2004.08.005
- Hoebel, B., & Teitelbaum, P. (1962). Hypothalamic Control of Feeding and Self-Stimulation Author (s): Bartley G. Published by: American Association for the Advancement of Science Stable URL: http://www.jstor.org/stable/1709352 Accessed: 15-07-2016 22: 49 U. *American Association for the Advancement of Science*, 135(3501), 375–377.
- Hollerman, J. R., & Schultz, W. (1998). Dopamine neurons report an error in the temporal prediction of reward during learning. *Nature Neuroscience*, *1*(4), 304–309. https://doi.org/10.1038/1124
- Hu, M., Crombag, H. S., Robinson, T. E., & Becker, J. B. (2004). Biological Basis of Sex Differences in the Propensity to Self-administer Cocaine. *Neuropsychopharmacology*, 29(1), 81–85. https://doi.org/10.1038/sj.npp.1300301

- Huang, H., & van den Pol, A. N. (2007). Rapid Direct Excitation and Long-Lasting Enhancement of NMDA Response by Group I Metabotropic Glutamate Receptor Activation of Hypothalamic Melanin- Concentrating Hormone Neurons. *The Journal of Neuroscience*, 27(43), 11560–11572. https://doi.org/10.1523/JNEUROSCI.2147-07.2007
- Huang, W., Ramsey, K. M., Marcheva, B., & Bass, J. (2011). *Huang 2011 circadian rhythms sleep food.pdf* (pp. 2133–2141).
- Hutchinson, R. R., & Renfrew, J. W. (1966). STALKING ATTACK AND EATING BEHAVIORS ELICITED FROM THE SAME SITES IN THE HYPOTHALAMUS 1. *Journal of Comparative and Physiological Psychology*, *61*(3), 360–367.
- Jego, S., Glasgow, S. D., Herrera, C. G., Ekstrand, M., Reed, S. J., Boyce, R., Friedman, J., Burdakov, D., & Adamantidis, A. R. (2013). Optogenetic identification of a rapid eye movement sleep modulatory circuit in the hypothalamus. *Nature Neuroscience*, *16*(11), 1637–1643. https://doi.org/10.1038/nn.3522
- Johnson, A. W. (2018). Characterizing ingestive behavior through licking microstructure: Underlying neurobiology and its use in the study of obesity in animal models. *International Journal of Developmental Neuroscience*, *64*(March 2017), 38–47. https://doi.org/10.1016/j.ijdevneu.2017.06.012
- Kacelnik, A., & Brunner, D. (2002). Timing and foraging: Gibbon's scalar expectancy theory and optimal patch exploitation. *Learning and Motivation*, 33(1), 177–195. https://doi.org/10.1006/lmot.2001.1110
- Karlsson, C., Aziz, A. M. A., Rehman, F., Pitcairn, C., Barchiesi, R., Barbier, E., Wendel Hansen, M., Gehlert, D., Steensland, P., Heilig, M., & Thorsell, A. (2016). Melanin-Concentrating Hormone and Its MCH-1 Receptor: Relationship Between Effects on Alcohol and Caloric Intake. *Alcoholism: Clinical and Experimental Research*, 40(10), 2199–2207. https://doi.org/10.1111/acer.13181
- Kelley, A. E. (2004). Ventral striatal control of appetitive motivation: Role in ingestive behavior and reward-related learning. *Neuroscience and Biobehavioral Reviews*, 27(8), 765–776. https://doi.org/10.1016/j.neubiorev.2003.11.015
- Kelley, A. E., Baldo, B. A., Pratt, W. E., & Will, M. J. (2005). Corticostriatal-hypothalamic circuitry and food motivation: Integration of energy, action and reward. *Physiology and Behavior*, *86*(5), 773–795. https://doi.org/10.1016/j.physbeh.2005.08.066
- Kelley, A. E., Bless, E. P., & Swanson, C. J. (1996). Investigation of the effects of opiate antagonists infused into the nucleus accumbens on feeding and sucrose drinking in rats. *Journal of Pharmacology and Experimental Therapeutics*, 278(3), 1499–1507.

- Kurti, A. N., & Matell, M. S. (2011). Nucleus accumbens dopamine modulates response rate but not response timing in an interval timing task. *Behavioral Neuroscience*, 125(2), 215–225. https://psycnet.apa.org/record/2011-06370-006
- Lafferty, C. K., Yang, A. K., Mendoza, J. A., & Britt, J. P. (2020). Nucleus Accumbens Cell Type- and Input-Specific Suppression of Unproductive Reward Seeking. *Cell Reports*, 30(11), 3729-3742.e3. https://doi.org/10.1016/j.celrep.2020.02.095
- Lee, J., Raycraft, L., & Johnson, A. W. (2021). The dynamic regulation of appetitive behavior through lateral hypothalamic orexin and melanin concentrating hormone expressing cells. *Physiology and Behavior*, 229(October 2020), 113234. https://doi.org/10.1016/j.physbeh.2020.113234
- Lewis, P. A., & Miall, R. C. (2003). Brain activation patterns during measurement of suband supra-second intervals. *Neuropsychologia*, *41*(12), 1583–1592. https://doi.org/10.1016/S0028-3932(03)00118-0
- Li, X., Schwartz, P. E., & Rissman, E. F. (1997). Distribution of estrogen receptor-β-like immunoreactivity in rat forebrain. *Neuroendocrinology*, *66*(2), 63–67. https://doi.org/10.1159/000127221
- López, M., & Tena-Sempere, M. (2015). Estrogens and the control of energy homeostasis: A brain perspective. *Trends in Endocrinology and Metabolism*, *26*(8), 411–421. https://doi.org/10.1016/j.tem.2015.06.003
- Ludwig, D. S., Flier, J. S., Maratos-flier, E., Ludwig, D. S., Tritos, N. A., Mastaitis, J. W., Kulkarni, R., Kokkotou, E., Elmquist, J., Lowell, B., Flier, J. S., & Maratos-flier, E. (2001). *Melanin-concentrating hormone overexpression in transgenic mice leads to obesity and insulin resistance Find the latest version: Melanin-concentrating hormone overexpression in transgenic mice leads to obesity and insulin resistance.* 107(3), 379–386.
- MacDonald, C. J., Cheng, R.-K., & Meck, W. H. (2012). Acquisition of "Start" and "Stop" response thresholds in peak-interval timing is differentially sensitive to protein synthesis inhibition in the dorsal and ventral striatum. *Frontiers in Integrative Neuroscience*, 6(March), 1–16. https://doi.org/10.3389/fnint.2012.00010
- Malapani, C., & Fairhurst, S. (2002). Scalar timing in animals and humans. *Learning and Motivation*, 33(1), 156–176. https://doi.org/10.1006/lmot.2001.1105
- Marsh, D. J., Weingarth, D. T., Novi, D. E., Chen, H. Y., Trumbauer, M. E., Chen, A. S., Guan, X. M., Jiang, M. M., Feng, Y., Camacho, R. E., Shen, Z., Frazier, E. G., Yu, H., Metzger, J. M., Kuca, S. J., Shearman, L. P., Gopal-Truter, S., MacNeil, D. J., Strack, A. M., ... Qian, S. (2002). Melanin-concentrating hormone 1 receptor-deficient mice are lean, hyperactive, and hyperphagic and have altered metabolism. *Proceedings of the National Academy of Sciences of the United States*

- of America, 99(5), 3240-3245. https://doi.org/10.1073/pnas.052706899
- Marshall, A. T., Smith, A. P., & Kirkpa. (2014). Mechanisms of Impulsive Choice: I. Individual Differences in Interval Timing and Reward Processing. *Journal of the Experimental Analysis of Behavior*, 102, 86–101. https://doi.org/10.1007/s10071-020-01456-2
- Matell, M. S., Bateson, M., & Meck, W. H. (2006). Single-trials analyses demonstrate that increases in clock speed contribute to the methamphetamine-induced horizontal shifts in peak-interval timing functions. *Psychopharmacology*, *188*(2), 201–212. https://doi.org/10.1007/s00213-006-0489-x
- Matell, M. S., & Meck, W. H. (2004). Cortico-striatal circuits and interval timing: Coincidence detection of oscillatory processes. *Cognitive Brain Research*, *21*(2), 139–170. https://doi.org/10.1016/j.cogbrainres.2004.06.012
- Matell, M. S., Meck, W. H., & Nicolelis, M. A. L. (2003). Interval timing and the encoding of signal duration by ensembles of cortical and striatal neurons. *Behavioral Neuroscience*, *117*(4), 760–773. https://doi.org/10.1037/0735-7044.117.4.760
- McEwen, B. S. (2002). Recent Progress in Hormone Research. In *Endocrine Reviews* (Vol. 57, Issue 1). https://doi.org/10.2307/1292058
- Meck, W. H. (1983). Selective adjustment of the speed of internal clock and memory processes. *Journal of Experimental Psychology: Animal Behavior Processes*, 9(2), 171–201. https://doi.org/10.1037/0097-7403.9.2.171
- Meck, W. H. (1996). Neuropharmacology of timing and time perception. *Cognitive Brain Research*, 3(3–4), 227–242. https://doi.org/10.1016/0926-6410(96)00009-2
- Meck, W. H. (2005). Neuropsychology of timing and time perception. *Brain and Cognition*, 58(1), 1–8. https://doi.org/10.1016/j.bandc.2004.09.004
- Meck, W. H. (2006). Frontal cortex lesions eliminate the clock speed effect of dopaminergic drugs on interval timing. *Brain Research*, 1108(1), 157–167. https://doi.org/10.1016/j.brainres.2006.06.046
- Meck, W. H., Cheng, R., Macdonald, C. J., Gainetdinov, R. R., Caron, M. G., & Özlem, M. (2012). Gene-dose dependent effects of methamphetamine on interval timing in dopamine-transporter knockout mice. *Neuropharmacology*, *62*(3), 1221–1229. https://doi.org/10.1016/j.neuropharm.2011.01.042
- Meck, W. H., & Church, R. M. (1987). Cholinergic Modulation of the Content of Temporal Memory. *Behavioral Neuroscience*, 101(4), 457–464. https://doi.org/10.1037/0735-7044.101.4.457

- Meck, W. H., Penney, T. B., & Pouthas, V. (2008). Cortico-striatal representation of time in animals and humans. *Current Opinion in Neurobiology*, *18*(2), 145–152. https://doi.org/10.1016/j.conb.2008.08.002
- Mello, G. B. M., Soares, S., & Paton, J. J. (2015). A Scalable Population Code for Time in the Striatum. *Current Biology*, 25(9), 1113–1122. https://doi.org/10.1016/j.cub.2015.02.036
- Merchant, H., Harrington, D. L., & Meck, W. H. (2013). Neural basis of the perception and estimation of time. *Annual Review of Neuroscience*, *36*, 313–336. https://doi.org/10.1146/annurev-neuro-062012-170349
- Messina, M. M., Boersma, G., Overton, J. M., & Eckel, L. A. (2006). Estradiol decreases the orexigenic effect of melanin-concentrating hormone in ovariectomized rats. *Physiology and Behavior*, 88(4–5), 523–528. https://doi.org/10.1016/j.physbeh.2006.05.002
- Micevych, P. E., & Mermelstein, P. G. (2008). Membrane estrogen receptors acting through metabotropic glutamate receptors: An emerging mechanism of estrogen action in brain. *Molecular Neurobiology*, 38(1), 66–77. https://doi.org/10.1007/s12035-008-8034-z
- Mickelsen, L. E., Bolisetty, M., Chimileski, B. R., Fujita, A., Beltrami, E. J., Costanzo, J. T., Naparstek, J. R., Robson, P., & Jackson, A. C. (2019). Single-cell transcriptomic analysis of the lateral hypothalamic area reveals molecularly distinct populations of inhibitory and excitatory neurons. *Nature Neuroscience*, 22(4), 642–656. https://doi.org/10.1038/s41593-019-0349-8
- Mickelsen, L. E., Kolling, F. W., Chimileski, B. R., Fujita, A., Norris, C., Chen, K., Nelson, C. E., & Jackson, A. C. (2017). Neurochemical heterogeneity among lateral hypothalamic hypocretin/orexin and melanin-concentrating hormone neurons identified through single-cell gene expression analysis. *ENeuro*, *4*(5). https://doi.org/10.1523/ENEURO.0013-17.2017
- Mieda, M., & Yanagisawa, M. (2002). Sleep, feeding, and neuropeptides: Roles of orexins and orexin receptors. *Current Opinion in Neurobiology*, *12*(3), 339–345. https://doi.org/10.1016/S0959-4388(02)00331-8
- Mistlberger, R. E., Antle, M. C., Kilduff, T. S., & Jones, M. (2003). Food- and light-entrained circadian rhythms in rats with hypocretin-2-saporin ablations of the lateral hypothalamus. *Brain Research*, *980*(2), 161–168. https://doi.org/10.1016/S0006-8993(03)02755-0
- Mogenson, G. J., Jones, D. L., & Yim, C. Y. (1980). From motivation to action: Functional interface between the limbic system and the motor system. *Progress in Neurobiology*, *14*(2–3), 69–97. https://doi.org/10.1016/0301-0082(80)90018-0

- Mogenson, G. J., Swanson, L. W., & Wu, M. (1983). Neural projections from nucleus accumbens to globus pallidus, substantia innominata, and lateral preoptic-lateral hypothalamic area: An anatomical and electrophysiological investigation in the rat. *Journal of Neuroscience*, *3*(1), 189–202. https://doi.org/10.1523/jneurosci.03-01-00189.1983
- Montes, G. S., & Luque, E. H. (1988). Effects of Ovarian Steroids on vaginal smears in Rat. *Acta Anat*, *133*, 192–199.
- Monti, J. M., Torterolo, P., & Lagos, P. (2013). Melanin-concentrating hormone control of sleep-wake behavior. *Sleep Medicine Reviews*, *17*(4), 293–298. https://doi.org/10.1016/j.smrv.2012.10.002
- Morin, L. P., & Fleming, A. S. (1978). Variation of food intake and body weight with estrous cycle, ovariectomy, and estradiol benzoate treatment in hamsters (Mesocricetus auratus). *Journal of Comparative and Physiological Psychology*, 92(1), 1–6. https://doi.org/10.1037/h0077435
- Morita, T., Nishijima, T., & Tokura, H. (2005). Time sense for short intervals during the follicular and luteal phases of the menstrual cycle in humans. *Physiology and Behavior*, *85*(2), 93–98. https://doi.org/10.1016/j.physbeh.2005.02.024
- Morofushi, M., Shinohara, K., & Kimura, F. (2001). Menstrual and circadian variations in time perception in healthy women and women with premenstrual syndrome. *Neuroscience Research*, *41*(4), 339–344. https://doi.org/10.1016/S0168-0102(01)00290-5
- Murray, J. F., Baker, B. I., Levy, A., & Wilson, C. A. (2000). The influence of gonadal steroids on pre-pro melanin-concentrating hormone mRNA in female rats. *Journal of Neuroendocrinology*, *12*(1), 53–59. https://doi.org/10.1046/j.1365-2826.2000.00425.x
- Muschamp, J. W., & Hull, E. M. (2007). Melanin concentrating hormone and estrogen receptor-α are coexstensive but not coexpressed in cells of male rat hypothalamus. *Neuroscience Letters*, *427*(3), 123–126. https://doi.org/10.1016/j.neulet.2007.09.031
- Mystkowski, P., Seeley, R. J., Hahn, T. M., Baskin, D. G., Havel, P. J., Matsumoto, A. M., Wilkinson, C. W., Peacock-kinzig, K., Blake, K. A., & Schwartz, M. W. (2000). *Hypothalamic Melanin-Concentrating Hormone and Estrogen- Induced Weight Loss.* 20(22), 8637–8642.
- Nieuwenhuys, R., Geeraedts, L. M. G., & Veening, J. G. (1982). The medial forebrain bundle of the rat. I. General introduction. In *Journal of Comparative Neurology* (Vol. 206, Issue 1). https://doi.org/10.1002/cne.902060106

- Noble, E. E., Hahn, J. D., Konanur, V. R., Hsu, T. M., Page, S. J., Cortella, A. M., Liu, C. M., Song, M. Y., Suarez, A. N., Szujewski, C. C., Rider, D., Clarke, J. E., Darvas, M., Appleyard, S. M., & Kanoski, S. E. (2018). Control of Feeding Behavior by Cerebral Ventricular Volume Transmission of Melanin-Concentrating Hormone. *Cell Metabolism*, 28(1), 55-68.e7. https://doi.org/10.1016/j.cmet.2018.05.001
- Noble, E. E., Wang, Z., Liu, C. M., Davis, E. A., Suarez, A. N., Stein, L. M., Tsan, L., Terrill, S. J., Hsu, T. M., Jung, A. H., Raycraft, L. M., Hahn, J. D., Darvas, M., Cortella, A. M., Schier, L. A., Johnson, A. W., Hayes, M. R., Holschneider, D. P., & Kanoski, S. E. (2019). Hypothalamus-hippocampus circuitry regulates impulsivity via melanin-concentrating hormone. *Nature Communications*, *10*(1), 1–16. https://doi.org/10.1038/s41467-019-12895-y
- O'Connor, E. C., Kremer, Y., Lefort, S., Harada, M., Pascoli, V., Rohner, C., & Lüscher, C. (2015). Accumbal D1R Neurons Projecting to Lateral Hypothalamus Authorize Feeding. *Neuron*, *88*(3), 553–564. https://doi.org/10.1016/j.neuron.2015.09.038
- Olds, J., & Milner, P. (1954). Positive Reinforcement Produced By Electrical Stimulation of Septal Area and Other Regions of Rat Brain. *Journal of Comparative and Physiological Psychology*, 47(6), 419–427. https://doi.org/10.1037/h0058775
- Panfil, K., Deavours, A., & Kirkpatrick, K. (2023). Effects of the estrous cycle on impulsive choice and interval timing in female rats. *Hormones and Behavior*, 149(January), 105315. https://doi.org/10.1016/j.yhbeh.2023.105315
- Paxinos, G., & Watson, C. (1998). The rat brain in stereotaxic coordinates (4th edition) (Fourth). Academic Press.
- Petrovich, G. D. (2018). Lateral hypothalamus as a motivation-cognition interface in the control of feeding behavior. *Frontiers in Systems Neuroscience*, *12*(April), 1–7. https://doi.org/10.3389/fnsys.2018.00014
- Pfeffer, M., Plenzig, S., Gispert, S., Wada, K., Korf, H. W., & von Gall, C. (2012). Disturbed sleep/wake rhythms and neuronal cell loss in lateral hypothalamus and retina of mice with a spontaneous deletion in the ubiquitin carboxyl-terminal hydrolase L1 gene. *Neurobiology of Aging*, 33(2), 393–403. https://doi.org/10.1016/j.neurobiologing.2010.02.019
- Pissios, P., Bradley, R. L., & Maratos-Flier, E. (2006). Expanding the scales: The multiple roles of MCH in regulating energy balance and other biological functions. *Endocrine Reviews*, 27(6), 606–620. https://doi.org/10.1210/er.2006-0021
- Pissios, P., Frank, L., Kennedy, A. R., Porter, D. R., Marino, F. E., Liu, F. F., Pothos, E. N., & Maratos-Flier, E. (2008). Dysregulation of the Mesolimbic Dopamine System and Reward in MCH-/- Mice. *Biological Psychiatry*, *64*(3), 184–191. https://doi.org/10.1016/j.biopsych.2007.12.011

- Pleil, K. E., Cordes, S., Meck, W. H., & Williams, L. C. (2011). Rapid and acute effects of estrogen on time perception in male and female rats. *Frontiers in Integrative Neuroscience*, *5*(October), 1–15. https://doi.org/10.3389/fnint.2011.00063
- Qu, D., Ludwig, D. S., Gammeltoft, S., Piper, M., Pelleymounter, M. a, Cullen, M. J., Mathes, W. F., Przypek, R., Kanarek, R., & Maratos-Flier, E. (1996). A role for melanin-concentrating hormone in the central regulation of feeding behaviour. *Nature*, *380*(6571), 243–247. https://doi.org/10.1038/380243a0
- Qualls-Creekmore, E., & Münzberg, H. (2018). Modulation of feeding and associated behaviors by lateral hypothalamic circuits. *Endocrinology*, *159*(11), 3631–3642. https://doi.org/10.1210/en.2018-00449
- Quigley, J. A., Logsdon, M. K., Graham, B. C., Beaudoin, K. G., & Becker, J. B. (2021). Activation of G protein-coupled estradiol receptor 1 in the dorsolateral striatum enhances motivation for cocaine and drug-induced reinstatement in female but not male rats. *Biology of Sex Differences*, *12*(1), 1–11. https://doi.org/10.1186/s13293-021-00389-w
- Rakitin, B. C., Penney, T. B., Gibbon, J., Malapani, C., Hinton, S. C., & Meck, W. H. (1998). Scalar expectancy theory and peak-interval timing in humans. *Journal of Experimental Psychology: Animal Behavior Processes*, 24(1), 15–33. https://doi.org/10.1037/0097-7403.24.1.15
- Reppert, S. M., & Weaver, D. R. (2002). Coordination of circadian timing in mammals. *Nature*, *418*(August), 935–941.
- Roberts, S. (1981). Isolation of an internal clock. *Journal of Experimental Psychology: Animal Behavior Processes*, 7(3), 242–268. https://doi.org/10.1037/0097-7403.7.3.242
- Roberts, S., & Church, R. M. (1978). Control of an internal clock. *Journal of Experimental Psychology: Animal Behavior Processes*, *4*(4), 318–337. https://doi.org/10.1037//0097-7403.4.4.318
- Robinson, T. E., Becker, J. B., & Ramirez, V. D. (1980). Sex differences in amphetamine-elicited rotational behavior and the lateralization of striatal dopamine in rats. *Brain Research Bulletin*, *5*(5), 539–545. https://doi.org/10.1016/0361-9230(80)90260-9
- Ross, L., & Santi, A. (2000). The effects of estrogen on temporal and numerical processing in ovariectomized female rats. *Psychobiology*, *28*(3), 394–405. https://doi.org/10.3758/BF03331997
- Roth, B. L. (2016). DREADDs for Neuroscientists. Neuron, 89(4), 683-694.

- https://doi.org/10.1016/j.neuron.2016.01.040
- Saito, Y., Nothacker, H., Wang, Z., Lin, S. H. S., Leslie, F., & Civelli, O. (1999). Molecular characterization of the melanin-concentrating- hormone receptor. *Letters to Nature*, *400*(July), 265–269.
- Sandstrom, N. J. (2007). Estradiol Modulation of the Speed of an Internal Clock. *Behavioral Neuroscience*, 121(2), 422–432. https://doi.org/10.1037/0735-7044.121.2.422
- Santollo, J., & Eckel, L. A. (2008). The orexigenic effect of melanin-concentrating hormone (MCH) is influenced by sex and stage of the estrous cycle. *Physiology and Behavior*, 93(4–5), 842–850. https://doi.org/10.1016/j.physbeh.2007.11.050
- Santollo, J., & Eckel, L. A. (2013). Oestradiol Decreases Melanin-Concentrating Hormone (MCH) and MCH Receptor Expression in the Hypothalamus of Female Rats. *Journal of Neuroendocrinology*, *25*(6), 570–579. https://doi.org/10.1111/jne.12032
- Saper, C.B., Swanson, L. W., & Cowan, W. M. (1979). An Autoradiographic Study of the Efferent Connections of the Lateral Hypothalamic Area in the Rat. *Journal of Comparative Neurology*, *183*(4), 689–706.
- Saper, Clifford B, Chou, T. C., & Elmquist, J. K. (2002). Review The Need to Feed: Homeostatic and Hedonic Control of Eating mechanisms that underlie regulation of feeding and make it such a rewarding experience (Figure 1). *Neuron*, 36, 199–211. https://ac-els-cdn-com.ep.fjernadgang.kb.dk/S0896627302009698/1-s2.0-S0896627302009698-main.pdf?_tid=fdb2abcc-804f-469e-a02d-22863bcb04cd&acdnat=1536577440_61c910faaf6419f9c0a00c7a54d2ea35
- Schneider, B. A. (1969). A Two-State Analysis of Fixed-Interval Responding in the Pigeion. *Journal of Experimental Analysis of Behavior*, 12, 677–687.
- Sherwood, A., Holland, P. C., Adamantidis, A., & Johnson, A. W. (2015). Deletion of Melanin Concentrating Hormone Receptor-1 disrupts overeating in the presence of food cues. *Physiology and Behavior*, 152, 402–407. https://doi.org/10.1016/j.physbeh.2015.05.037
- Sherwood, A., Wosiski-Kuhn, M., Nguyen, T., Holland, P. C., Lakaye, B., Adamantidis, A., & Johnson, A. W. (2012). The role of melanin-concentrating hormone in conditioned reward learning. *European Journal of Neuroscience*, *36*(8), 3126–3133. https://doi.org/10.1111/j.1460-9568.2012.08207.x
- Shimada, M., Tritos, N. A., Lowell, B. B., Flier, J. S., & Maratos-Flier, E. (1998). Mice lacking melanin-concentrating hormone receptor are hypophagic and lean. *Nature*, 396(December), 670–674.

- Shughrue, P. J., Lane, M. V, & Merchenthaler, I. (1997). Comparative Distribution of Estrogen Receptor- a and B mRNA in Rat CNS. *The Journal of Comparative Neurology*, 388, 507–525.
- Skinner, B. F. (1938). *The Behavior of Organisms*. https://doi.org/10.1037/13145-003
- Smith, G. P. (2001). John Davis and the meanings of licking. *Appetite*, *36*(1), 84–92. https://doi.org/10.1006/appe.2000.0371
- Stelzer, G., Rosen, N., Plaschkes, I., Zimmerman, S., Twik, M., Fishilevich, S., Stein, T. I., Nudel, R., Lieder, I., Mazor, Y., Kaplan, S., Dahary, D., Warshawsky, D., Guangolan, Y., Kohn, A., Rappaport, N., & Safran, M. (2016). *The GeneCards Suite:*From Gene Data Mining to Disease Genome Sequence Analyses. June, 1–33. https://doi.org/10.1002/cpbi.5
- Stratford, T. R., & Kelley, A. E. (1997). GABA in the nucleus accumbens shell participates in the central regulation of feeding behavior. *Journal of Neuroscience*, 17(11), 4434–4440. https://doi.org/10.1523/jneurosci.17-11-04434.1997
- Stuber, G. D., & Wise, R. A. (2016). Lateral hypothalamic circuits for feeding and reward. *Nature Neuroscience*, 19(2), 198–205. https://doi.org/10.1038/nn.4220
- Subramanian, K. S., Lauer, L. T., Hayes, A. M. R., Décarie-spain, L., Mcburnett, K., Nourbash, A. C., Donohue, K. N., Kao, A. E., Bashaw, A. G., Burdakov, D., Noble, E. E., Schier, L. A., & Kanoski, S. E. (2023). *Hypothalamic melanin-concentrating hormone neurons integrate food-motivated appetitive and consummatory processes in rats*. 1–14. https://doi.org/10.1038/s41467-023-37344-9
- Swanson, L. W., Sanchez-Watts, G., & Watts, A. G. (2005). Comparison of melanin-concentrating hormone and hypocretin/orexin mRNA expression patterns in a new parceling scheme of the lateral hypothalamic zone. *Neuroscience Letters*, 387(2), 80–84. https://doi.org/10.1016/j.neulet.2005.06.066
- Tan, C. P., Sano, H., Iwaasa, H., Pan, J., Sailer, A. W., Hreniuk, D. L., Feighner, S. D., Palyha, O. C., Pong, S. S., Figueroa, D. J., Austin, C. P., Jiang, M. M., Yu, H., Ito, J., Ito, M., Ito, M., Guan, X. M., MacNeil, D. J., Kanatani, A., ... Howard, A. D. (2002). Melanin-concentrating hormone receptor subtypes 1 and 2: Species-specific gene expression. *Genomics*, 79(6), 785–792. https://doi.org/10.1006/geno.2002.6771
- ter Haar, M. B. (1972). Circadian and estrual rhythms in food intake in the rat. *Hormones and Behavior*, *3*(3), 213–219. https://doi.org/10.1016/0018-506X(72)90034-7
- Terrill, S. J., Subramanian, K. S., Lan, R., Liu, C. M., Cortella, A. M., Noble, E. E., &

- Kanoski, S. E. (2020). Nucleus accumbens melanin-concentrating hormone signaling promotes feeding in a sex-specific manner. *Neuropharmacology*, *178*, 108270. https://doi.org/10.1016/j.neuropharm.2020.108270
- Toran-Allerand, C. D. (2004). Minireview: A Plethora of Estrogen Receptors in the Brain: Where Will It End? *Endocrinology*, *145*(3), 1069–1074. https://doi.org/10.1210/en.2003-1462
- Toran-Allerand, C. D., Guan, X., MacLusky, N. J., Horvath, T. L., Diano, S., Singh, M., Connolly, E. S., Nethrapalli, I. S., & Tinnikov, A. A. (2002). ER-X: A novel, plasma membrane-associated, putative estrogen receptor that is regulated during development and after ischemic brain injury. *Journal of Neuroscience*, 22(19), 8391–8401. https://doi.org/10.1523/jneurosci.22-19-08391.2002
- Turek, F. W., Joshu, C., Kohsaka, A., Lin, E., Ivanova, G., Mcdearmon, E., Laposky, A., Losee-olson, S., Easton, A., Jensen, D. R., Eckel, R. H., Takahashi, J. S., & Bass, J. (2005). *Obesity and Metabolic Syndrome in Circadian Clock Mutant Mice*. 308(May), 1043–1046.
- Valenstein, E. S., Cox, V. C., & Kakolewski, J. W. (1968). Modification of Motivated Behavior Elicited by Electrical Stimulation of the Hypothalamus. *Science*, *159*(3819), 1119–1121.
- Varma, M., Chai, J. K., Meguid, M. M., Laviano, A., Gleason, J. R., Yang, Z. J., & Blaha, V. (1999). Effect of estradiol and progesterone on daily rhythm in food intake and feeding patterns in Fischer rats. *Physiology and Behavior*, 68(1–2), 99–107. https://doi.org/10.1016/S0031-9384(99)00152-3
- Williams, C. L. (2011). Sex differences in counting and timing. *Frontiers in Integrative Neuroscience*, *5*(DECEMBER), 1–4. https://doi.org/10.3389/fnint.2011.00088
- Zamorano, F., Billeke, P., Hurtado, J. M., López, V., Carrasco, X., Ossandón, T., & Aboitiz, F. (2014). Temporal constraints of behavioral inhibition: Relevance of interstimulus interval in a go-nogo task. *PLoS ONE*, 9(1). https://doi.org/10.1371/journal.pone.0087232
- Zhou, D., Shen, Z., Strack, A. M., Marsh, D. J., & Shearman, L. P. (2005). Enhanced running wheel activity of both Mch1r- and Pmch-deficient mice. *Regulatory Peptides*, 124(1–3), 53–63. https://doi.org/10.1016/j.regpep.2004.06.026

APPENDIX

Chapter 2 Supplemental Materials

 Table S2.1 Results from the overall model examining estrous cycle within vehicle.

	F	df	р
Pre-peak:			_
Estrous	0.372	239.983	0.543
Time	65.264	1326.782	<.001
Time ²	0.304	1938.129	0.581
Time ³	3.499	2670.165	0.061
Estrous x time	0.004	1326.782	0.95
Estrous x time ²	0.326	1938.129	0.568
Estrous x time ³	0.045	2670.165	0.831
Post-peak:			
Estrous	0.089	174.311	0.766
Time	32.686	499.686	<.001
Time ²	14.096	637.7	<.001
Time ³	3.36	1241.077	0.067
Estrous x time	0.033	499.686	0.856
Estrous x time ²	0.375	637.7	0.54
Estrous x time ³	0.194	1241.077	0.66

Table S2.2 Results from the interaction model examining effects of time within vehicle treated rats tested in P/E and M/D.

	F	df	р	Regression slope (b)	standard error (se)
Pre-peak P/E:					
Intercept	29.241	244.997	<.001	0.410928	0.075992
Time	30.25	1377.804	<.001	0.062273	0.011322
Time ²	0.538	2065.577	0.463	0.000628	0.000856
Time ³	1.106	2717.457	0.293	-0.000122	0.000116
Pre-peak M/D:					
Intercept	40.38	234.978	<.001	0.475981	0.074904
Time	35.333	1271.433	<.001	0.063246	0.01064
Time ²	0	1764.583	0.988	-1.089E-05	0.00072
Time ³	2.864	2582.134	0.091	-0.000154	9.0901E-05
Post-peak P/E:					
Intercept	5.864	174.361	0.016	0.156647	0.064689
Time	15.128	503.14	<.001	-0.022848	0.005874
Time ²	9.642	633.292	0.002	0.00059	0.00019
Time ³	0.955	1245.794	0.329	1.3229E-05	1.354E-05
Post-peak M/D:					
Intercept	8.095	174.261	0.005	0.183905	0.064639
Time	17.622	496.179	<.001	-0.024352	0.005801
Time ²	4.881	642.053	0.028	0.000424	0.000192
Time ³	2.626	1236.227	0.105	2.1591E-05	1.3323E-05

Table S2.3 Results from the overall models examining estrous cycle within vehicle at 5s intervals.

			df	p
		·	<u> </u>	Р
5s	Estrous	0.075	276.246	0.784
	Time	52.608	1437.004	<.001
	Time ²	4.052	2679.487	0.044
	Time ³	9.858	2790.363	0.002
	Estrous x time	0.003	1437.004	0.959
	Estrous x time ²	0.026	2679.487	0.871
	Estrous x time ³	0.021	2790.363	0.884
10s	Estrous	0.061	242.194	0.806
	Time	83.33	1338.594	<.001
	Time ²	0.193	2293.232	0.661
	Time ³	9.858	2790.363	0.002
	Estrous x time	0.021	1338.594	0.884
	Estrous x time ²	0.02	2293.232	0.887
	Estrous x time ³	0.021	2790.363	0.884
15s	Estrous	2.978	272.248	0.086
	Time	44.83	1346.098	<.001
	Time ²	11.401	2776.309	<.001
	Time ³	7.24	2794.018	0.007
	Estrous x time	0.357	1346.098	0.55
	Estrous x time ²	0.589	2776.309	0.443
	Estrous x time ³	0.297	2794.018	0.586
20s	Estrous	2.111	243.658	0.148
	Time	35.574	862.511	<.001
	Time ²	0.024	2084.304	0.876
	Time ³	0.025	2511.09	0.874
	Estrous x time	0.968	862.511	0.325
	Estrous x time ²	1.87	2084.304	0.172
	Estrous x time ³	0.529	2511.09	0.467
25s	Estrous	0.77	238.624	0.381
	Time	64.073	1170.708	<.001
	Time ²	0.243	1827.767	0.622
	Time ³	1.826	2597.625	0.177
	Estrous x time	0.467	1170.708	0.494
	Estrous x time ²	0.185	1827.767	0.667
	Estrous x time ³	0.388	2597.625	0.534
30s	Estrous	0.466	242.314	0.496
	Time	61.366	1344.277	<.001

Table S2.3 (cont'd)

	Time ²	0.15	1777.786	0.698
	Time ³	3.536	2615.946	0.06
	Estrous x time	0.022	1344.277	0.882
	Estrous x time ²	0.271	1777.786	0.602
	Estrous x time ³	0.052	2615.946	0.82
35s	Estrous	0.466	242.314	0.496
	Time	61.366	1344.277	<.001
	Time ²	0.15	1777.786	0.698
	Time ³	3.536	2615.946	0.06
	Estrous x time	0.022	1344.277	0.882
	Estrous x time ²	0.271	1777.786	0.602
	Estrous x time ³	0.052	2615.946	0.82
40s	Estrous	26.48	246.256	0.496
	Time	27.575	1344.277	<.001
	Time ²	0.357	1777.786	0.698
	Time ³	1.099	2615.946	0.06
	Estrous x time	38.429	1344.277	0.882
	Estrous x time ²	34.288	1777.786	0.602
	Estrous x time ³	0.011	2615.946	0.82

Table S2.4 Results from the interaction models examining estrous cycle within vehicle at 5s intervals.

		F	df	р	Regression slope (b)	standard error (se)
5s P/E:	Intercept	4.574	282.849	0.033	0.17128	0.080086
	Time	25.903	1434.992	<.001	0.053641	0.01054
	Time ²	2.125	2674.622	0.145	0.002801	0.001921
	Time ³	4.417	2784.029	0.036	-0.000198	9.4009E-05
5s M/D:	Intercept	6.655	269.572	0.01	0.201969	0.078291
	Time	26.708	1439.024	<.001	0.054401	0.010526
	Time ²	1.931	2685.523	0.165	0.002383	0.001715
	Time ³	5.759	2799.817	0.016	-0.00018	7.5037E-05
10s P/E:	Intercept	41.436	242.554	<.001	0.484817	0.075316
	Time	38.488	1344.466	<.001	0.066834	0.010773
	Time ²	0.043	2325.075	0.837	-0.000163	0.000788
	Time ³	4.417	2784.029	0.036	-0.000198	9.4009E-05
10s M/D:	Intercept	46.133	241.835	<.001	0.511036	0.075239
	Time	45.714	1331.197	<.001	0.064724	0.009573
	Time ²	0.175	2258.8	0.676	-0.000318	0.000761
	Time ³	5.759	2799.817	0.016	-0.00018	7.5037E-05
15s P/E:	Intercept	90.402	270.813	<.001	0.789514	0.083037
	Time	25.041	1518.543	<.001	0.050189	0.01003
	Time ²	6.273	2779.731	0.012	-0.003116	0.001244
	Time ³	4.309	2803.359	0.038	-0.000196	9.4613E-05
15s M/D:	Intercept	69.405	274.174	<.001	0.599857	0.072003
	Time	19.823	1175.501	<.001	0.04196	0.009424
	Time ²	5.392	2768.679	0.02	-0.001962	0.000845
	Time ³	2.933	2778.355	0.087	-0.00013	7.6059E-05
20s P/E:	Intercept	22.163	241.854	<.001	0.396332	0.084187
	Time	23.088	889.565	<.001	0.042124	0.008767
	Time ²	1.207	2111.114	0.272	0.001151	0.001048
	Time ³	0.152	2497.711	0.697	2.4309E-05	6.2355E-05
20s M/D:	Intercept	46.018	245.496	<.001	0.569005	0.083878
	Time	12.994	834.079	<.001	0.030195	0.008376
	Time ²	0.707	2059.542	0.401	-0.000916	0.001089
	Time ³	0.419	2526.084	0.518	-3.789E-05	5.8558E-05
25s P/E:	Intercept	25.567	242.948	<.001	0.393172	0.077758
	Time	27.216	1416.741	<.001	0.060161	0.011532
	Time ²	0.358	1936.315	0.55	0.000518	0.000866
	Time ³	1.078	2665.554	0.299	-0.000124	0.00012
25s M/D:	Intercept	41.353	234.214	<.001	0.488577	0.075977
	Time	43.699	778.542	<.001	0.050696	0.007669
	Time ²	0.002	1675.061	0.961	3.5218E-05	0.000713

Table S2.4 (cont'd)

	Time ³	1.378	1806.83	0.241	-4.582E-05	3.9037E-05
30s P/E:	Intercept	26.48	246.256	<.001	0.430583	0.053715
	Time	27.575	1396.705	<.001	-0.036651	0.053715
	Time ²	0.357	1911.721	0.55	0.06142	0.007841
	Time ³	1.099	2650.47	0.295	0.00022	0.000567
30s M/D:	Intercept	44.883	201.424	<.001	0.458512	0.06844
	Time	28.515	421.285	<.001	-0.025844	0.00484
	Time ²	1.433	1373.365	0.231	-0.000377	0.000315
	Time ³	5.167	1388.455	0.023	2.6251E-05	1.1548E-05
35s P/E:	Intercept	21.211	181.636	<.001	0.300112	0.065163
	Time	28.374	469.314	<.001	-0.029491	0.005536
	Time ²	0.668	908.95	0.414	0.000178	0.000217
	Time ³	3.895	1317.578	0.049	2.4911E-05	1.2622E-05
35s M/D:	Intercept	25.441	178.927	<.001	0.323158	0.064069
	Time	25.65	473.044	<.001	-0.027641	0.005458
	Time ²	0.008	982.323	0.929	1.7238E-05	0.000195
	Time ³	5.167	1388.455	0.023	2.6251E-05	1.1548E-05
40s P/E:	Intercept	26.48	246.256	<.001	0.393932	0.076553
	Time	27.575	1396.705	<.001	0.060252	0.011474
	Time ²	0.357	1911.721	0.55	0.000515	0.000862
	Time ³	1.099	2650.47	0.295	-0.000125	0.000119
40s M/D:	Intercept	8.598	176.354	0.004	0.188667	0.064342
	Time	22.18	488.893	<.001	-0.0255	0.005414
	Time ²	4.576	719.182	0.033	0.000411	0.000192
	Time ³	5.167	1388.455	0.023	2.6251E-05	1.1548E-05

 Table S2.5
 Results from the overall model examining drug treatment within P/E.

	F	df	р
Pre-peak:			_
Drug	0.047	232.575	0.828
Time	59.179	1365.987	<.001
Time ²	1.688	2041.091	0.194
Time ³	2.223	2713.98	0.136
Drug x time	0.075	1365.987	0.785
Drug x time ²	0.038	2041.091	0.845
Drug x time ³	0.03	2713.98	0.863
Post-peak:			
Drug	25.845	536.238	<.001
Time	14.223	688.659	<.001
Time ²	2.251	1379.884	0.134
Time ³	0.043	170.805	0.837
Drug x time	0.046	536.238	0.831
Drug x time ²	0.103	688.659	0.749
Drug x time ³	0.027	1379.884	0.87

Table S2.6 Results from the interaction model examining drug treatment within P/E.

	F	df	р	Regression slope (b)	standard error (se)
Pre-peak P/E:					
Intercept	26.474	237.682	<.001	0.410428	0.079768
Table S2.6 (cor	nt'd)				
Time	29.161	1450.839	<.001	0.062061	0.011493
Time ²	0.515	2153.858	0.473	0.00062	0.000863
Time ³	1.07	2754.569	0.301	-0.000121	0.000117
Pre-peak M/D:					
Intercept	24.178	227.471	<.001	0.386111	0.078523
Time	30.183	1271.489	<.001	0.057801	0.010521
Time ²	1.368	1880.777	0.242	0.000839	0.000717
Time ³	1.23	2626.688	0.268	-9.571E-05	8.631E-05
Post-peak P/E:					
Intercept	5.325	169.781	0.022	0.158222	0.068564
Time	14.321	527.6	<.001	-0.022939	0.006062
Time ²	8.878	672.116	0.003	0.000581	0.000195
Time ³	0.961	1350.168	0.327	1.349E-05	1.3761E-05
Post-peak M/D:					
Intercept	4.007	171.824	0.047	0.138164	0.06902
Time	11.625	544.719	<.001	-0.021089	0.006185
Time ²	5.633	703.883	0.018	0.00049	0.000207
Time ³	1.294	1406.277	0.256	1.6784E-05	1.4757E-05

Table S2.7 Results from the overall models examining drug (VEH, CNO) during P/E at 5s intervals.

		F	df	р
.	Davis	0.000	064.007	0.007
5s	Drug Time	0.028 42.406	264.307 1497.739	0.867 <.001
	Time ²	3.528	2696.84	0.06
	Time ³	7.052	2804.575	0.008
		0.326	1497.739	0.568
	Drug x time Drug x time ²	0.320	2696.84	0.366
	Drug x time ³	0.093	2804.575	0.761
100	_	0.409	235.14	
10s	Drug Time	73.886	235.14 1318.461	0.523 <.001
	Time ²	0.02	2365.82	0.888
	Time ³	7.052	2804.575	0.008
	Drug x time	0.486	1318.461	0.486
	Drug x time ²	0.203	2365.82	0.653
	Drug x time ³	0.541	2804.575	0.462
15s	Drug X time	3.986	260.022	0.402
103	Time	47.484	1397.062	<.001
	Time ²	8.029	2774.13	0.005
	Time ³	6.15	2801.157	0.013
	Drug x time	0.087	1397.062	0.768
	Drug x time ²	2.232	2774.13	0.135
	Drug x time ³	0.798	2801.157	0.372
20s	Drug	0.206	236.562	0.65
	Time	45.14	904.926	<.001
	Time ²	1.156	2142.29	0.282
	Time ³	0.033	2544.887	0.855
	Drug x time	0.051	904.926	0.821
	Drug x time ²	0.323	2142.29	0.57
	Drug x time ³	0.184	2544.887	0.668
25s	Drug	0.011	231.584	0.916
	Time	58.42	1221.622	<.001
	Time ²	0.808	1933.017	0.369
	Time ³	1.367	2649.329	0.242
	Drug x time	0.764	1221.622	0.382
	Drug x time ²	0.001	1933.017	0.979
	Drug x time ³	0.555	2649.329	0.456
30s	Drug	0.029	233.978	0.866
	Time	54.628	1386.611	<.001
	Time ²	1.311	1892.158	0.252

Table S2.7 (cont'd)

	Time ³	2.187	2663.537	0.139
	Drug x time	0.047	1386.611	0.828
	Drug x time ²	0.05	1892.158	0.824
	Drug x time ³	0.024	2663.537	0.876
35s	Drug	0.029	233.978	0.866
	Time	54.628	1386.611	<.001
	Time ²	1.311	1892.158	0.252
	Time ³	2.187	2663.537	0.139
	Drug x time	0.047	1386.611	0.828
	Drug x time ²	0.05	1892.158	0.824
	Drug x time ³	0.024	2663.537	0.876
40s	Drug	23.628	238.903	0.866
	Time	26.484	1386.611	<.001
	Time ²	0.361	1892.158	0.252
	Time ³	1.033	2663.537	0.139
	Drug x time	22.088	1386.611	0.828
	Drug x time ²	28.365	1892.158	0.824
	Drug x time ³	1.139	2663.537	0.876

Table S2.8 Results from the interaction model examining the effects of drug (VEH, CNO) during P/E at 5s intervals.

					_	
		F	df	р	Regression slope (b)	standard error (se)
5s VEH:	Intercept	4.25	272.913	0.04	0.17285	0.083848
	Time	25.045	1485.706	<.001	0.053567	0.010704
	Time ²	2.055	2724.516	0.152	0.002767	0.00193
	Time ³	4.317	2811.623	0.038	-0.000196	9.4318E-05
5s CNO:	Intercept	3.49	255.719	0.063	0.153154	0.081982
	Time	17.676	1509.901	<.001	0.044934	0.010688
	Time ²	1.473	2655.395	0.225	0.001994	0.001643
	Time ³	2.759	2789.303	0.097	-0.000111	6.6821E-05
10s VEH:	Intercept	37.592	234.913	<.001	0.485368	0.079163
	Time	36.926	1412.648	<.001	0.066541	0.01095
	Time ²	0.047	2405.077	0.828	-0.000172	0.000794
	Time ³	4.317	2811.623	0.038	-0.000196	9.4318E-05
10s CNO:	Intercept	27.365	235.369	<.001	0.413813	0.079106
	Time	37.552	1197.173	<.001	0.056555	0.009229
	Time ²	0.177	2324.852	0.674	0.00033	0.000783
	Time ³	2.759	2789.303	0.097	-0.000111	6.6821E-05
15s VEH:	Intercept	86.278	266.525	<.001	0.789023	0.084945
	Time	24.597	1553.309	<.001	0.050051	0.010092
	Time ²	6.238	2791.729	0.013	-0.003108	0.001245
	Time ³	4.271	2816.533	0.039	-0.000196	9.4628E-05
15s CNO:	Intercept	56.229	252.022	<.001	0.562726	0.075044
	Time	22.889	1243.134	<.001	0.045948	0.009604
	Time ²	1.798	2711.189	0.18	-0.000962	0.000718
	Time ³	1.884	2764.624	0.17	-9.198E-05	6.7007E-05
20s VEH:	Intercept	20.569	235.503	<.001	0.393868	0.086844
	Time	22.801	919.974	<.001	0.042411	0.008882
	Time ²	1.228	2189.665	0.268	0.001166	0.001052
	Time ³	0.166	2550.355	0.684	2.5425E-05	6.2496E-05
20s CNO:	Intercept	27.245	237.646	<.001	0.449436	0.086104
	Time	22.366	888.405	<.001	0.039646	0.008383
	Time ²	0.143	2084.395	0.706	0.000359	0.000951
	Time ³	0.035	2537.763	0.852	-1.025E-05	5.4917E-05
25s VEH:	Intercept	22.91	236.113	<.001	0	0
	Time	26.162	1493.523	<.001	0.390766	0.081639
	Time ²	0.361	2026.694	0.548	0.059899	0.011711
	Time ³	1.015	2712.69	0.314	0.000526	0.000875
25s CNO:	Intercept	25.472	226.98	<.001	-0.000121	0.00012
	Time	37.343	793.768	<.001	0.402856	0.079821
	Time ²	0.467	1800.66	0.495	0.047608	0.007791

Table S2.8 (cont'd)

	Time ³	0.459	1866.364	0.498	0.000496	0.000726
30s VEH:	Intercept	23.628	238.903	<.001	0.381842	0.056477
	Time	26.484	1477.058	<.001	0.009557	0.056477
	Time ²	0.361	2006.41	0.548	0.058256	0.007882
	Time ³	1.033	2702.394	0.309	0.00065	0.000568
30s CNO:	Intercept	31.07	201.025	<.001	0.411853	0.073888
	Time	23.141	453.943	<.001	-0.024265	0.005044
	Time ²	0.851	1499.161	0.357	-0.000355	0.000385
	Time ³	3.756	1556.809	0.053	2.548E-05	1.3147E-05
35s VEH:	Intercept	19.306	176.092	<.001	0.303885	0.069161
	Time	26.58	491.347	<.001	-0.029539	0.00573
	Time ²	0.514	967.362	0.474	0.000159	0.000222
	Time ³	3.906	1426.449	0.048	2.535E-05	1.2827E-05
35s CNO:	Intercept	16.841	179.341	<.001	0.284831	0.069407
	Time	20.503	502.759	<.001	-0.025906	0.005721
	Time ²	0.013	1138.357	0.909	2.6976E-05	0.000235
	Time ³	3.756	1556.809	0.053	2.548E-05	1.3147E-05
40s VEH:	Intercept	23.628	238.903	<.001	0.391399	0.080521
	Time	26.484	1477.058	<.001	0.059964	0.011652
	Time ²	0.361	2006.41	0.548	0.000524	0.000872
	Time ³	1.033	2702.394	0.309	-0.000122	0.00012
40s CNO:	Intercept	5.379	171.928	0.022	0.159158	0.068626
	Time	16.277	539.627	<.001	-0.023726	0.005881
	Time ²	4.183	771.938	0.041	0.000409	0.0002
	Time ³	3.756	1556.809	0.053	2.548E-05	1.3147E-05

Table S2.9 Results from the overall model examining drug treatment within M/D.

	F	df	р
Pre-peak:			
Drug	0.245	236.66	0.621
Time	70.478	1263.682	<.001
Time ²	0.257	1744.578	0.612
Time ³	4.72	2554.977	0.03
Drug x time	0.003	1263.682	0.959
Drug x time ²	0.276	1744.578	0.6
Drug x time ³	0.04	2554.977	0.841
Post-peak:			
Drug	0.134	174.29	0.715
Time	42.529	483.83	<.001
Time ²	8.639	621.096	0.003
Time ³	8.033	1189.501	0.005
Drug x time	0.208	483.83	0.649
Drug x time ²	0.093	621.096	0.76
Drug x time ³	0.209	1189.501	0.647

Table S2.10 Results from the interaction model examining drug treatment within M/D.

	F	df	р	Regression slope (b)	standard error (se)
Pre-peak P/E:					
Intercept	41.713	236.243	<.001	0.476073	0.073712
Time	35.954	1253.967	<.001	0.063287	0.010555
Time ²	0	1742.861	0.99	-9.397E-06	0.000715
Time ³	2.906	2566.263	0.088	-0.000154	9.0431E-05
Pre-peak M/D:					
Intercept	33.044	237.077	<.001	0.424479	0.073843
Time	34.539	1273.325	<.001	0.062524	0.010639
Time ²	0.51	1746.152	0.475	0.000534	0.000747
Time ³	1.886	2544.245	0.17	-0.000128	9.3263E-05
Post-peak P/E:					
Intercept	8.359	175.169	0.004	0.183521	0.063476
Time	18.027	490.337	<.001	-0.024339	0.005732
Time ²	5.037	632.904	0.025	0.000426	0.00019
Time ³	2.66	1212.484	0.103	2.1551E-05	1.3215E-05
Post-peak M/D:					
Intercept	11.749	173.407	<.001	0.216243	0.063087
Time	24.849	477.177	<.001	-0.027995	0.005616
Time ²	3.631	608.518	0.057	0.000346	0.000182
Time ³	5.776	1164.074	0.016	2.9845E-05	1.2418E-05

Table S2.11 Results from the overall models examining drug (VEH, CNO) during M/D at 5s intervals.

		F	df	р
	_			
5s	Drug	0.011	272.127	0.916
	Time	52.751	1439.288	<.001
	Time ²	2.243	2686.017	0.134
	Time ³	7.21	2797.677	0.007
	Drug x time	0.007	1439.288	0.935
	Drug x time ²	0.194	2686.017	0.659
	Drug x time ³	0.41	2797.677	0.522
10s	Drug	0.015	242.855	0.903
	Time	79.58	1368.551	<.001
	Time ²	0.398	2268.58	0.528
	Time ³	7.21	2797.677	0.007
	Drug x time	0.249	1368.551	0.618
	Drug x time ²	0.002	2268.58	0.967
	Drug x time ³	0.41	2797.677	0.522
15s	Drug	0.003	267.535	0.955
	Time	42.39	1218.29	<.001
	Time ²	7.58	2775.304	0.006
	Time ³	4.652	2778.648	0.031
	Drug x time	0.108	1218.29	0.742
	Drug x time ²	0.205	2775.304	0.651
	Drug x time ³	0.038	2778.648	0.846
20s	Drug	0.984	245.306	0.322
	Time	41.781	842.279	<.001
	Time ²	0	2076.088	0.994
	Time ³	0.217	2520.711	0.642
	Drug x time	2.055	842.279	0.152
	Drug x time ²	1.413	2076.088	0.235
	Drug x time ³	0.187	2520.711	0.666
25s	Drug	0.544	237.419	0.462
	Time	73.132	1081.248	<.001
	Time ²	0.339	1627.39	0.56
	Time ³	2.723	2435.242	0.099
	Drug x time	0.68	1081.248	0.41
	Drug x time ²	0.258	1627.39	0.611
	Drug x time ³	0.576	2435.242	0.448
30s	Drug	0.289	241.027	0.591
	Time	68.489	1271.952	<.001
	Time ²	0.214	1581.628	0.643

Table S2.11 (cont'd)

	 : 3	4.005	0500 005	0.000
	Time ³	4.605	2522.825	0.032
	Drug x time	0.005	1271.952	0.944
	Drug x time ²	0.369	1581.628	0.544
	Drug x time ³	0.069	2522.825	0.793
35s	Drug	0.289	241.027	0.591
	Time	68.489	1271.952	<.001
	Time ²	0.214	1581.628	0.643
	Time ³	4.605	2522.825	0.032
	Drug x time	0.005	1271.952	0.944
	Drug x time ²	0.369	1581.628	0.544
	Drug x time ³	0.069	2522.825	0.793
40s	Drug	40.132	240.594	0.591
	Time	35.059	1271.952	<.001
	Time ²	0.011	1581.628	0.643
	Time ³	2.992	2522.825	0.032
	Drug x time	30.971	1271.952	0.944
	Drug x time ²	33.446	1581.628	0.544
	Drug x time ³	0.548	2522.825	0.793

Table S2.12 Results from the interaction model examining the effects of drug (VEH, CNO) during M/D at 5s intervals.

	F	df	р	Regression slope (b)	standard error (se)
Intercept	6.763	270.26	0.01	0.201852	0.077616
					0.010474
					0.001709
Time ³		2796.342	0.016	-0.00018	7.4773E-05
Intercept		273.993	0.007		0.078029
					0.010476
					0.00177
Time ³	1.997	2798.881	0.158	-0.000111	7.8399E-05
Intercept	46.957	242.333	<.001	0.510958	0.074565
Time					0.009524
Time ²	0.176	2248.267	0.675	-0.000318	0.000757
Time ³	5.803	2796.342	0.016	-0.00018	7.4773E-05
Intercept	44.46	243.377	<.001	0.498137	0.074708
Time	34.107		<.001	0.05788	0.009911
	0.223	2288.355	0.637	-0.000362	0.000766
Time ³	1.997	2798.881	0.158	-0.000111	7.8399E-05
Intercept	65.951	262.798	<.001	0.597001	0.073513
	19.594	1181.061	<.001	0.042038	0.009497
	5.33	2778.188	0.021	-0.001952	0.000845
Time ³	2.919	2788.104	0.088	-0.00013	7.6109E-05
Intercept	65.765	272.288	<.001	0.60286	0.074339
			<.001		0.009735
Time ²	2.555	2772.581	0.11	-0.001401	0.000876
Time ³	1.829	2769.721	0.176	-0.000109	8.0282E-05
Intercept	47.198	248.056	<.001	0.569551	0.082903
Time	13.158	830.66	<.001	0.030154	0.008313
	0.721	2043.716	0.396	-0.00092	0.001083
Time ³	0.428	2512.435	0.513	-3.813E-05	5.8282E-05
Intercept	30.093	242.584	<.001	0.453438	0.082657
	30.029		<.001	0.047341	0.008639
	0.692	2107.97	0.406	0.000909	0.001093
Time ³	0.001	2528.022	0.982	-1.42E-06	6.1797E-05
Intercept	43.087	236.642	<.001	0.488805	0.074467
	44.774	769.515	<.001	0.050692	0.007576
Time ²	0.003	1647.817	0.956	3.8773E-05	0.000707
Time ³	1.414	1782.856	0.235	-4.603E-05	3.8717E-05
Intercept	29.862	238.184	<.001	0.41077	0.075169
Time	32.971	1294.461	<.001	0.061511	0.010712
Time ²	0.55	1610.184	0.458	0.000569	0.000767
	Time Time² Time³ Intercept Time Time²	Intercept 6.763 Time 26.978 Time² 1.947 Time³ 5.803 Intercept 7.489 Time 25.78 Time² 0.539 Time³ 1.997 Intercept 46.957 Time 46.202 Time² 0.176 Time³ 5.803 Intercept 44.46 Time 34.107 Time² 0.223 Time³ 1.997 Intercept 65.951 Time 19.594 Time² 5.33 Time² 5.33 Time² 5.33 Time² 22.824 Time² 22.824 Time² 22.824 Time² 13.158 Time² 0.721 Time³ 0.428 Intercept 30.093 Time² 0.692 Time³ 0.001 Intercept 43.087 <th>Intercept 6.763 270.26 Time 26.978 1431.826 Time² 1.947 2679.35 Time³ 5.803 2796.342 Intercept 7.489 273.993 Time 25.78 1446.785 Time² 0.539 2692.143 Time³ 1.997 2798.881 Intercept 46.957 242.333 Time 46.202 1323.282 Time² 0.176 2248.267 Time³ 5.803 2796.342 Intercept 44.46 243.377 Time 34.107 1411.791 Time² 0.223 2288.355 Time³ 1.997 2798.881 Intercept 65.951 262.798 Time 19.594 1181.061 Time² 5.33 2778.188 Time³ 2.919 2788.104 Intercept 65.765 272.288 Time 22.824 1254.954 Time</th> <th> Intercept 6.763 270.26 0.01 </th> <th> Intercept</th>	Intercept 6.763 270.26 Time 26.978 1431.826 Time² 1.947 2679.35 Time³ 5.803 2796.342 Intercept 7.489 273.993 Time 25.78 1446.785 Time² 0.539 2692.143 Time³ 1.997 2798.881 Intercept 46.957 242.333 Time 46.202 1323.282 Time² 0.176 2248.267 Time³ 5.803 2796.342 Intercept 44.46 243.377 Time 34.107 1411.791 Time² 0.223 2288.355 Time³ 1.997 2798.881 Intercept 65.951 262.798 Time 19.594 1181.061 Time² 5.33 2778.188 Time³ 2.919 2788.104 Intercept 65.765 272.288 Time 22.824 1254.954 Time	Intercept 6.763 270.26 0.01	Intercept

Table S2.12 (cont'd)

	Time ³	1.688	2533.933	0.194	-0.000124	9.5777E-05
30s VEH:	Intercept	40.132	240.594	<.001	0.439596	0.052244
	Time	35.059	1266.146	<.001	0.028109	0.052244
	Time ²	0.011	1576.641	0.917	0.062125	0.007507
	Time ³	2.992	2532.835	0.084	0.000244	0.000528
30s CNO:	Intercept	58.358	200.336	<.001	0.505951	0.066231
	Time	34.196	405.872	<.001	-0.027563	0.004714
	Time ²	5.194	1262.226	0.023	-0.000651	0.000286
	Time ³	11.019	1316.905	<.001	3.6055E-05	1.0861E-05
35s VEH:	Intercept	26.542	180.851	<.001	0.322462	0.06259
	Time	26.539	467.307	<.001	-0.027681	0.005373
	Time ²	0.012	966.937	0.914	2.0772E-05	0.000192
	Time ³	5.272	1358.022	0.022	2.6259E-05	1.1437E-05
35s CNO:	Intercept	32.896	178.094	<.001	0.356366	0.062133
	Time	34.946	464.813	<.001	-0.031369	0.005306
	Time ²	0.38	866.968	0.538	-0.00011	0.000179
	Time ³	11.019	1316.905	<.001	3.6055E-05	1.0861E-05
40s VEH:	Intercept	40.132	240.594	<.001	0.467705	0.073829
	Time	35.059	1266.146	<.001	0.062653	0.010581
	Time ²	0.011	1576.641	0.917	-7.605E-05	0.00073
	Time ³	2.992	2532.835	0.084	-0.00016	9.2703E-05
40s CNO:	Intercept	10.275	177.588	0.002	0.201271	0.062791
	Time	32.748	472.845	<.001	-0.029767	0.005202
	Time ²	5.235	693.796	0.022	0.000431	0.000188
	Time ³	11.019	1316.905	<.001	3.6055E-05	1.0861E-05

Chapter 3 Supplemental Materials

 Table S3.1 Results from the overall model examining estrous cycle within vehicle.

	F	df	р
Pre-peak:			-
Estrous	0.052	312.224	0.82
Time	64.172	1864.046	<.001
Time ²	0.811	2685.781	0.368
Time ³	0.497	3596.903	0.481
Estrous x time	0.586	1864.046	0.444
Estrous x time ²	0.039	2685.781	0.844
Estrous x time ³	0.614	3596.903	0.433
Post-peak:			
Estrous	1.069	226.476	0.302
Time	61.607	695.345	<.001
Time ²	4.325	897.092	0.038
Time ³	19.627	1787.695	<.001
Estrous x time	1.111	695.345	0.292
Estrous x time ²	1.494	897.092	0.222
Estrous x time ³	2.855	1787.695	0.091

Table S3.2 Results from the interaction model examining effects of time within vehicle treated rats tested in P/E and M/D.

	F	df	р	Regression slope (b)	standard error (se)
Pre-peak P/E:					
Intercept	40.047	314.713	<.001	0.436405	0.068961
Time	36.805	1917.777	<.001	0.059504	0.009808
Time ²	0.231	2748.883	0.631	0.000348	0.000724
Time ³	0.977	3620.92	0.323	-9.412E-05	9.5202E-05
Pre-peak M/D:					
Intercept	36.539	309.734	<.001	0.414294	0.068538
Time	27.523	1806.867	<.001	0.049126	0.009364
Time ²	0.648	2613.667	0.421	0.000543	0.000675
Time ³	0.004	3563.911	0.952	4.9866E-06	8.329E-05
Post-peak P/E:					
Intercept	9.45	225.855	0.002	0.182097	0.059237
Time	23.254	690.099	<.001	-0.024849	0.005153
Time ²	5.59	887.017	0.018	0.00039	0.000165
Time ³	3.864	1764.49	0.049	2.2316E-05	1.1352E-05
Post-peak M/D:					
Intercept	20.48	227.096	<.001	0.268842	0.059406
Time	39.348	700.57	<.001	-0.032558	0.00519
Time ²	0.359	906.822	0.549	0.000101	0.000169
Time ³	18.213	1809.924	<.001	4.9833E-05	1.1677E-05

Table S3.3 Results from the overall models examining estrous cycle within vehicle at 5s intervals.

		F	df	р
5s	Estrous	0.014	350.773	0.906
35	Time	66.102	2005.66	<.001
	Time ²	0.229	3666.405	0.632
	Time ³	2.141	3791.698	0.144
	Estrous x time	0.138	2005.66	0.71
	Estrous x time ²	0.47	3666.405	0.493
	Estrous x time ³	1.146	3791.698	0.284
10s	Estrous	0.141	315.39	0.708
	Time	76.278	1923.956	<.001
	Time ²	1.357	3169.915	0.244
	Time ³	2.141	3791.698	0.144
	Estrous x time	0.942	1923.956	0.332
	Estrous x time ²	0.009	3169.915	0.925
	Estrous x time ³	1.146	3791.698	0.284
15s	Estrous	0.737	350.252	0.391
	Time	51.601	1703.555	<.001
	Time ²	2.65	3742.014	0.104
	Time ³	1.316	3773.399	0.251
	Estrous x time	0.784	1703.555	0.376
	Estrous x time ²	0.136	3742.014	0.713
	Estrous x time ³	0.005	3773.399	0.944
20s	Estrous	0.115	317.171	0.734
	Time	72.56	1228.604	<.001
	Time ²	1.573	2947.16	0.21
	Time ³	0.001	3411.074	0.98
	Estrous x time	0.001	1228.604	0.97
	Estrous x time ²	0.037	2947.16	0.848
	Estrous x time ³	0.036	3411.074	0.849
25s	Estrous	0.056	314.772	0.812
	Time	75.904	1623.396	<.001
	Time ²	2.696	2504.759	0.101
	Time ³	0.494	3455.586	0.482
	Estrous x time	0.632	1623.396	0.427
	Estrous x time ²	0.853	2504.759	0.356
	Estrous x time ³	0.849	3455.586	0.357
30s	Estrous	0.066	315.963	0.798
	Time	59.668	1879.115	<.001
	Time ²	1.367	2481.12	0.242

Table S3.3 (cont'd)

	Time ³	0.18	3556.533	0.672
	Estrous x time	0.526	1879.115	0.469
	Estrous x time ²	0.203	2481.12	0.652
	Estrous x time ³	0.808	3556.533	0.369
35s	Estrous	0.066	315.963	0.798
	Time	59.668	1879.115	<.001
	Time ²	1.367	2481.12	0.242
	Time ³	0.18	3556.533	0.672
	Estrous x time	0.526	1879.115	0.469
	Estrous x time ²	0.203	2481.12	0.652
	Estrous x time ³	0.808	3556.533	0.369
40s	Estrous	36.236	318.673	0.798
	Time	33.984	1879.115	<.001
	Time ²	0.241	2481.12	0.242
	Time ³	0.768	3556.533	0.672
	Estrous x time	32.501	1879.115	0.469
	Estrous x time ²	25.798	2481.12	0.652
	Estrous x time ³	1.412	3556.533	0.369

Table S3.4 Results from the interaction models examining estrous cycle within vehicle at 5s intervals.

		F	df	р	Regression slope (b)	standard error (se)
5s P/E:	Intercept	9.886	358.985	0.002	0.225773	0.071805
	Time	36.127	1990.93	<.001	0.055749	0.009275
	Time ²	0.611	3686.695	0.435	0.001254	0.001605
	Time ³	2.631	3788.321	0.105	-0.000124	7.6198E-05
5s M/D:	Intercept	11.295	342.587	<.001	0.237632	0.070708
	Time	30.111	2020.504	<.001	0.050879	0.009272
	Time ²	0.024	3639.375	0.877	-0.000223	0.001436
	Time ³	0.099	3796.651	0.753	-1.915E-05	6.0933E-05
10s P/E:	Intercept	57.587	315.049	<.001	0.520415	0.068578
	Time	41.966	2005.676	<.001	0.059018	0.00911
	Time ²	0.792	3195.418	0.373	-0.0006	0.000674
	Time ³	2.631	3788.321	0.105	-0.000124	7.6198E-05
10s M/D:	Intercept	49.814	315.731	<.001	0.484057	0.068584
	Time	34.322	1824.33	<.001	0.047212	0.008059
	Time ²	0.573	3144.216	0.449	-0.00051	0.000674
	Time ³	0.099	3796.651	0.753	-1.915E-05	6.0933E-05
15s P/E:	Intercept	72.05	368.058	<.001	0.576479	0.067915
	Time	19.978	1696.239	<.001	0.037746	0.008445
	Time ²	1.548	3734.019	0.214	-0.001185	0.000953
	Time ³	0.477	3782.444	0.49	-5.373E-05	7.7773E-05
15s M/D:	Intercept	97.987	332.97	<.001	0.658089	0.066481
	Time	32.317	1710.798	<.001	0.048362	0.008507
	Time ²	1.113	3755.57	0.292	-0.000748	0.000709
	Time ³	0.945	3757.677	0.331	-6.067E-05	6.242E-05
20s P/E:	Intercept	37.346	314.217	<.001	0.447649	0.073251
	Time	35.028	1235.916	<.001	0.045422	0.007675
	Time ²	0.549	2972.221	0.459	0.000643	0.000868
	Time ³	0.013	3412.389	0.909	-6.005E-06	5.2313E-05
20s M/D:	Intercept	43.503	320.169	<.001	0.482825	0.073203
	Time	37.602	1220.953	<.001	0.045828	0.007474
	Time ²	1.077	2920.538	0.299	0.000875	0.000843
	Time ³	0.024	3409.637	0.876	7.7887E-06	5.0085E-05
25s P/E:	Intercept	35.708	316.637	<.001	0.417402	0.069851
	Time	33.774	1956.412	<.001	0.05753	0.009899
	Time ²	0.241	2543.598	0.623	0.000362	0.000737
	Time ³	0.759	3579.588	0.384	-8.529E-05	9.7869E-05
25s M/D:	Intercept	32.428	312.887	<.001	0.394041	0.069196
	Time	47.351	1131.302	<.001	0.047912	0.006963
	Time ²	3.532	2460.631	0.06	0.001294	0.000689

Table S3.4 (cont'd)

	Time ³	0.091	2430.566	0.763	1.1477E-05	3.8086E-05
30s P/E:	Intercept	36.236	318.673	<.001	0.405134	0.048879
	Time	33.984	1948.092	<.001	0.012537	0.048879
	Time ²	0.241	2531.879	0.623	0.05262	0.006812
	Time ³	0.768	3572.948	0.381	0.000588	0.000503
30s M/D:	Intercept	83.732	260.712	<.001	0.570606	0.062358
	Time	27.612	578.741	<.001	-0.022652	0.004311
	Time ²	25.909	1979.757	<.001	-0.001422	0.000279
	Time ³	29.08	2055.239	<.001	5.4712E-05	1.0146E-05
35s P/E:	Intercept	29.31	231.372	<.001	0.318903	0.058904
	Time	35.058	655.659	<.001	-0.028859	0.004874
	Time ²	0.07	1269.628	0.792	-4.535E-05	0.000172
	Time ³	8.92	1930.204	0.003	3.0415E-05	1.0184E-05
35s M/D:	Intercept	53.012	232.633	<.001	0.428638	0.058871
	Time	45.882	663.752	<.001	-0.032768	0.004838
	Time ²	11.892	1383.642	<.001	-0.000601	0.000174
	Time ³	29.08	2055.239	<.001	5.4712E-05	1.0146E-05
40s P/E:	Intercept	36.236	318.673	<.001	0.417671	0.069385
	Time	33.984	1948.092	<.001	0.057558	0.009874
	Time ²	0.241	2531.879	0.623	0.000361	0.000736
	Time ³	0.768	3572.948	0.381	-8.567E-05	9.7738E-05
40s M/D:	Intercept	18.797	229.701	<.001	0.256609	0.059187
	Time	51.932	691.095	<.001	-0.034677	0.004812
	Time ²	1.656	1014.523	0.198	0.000219	0.000171
	Time ³	29.08	2055.239	<.001	5.4712E-05	1.0146E-05

 Table S3.5
 Results from the overall model examining drug treatment within P/E.

	F	df	р
Pre-peak:			_
Drug	0.015	318.271	0.901
Time	69.944	1815.933	<.001
Time ²	1.046	2659.667	0.307
Time ³	1.361	3591.193	0.244
Drug x time	0.158	1815.933	0.691
Drug x time ²	0.091	2659.667	0.763
Drug x time ³	0.111	3591.193	0.739
Post-peak:			
Drug	42.308	703.798	<.001
Time	13.471	901.344	<.001
Time ²	4.233	1787.802	0.04
Time ³	0.076	232.687	0.783
Drug x time	0.031	703.798	0.861
Drug x time ²	0.193	901.344	0.661
Drug x time ³	0.244	1787.802	0.622

Table S3.6 Results from the interaction model examining drug treatment within P/E.

	F	df	р	Regression slope (b)	standard error (se)
Pre-peak P/E:					
Intercept	41.493	320.893	<.001	0.436706	0.067796
Time	36.973	1874.617	<.001	0.059616	0.009804
Time ²	0.234	2695.946	0.628	0.000351	0.000726
Time ³	0.989	3593.605	0.32	-9.517E-05	9.5689E-05
Pre-peak M/D:					
Intercept	39.857	315.642	<.001	0.424872	0.067299
Time	32.978	1754.791	<.001	0.054214	0.009441
Time ²	0.985	2614.687	0.321	0.000645	0.00065
Time ³	0.402	3587.998	0.526	-5.283E-05	8.3331E-05
Post-peak P/E:					
Intercept	9.788	229.979	0.002	0.181344	0.057965
Time	23.566	677.152	<.001	-0.024802	0.005109
Time ²	5.774	864.892	0.016	0.000394	0.000164
Time ³	3.828	1701.462	0.051	2.2186E-05	1.134E-05
Post-peak M/D:					
Intercept	12.059	235.367	<.001	0.204062	0.058764
Time	19.016	728.996	<.001	-0.023504	0.00539
Time ²	7.705	932.986	0.006	0.000501	0.000181
Time ³	1.063	1854.648	0.303	1.3599E-05	1.3187E-05

Table S3.7 Results from the overall models examining drug (VEH, CNO) during P/E at 5s intervals.

		F	df	р
.	Davis	0.400	204 722	0.700
5s	Drug Time	0.126 62.882	364.738 1978.373	0.722 <.001
	Time ²	1.344	3592.099	0.246
	Time ³	4.117	3736.59	0.240
		0.347	1978.373	0.043
	Drug x time Drug x time ²	0.001	3592.099	0.556
	Drug x time ³	0.001	3736.59	0.978
100	•		321.812	0.699
10s	Drug Time	0.503 82.151	1784.365	<.001
	Time ²	0.307	3104.424	0.579
	Time ³	4.117	3736.59	0.043
	Drug x time	0.106	1784.365	0.745
	Drug x time ²	0.468	3104.424	0.494
	Drug x time ³	0.149	3736.59	0.699
15s	Drug X time	1.994	354.253	0.055
103	Time	52.164	1729.808	<.001
	Time ²	3.736	3660.579	0.053
	Time ³	1.783	3736.784	0.182
	Drug x time	0.926	1729.808	0.336
	Drug x time ²	0	3660.579	0.986
	Drug x time ³	0.074	3736.784	0.785
20s	Drug	0.207	320.817	0.649
	Time	70.181	1186.233	<.001
	Time ²	0.024	2780.328	0.877
	Time ³	0.871	3343.444	0.351
	Drug x time	0.035	1186.233	0.852
	Drug x time ²	0.829	2780.328	0.363
	Drug x time ³	0.572	3343.444	0.449
25s	Drug	0.002	320.943	0.962
	Time	64.935	1842.733	<.001
	Time ²	0.848	2444.441	0.357
	Time ³	1.251	3521.115	0.263
	Drug x time	0.11	1842.733	0.741
	Drug x time ²	0.039	2444.441	0.844
	Drug x time ³	0.049	3521.115	0.825
30s	Drug	0.002	320.943	0.962
	Time	64.935	1842.733	<.001
	Time ²	0.848	2444.441	0.357

Table S3.7 (cont'd)

	Time ³	1.251	3521.115	0.263
	Drug x time	0.11	1842.733	0.741
	Drug x time ²	0.039	2444.441	0.844
	Drug x time ³	0.049	3521.115	0.825
35s	Drug	0.002	320.943	0.962
	Time	64.935	1842.733	<.001
	Time ²	0.848	2444.441	0.357
	Time ³	1.251	3521.115	0.263
	Drug x time	0.11	1842.733	0.741
	Drug x time ²	0.039	2444.441	0.844
	Drug x time ³	0.049	3521.115	0.825
40s	Drug	37.645	324.669	0.962
	Time	34.076	1842.733	<.001
	Time ²	0.234	2444.441	0.357
	Time ³	0.788	3521.115	0.263
	Drug x time	37.351	1842.733	0.741
	Drug x time ²	30.864	2444.441	0.844
	Drug x time ³	0.709	3521.115	0.825

Table S3.8 Results from the interaction model examining the effects of drug (VEH, CNO) during P/E at 5s intervals.

		F	df	p	Regression slope (b)	standard error (se)
5s VEH:	Intercept	10.112	366.856	0.002	0.225035	0.070768
	Time	36.203	1962.42	<.001	0.055797	0.009273
	Time ²	0.618	3663.962	0.432	0.001268	0.001613
	Time ³	2.632	3777.54	0.105	-0.000124	7.6631E-05
5s CNO:	Intercept	7.115	362.651	0.008	0.189404	0.071007
	Time	27.005	1994.524	<.001	0.048083	0.009253
	Time ²	0.73	3503.502	0.393	0.001331	0.001557
	Time ³	1.513	3669.495	0.219	-8.455E-05	6.8744E-05
10s VEH:	Intercept	59.42	321.141	<.001	0.520183	0.067482
	Time	42.171	1970.822	<.001	0.059154	0.009109
	Time ²	0.779	3150.778	0.378	-0.000597	0.000676
	Time ³	2.632	3777.54	0.105	-0.000124	7.6631E-05
10s CNO:	Intercept	45.098	322.486	<.001	0.452518	0.067384
	Time	39.987	1601.515	<.001	0.055049	0.008705
	Time ²	0.008	3059.067	0.928	6.2493E-05	0.000687
	Time ³	1.513	3669.495	0.219	-8.455E-05	6.8744E-05
15s VEH:	Intercept	77.936	389.52	<.001	0.581562	0.065876
	Time	20.192	1662.679	<.001	0.037642	0.008377
	Time ²	1.631	3706.615	0.202	-0.001221	0.000956
	Time ³	0.503	3763.414	0.478	-5.54E-05	7.8081E-05
15s CNO:	Intercept	102.134	327.542	<.001	0.718424	0.071088
	Time	32.533	1795.789	<.001	0.049214	0.008628
	Time ²	2.2	3585.583	0.138	-0.001199	0.000809
	Time ³	1.472	3696.353	0.225	-8.385E-05	6.9103E-05
20s VEH:	Intercept	37.813	316.547	<.001	0.44834	0.07291
	Time	34.719	1216.471	<.001	0.045339	0.007695
	Time ²	0.539	2933.514	0.463	0.000641	0.000873
	Time ³	0.014	3386.008	0.905	-6.304E-06	5.2673E-05
20s CNO:	Intercept	45.586	325.116	<.001	0.49542	0.073376
	Time	35.543	1153.524	<.001	0.043367	0.007274
	Time ²	0.301	2611.675	0.583	-0.000454	0.000828
	Time ³	1.565	3291.273	0.211	-6.034E-05	4.8241E-05
25s VEH:	Intercept	37.645	324.669	<.001	0.418801	0.068258
	Time	34.076	1902.558	<.001	0.057683	0.009882
	Time ²	0.234	2472.417	0.628	0.000357	0.000738
	Time ³	0.788	3538.491	0.375	-8.73E-05	9.8341E-05
25s CNO:	Intercept	37.351	317.227	<.001	0.414209	0.067775
	Time	30.864	1781.003	<.001	0.053128	0.009563
	Time ²	0.709	2409.244	0.4	0.000552	0.000655

Table S3.8 (cont'd)

	Time ³	0.468	3497.548	0.494	-5.848E-05	8.55E-05
30s VEH:	Intercept	37.645	324.669	<.001	0.416505	0.048095
	Time	34.076	1902.558	<.001	0.002296	0.048095
	Time ²	0.234	2472.417	0.628	0.055406	0.006876
	Time ³	0.788	3538.491	0.375	0.000454	0.000493
30s CNO:	Intercept	64.292	277.695	<.001	0.509811	0.063581
	Time	41.36	611.286	<.001	-0.028026	0.004358
	Time ²	0.699	1863.603	0.403	-0.000307	0.000367
	Time ³	3.999	1962.765	0.046	2.4304E-05	1.2154E-05
35s VEH:	Intercept	30.269	235.877	<.001	0.317345	0.057681
	Time	35.629	643.627	<.001	-0.028854	0.004834
	Time ²	0.05	1236.636	0.823	-3.83E-05	0.000171
	Time ³	8.83	1863.174	0.003	3.0282E-05	1.0191E-05
35s CNO:	Intercept	37.535	249.374	<.001	0.365056	0.059586
	Time	34.688	657.822	<.001	-0.029268	0.004969
	Time ²	0.068	1475.878	0.794	5.8029E-05	0.000222
	Time ³	3.999	1962.765	0.046	2.4304E-05	1.2154E-05
40s VEH:	Intercept	37.645	324.669	<.001	0.418801	0.068258
	Time	34.076	1902.558	<.001	0.057683	0.009882
	Time ²	0.234	2472.417	0.628	0.000357	0.000738
	Time ³	0.788	3538.491	0.375	-8.73E-05	9.8341E-05
40s CNO:	Intercept	14.665	235.367	<.001	0.223203	0.058286
	Time	26.508	715.757	<.001	-0.026865	0.005218
	Time ²	5.876	1004.491	0.016	0.000423	0.000174
	Time ³	3.999	1962.765	0.046	2.4304E-05	1.2154E-05

Table S3.9 Results from the overall model examining drug treatment within M/D.

	F	df	р
Pre-peak:			
Drug	0.105	294.992	0.746
Time	67.789	1597.905	<.001
Time ²	1.376	2346.847	0.241
Time ³	0.066	3438.556	0.797
Drug x time	0.011	1597.905	0.915
Drug x time ²	0.013	2346.847	0.911
Drug x time ³	0.139	3438.556	0.709
Post-peak:			
Drug	1.211	228.086	0.272
Time	50.393	728.068	<.001
Time ²	4.991	927.629	0.026
Time ³	13.232	1882.963	<.001
Drug x time	2.574	728.068	0.109
Drug x time ²	2.039	927.629	0.154
Drug x time ³	4.351	1882.963	0.037

Table S3.10 Results from the interaction model examining drug treatment within M/D.

	F	df	р	Regression slope (b)	standard error (se)
Pre-peak P/E:					
Intercept	36.375	308.48	<.001	0.414123	0.068663
Time	27.6	1818.035	<.001	0.049077	0.009342
Time ²	0.651	2628.126	0.42	0.000542	0.000673
Time ³	0.004	3571.668	0.948	5.3991E-06	8.2972E-05
Pre-peak M/D:					
Intercept	45.004	281.479	<.001	0.445084	0.066346
Time	43.28	1324.524	<.001	0.050366	0.007656
Time ²	0.77	1912.845	0.38	0.000448	0.00051
Time ³	0.45	2864.897	0.502	-2.962E-05	4.4144E-05
Post-peak P/E:					
Intercept	20.411	226.262	<.001	0.269175	0.059581
Time	39.441	704.575	<.001	-0.03258	0.005188
Time ²	0.348	913.556	0.556	9.9636E-05	0.000169
Time ³	18.347	1827.397	<.001	4.9897E-05	1.1649E-05
Post-peak M/D:					
Intercept	8.564	229.898	0.004	0.175996	0.06014
Time	14.517	750.736	<.001	-0.020569	0.005398
Time ²	6.294	940.218	0.012	0.000453	0.00018
Time ³	1.087	1929.013	0.297	1.3527E-05	1.2973E-05

Table S3.11 Results from the overall models examining drug (VEH, CNO) during M/D at 5s intervals.

		F	df	р
5s	Drug	0.06	325.897	0.806
	Time	58.041	2004.507	<.001
	Time ²	0	3537.178	0.986
	Time ³	0.461	3774.461	0.497
	Drug x time	0.031	2004.507	0.86
	Drug x time ²	0.074	3537.178	0.786
	Drug x time ³	0.015	3774.461	0.903
10s	Drug	0.064	313.892	0.8
	Time	89.679	1555.549	<.001
	Time ²	0.497	3085.682	0.481
	Time ³	0.461	3774.461	0.497
	Drug x time	0.036	1555.549	0.849
	Drug x time ²	0.149	3085.682	0.699
	Drug x time ³	0.015	3774.461	0.903
15s	Drug	0.17	312.698	0.681
	Time	67.491	1772.53	<.001
	Time ²	2.773	3588.446	0.096
	Time ³	1.645	3729.05	0.2
	Drug x time	0.063	1772.53	0.801
	Drug x time ²	0.066	3588.446	0.797
	Drug x time ³	0.247	3729.05	0.619
20s	Drug	0.023	300.552	0.88
	Time	62.963	1160.092	<.001
	Time ²	1.761	3093.825	0.185
	Time ³	0.071	3422.7	0.79
	Drug x time	0.911	1160.092	0.34
	Drug x time ²	0.231	3093.825	0.631
	Drug x time ³	0	3422.7	0.997
25s	Drug	0.085	305.558	0.77
	Time	83.746	1097.628	<.001
	Time ²	4.186	2540.216	0.041
	Time ³	0.034	2598.449	0.854
	Drug x time	0.611	1097.628	0.434
	Drug x time ²	0.457	2540.216	0.499
	Drug x time ³	0.088	2598.449	0.767
30s	Drug	0.305	300.752	0.581
	Time	63.08	1499.56	<.001
	Time ²	2.867	2374.49	0.091

Table S3.11 (cont'd)

	Time ³	0.099	3465.124	0.753
	Drug x time	0.208	1499.56	0.648
	Drug x time ²	0.017	2374.49	0.896
	Drug x time ³	0.163	3465.124	0.686
35s	Drug	0.26	297.046	0.61
	Time	65.656	1572.331	<.001
	Time ²	1.57	2186.788	0.21
	Time ³	0.027	3394.433	0.869
	Drug x time	0.052	1572.331	0.82
	Drug x time ²	0.427	2186.788	0.513
	Drug x time ³	0.669	3394.433	0.414
40s	Drug	32.286	312.328	0.61
	Time	25.855	1572.331	<.001
	Time ²	1.424	2186.788	0.21
	Time ³	0.137	3394.433	0.869
	Drug x time	43.777	1572.331	0.82
	Drug x time ²	43.336	2186.788	0.513
	Drug x time ³	0.248	3394.433	0.414

Table S3.12 Results from the interaction model examining the effects of drug (VEH, CNO) during M/D at 5s intervals.

		F	df	р	Regression slope (b)	standard error (se)
5s VEH:	Intercept	11.311	341.528	<.001	0.237809	0.070708
	Time	30.272	2028.294	<.001	0.05085	0.009242
	Time ²	0.025	3644.755	0.874	-0.000227	0.00143
	Time ³	0.097	3798.384	0.755	-1.892E-05	6.0661E-05
5s CNO:	Intercept	9.767	310.301	0.002	0.213641	0.068362
	Time	27.791	1980.823	<.001	0.048556	0.009211
	Time ²	0.058	3302.734	0.809	0.000258	0.00107
	Time ³	0.799	3609.4	0.372	-2.716E-05	3.0389E-05
10s VEH:	Intercept	49.785	314.871	<.001	0.484024	0.068599
	Time	34.462	1831.668	<.001	0.047163	0.008034
	Time ²	0.579	3154.949	0.447	-0.000511	0.000671
	Time ³	0.097	3798.384	0.755	-1.892E-05	6.0661E-05
10s CNO:	Intercept	45.221	312.91	<.001	0.459476	0.068327
	Time	62.156	1196.802	<.001	0.049099	0.006228
	Time ²	0.052	3011.282	0.819	-0.000149	0.000652
	Time ³	0.799	3609.4	0.372	-2.716E-05	3.0389E-05
15s VEH:	Intercept	104.254	347.338	<.001	0.659207	0.064562
	Time	33.441	1704.18	<.001	0.048445	0.008377
	Time ²	1.155	3747.043	0.283	-0.000755	0.000703
	Time ³	0.984	3747.841	0.321	-6.136E-05	6.1868E-05
15s CNO:	Intercept	106.44	285.338	<.001	0.697703	0.067627
	Time	34.165	1855.123	<.001	0.045564	0.007795
	Time ²	2.478	2547.544	0.116	-0.000553	0.000351
	Time ³	0.791	3632.277	0.374	-2.709E-05	3.0467E-05
20s VEH:	Intercept	43.225	315.811	<.001	0.482585	0.073402
	Time	37.679	1220.304	<.001	0.045854	0.00747
	Time ²	1.079	2930.84	0.299	0.000874	0.000841
	Time ³	0.025	3417.818	0.875	7.8304E-06	4.9967E-05
20s CNO:	Intercept	58.137	282.733	<.001	0.497457	0.065242
	Time	25.609	1098.065	<.001	0.036006	0.007115
	Time ²	0.738	3546.882	0.39	0.000409	0.000477
	Time ³	0.062	3434.377	0.803	8.0356E-06	3.2197E-05
25s VEH:	Intercept	31.051	304.572	<.001	0.393216	0.070566
	Time	46.668	1143.389	<.001	0.047918	0.007014
	Time ²	3.507	2509.313	0.061	0.001292	0.00069
	Time ³	0.101	2462.088	0.75	1.2156E-05	3.8168E-05
25s CNO:	Intercept	36.706	306.573	<.001	0.422212	0.069689
	Time	37.145	1049.11	<.001	0.040374	0.006624
	Time ²	0.994	2575.028	0.319	0.00065	0.000652

Table S3.12 (cont'd)

	Time ³	0.007	2782.542	0.932	-2.851E-06	3.3272E-05
30s VEH:	Intercept	31.605	308.532	<.001	0.418851	0.048832
	Time	25.549	1822.154	<.001	-0.026961	0.048832
	Time ²	1.417	2450.906	0.234	0.045008	0.005667
	Time ³	0.14	3550.616	0.708	0.000759	0.000448
30s CNO:	Intercept	43.925	266.797	<.001	0.431005	0.065032
	Time	28.674	605.54	<.001	-0.023455	0.00438
	Time ²	1.982	1877.179	0.159	-0.000485	0.000345
	Time ³	5.831	2026.334	0.016	2.8554E-05	1.1825E-05
35s VEH:	Intercept	52.759	231.923	<.001	0.429145	0.059082
	Time	45.874	668.217	<.001	-0.03277	0.004838
	Time ²	12.027	1395.022	<.001	-0.000604	0.000174
	Time ³	29.265	2075.426	<.001	5.4761E-05	1.0123E-05
35s CNO:	Intercept	25.665	245.861	<.001	0.308021	0.060801
	Time	23.781	704.067	<.001	-0.023953	0.004912
	Time ²	0.272	1625.294	0.602	0.000111	0.000212
	Time ³	2.464	2248.109	0.117	1.8305E-05	1.1661E-05
40s VEH:	Intercept	32.286	312.328	<.001	0.392254	0.069034
	Time	25.855	1818.453	<.001	0.047638	0.009369
	Time ²	1.424	2441.21	0.233	0.000816	0.000683
	Time ³	0.137	3543.773	0.712	3.1275E-05	8.4637E-05
40s CNO:	Intercept	10.463	231.408	0.001	0.193312	0.059763
	Time	17.581	777.979	<.001	-0.021473	0.005121
	Time ²	4.967	1043.473	0.026	0.000385	0.000173
	Time ³	2.464	2248.109	0.117	1.8305E-05	1.1661E-05

Chapter 4 Supplemental Materials

 Table S4.1 Results from the overall model examining hormone effects under vehicle.

	F	df	р
Pre-peak:			
Hormone	0.989	228.568	0.321
Time	68.467	1899.678	<.001
Time ²	0.952	2616.922	0.329
Time ³	0.054	3281.154	0.815
Hormone x time	0.279	1899.678	0.598
Hormone x time ²	1.665	2616.922	0.197
Hormone x time ³	1.454	3281.154	0.228
Post-peak:			
Hormone	0.149	180.123	0.7
Time	54.08	845.436	<.001
Time ²	17.257	1213.586	<.001
Time ³	8.753	2368.068	0.003
Hormone x time	0.127	845.436	0.722
Hormone x time ²	0.213	1213.586	0.645
Hormone x time ³	0.239	2368.068	0.625

Table S4.2 Results from the interaction model examining effects of time within vehicle treated rats tested under oil and EB.

					-
	F	df	p	Regression slope (b)	standard error (se)
Pre-peak Oil:					_
Intercept	56.433	231.381	<.001	0.044892	0.008382
Time	28.681	1969.441	<.001	-0.000815	0.000542
Time ²	2.263	2678.835	0.133	4.1289E-05	6.5437E-05
Time ³	0.398	3292.53	0.528	0.446805	0.072532
Pre-peak EB:					
Intercept	37.947	225.761	<.001	0.05101	0.008004
Time	40.615	1825.575	<.001	0.000113	0.000473
Time ²	0.057	2535.033	0.811	-6.11E-05	5.409E-05
Time ³	1.276	3262.595	0.259	0.19498	0.066394
Post-peak Oil:					
Intercept	8.624	178.329	0.004	-0.028162	0.005068
Time	30.876	817.705	<.001	0.000451	0.000166
Time ²	7.434	1165.589	0.006	2.8428E-05	1.0925E-05
Time ³	6.771	2304.139	0.009	0.15864	0.066961
Post-peak EB:					
Intercept	5.613	181.913	0.019	-0.02556	0.005261
Time	23.603	872.302	<.001	0.000564	0.00018
Time ²	9.838	1256.136	0.002	2.0369E-05	1.2357E-05
Time ³	2.717	2418.393	0.099	0	0

Table S4.3 Results from the overall models examining the effects of hormone under treatment vehicle at 5s intervals.

		F	df	р
50	Hormone	2.326	255.152	0.128
5s	Hormone Time	2.326 88.021	2093.576	<.001
	Time ²	0.829	3303.262	0.363
	Time ³	0.026	3341.039	0.77
	Hormone x time	2.342	2093.576	0.126
	Hormone x time ²	5.66	3303.262	0.017
	Hormone x time ³	4.762	3341.039	0.029
10s	Hormone	2.637	237.169	0.106
100	Time	82.254	1765.341	<.001
	Time ²	5.232	3090.815	0.022
	Time ³	0.086	3341.039	0.77
	Hormone x time	1.302	1765.341	0.254
	Hormone x time ²	4.861	3090.815	0.028
	Hormone x time ³	4.762	3341.039	0.029
15s	Hormone	1.871	227.118	0.173
	Time	46.542	1763.111	<.001
	Time ²	4.121	3278.453	0.042
	Time ³	0.07	3327.746	0.792
	Hormone x time	1.445	1763.111	0.23
	Hormone x time ²	0.063	3278.453	0.802
	Hormone x time ³	2.937	3327.746	0.087
20s	Hormone	0.076	216.372	0.784
	Time	38.137	1288.669	<.001
	Time ²	1.836	2963.595	0.176
	Time ³	0.36	3276.423	0.548
	Hormone x time	0.022	1288.669	0.883
	Hormone x time ²	0.445	2963.595	0.505
	Hormone x time ³	0.769	3276.423	0.381
25s	Hormone	0.191	214.574	0.663
	Time	86.139	1159.747	<.001
	Time ²	0.16	2616.049	0.689
	Time ³	1.05	2667.625	0.306
	Hormone x time	0.981	1159.747	0.322
	Hormone x time ²	0.315	2616.049	0.575
	Hormone x time ³	0.147	2667.625	0.702
30s	Hormone	0.992	230.826	0.32
	Time	65.486	1899.36	<.001
	Time ²	8.0	2494.223	0.371

Table S4.3 (cont'd)

	Time ³	0.04	3275.139	0.841
	Hormone x time	0.246	1899.36	0.62
	Hormone x time ²	1.284	2494.223	0.257
	Hormone x time ³	1.528	3275.139	0.216
35s	Hormone	0.992	230.826	0.32
	Time	65.486	1899.36	<.001
	Time ²	0.8	2494.223	0.371
	Time ³	0.04	3275.139	0.841
	Hormone x time	0.246	1899.36	0.62
	Hormone x time ²	1.284	2494.223	0.257
	Hormone x time ³	1.528	3275.139	0.216
40s	Hormone	52.476	233.594	0.32
	Time	27.629	1899.36	<.001
	Time ²	1.809	2494.223	0.371
	Time ³	0.453	3275.139	0.841
	Hormone x time	34.607	1899.36	0.62
	Hormone x time ²	38.588	2494.223	0.257
	Hormone x time ³	0.033	3275.139	0.216

Table S4.4 Results from the interaction models examining the effects of hormone under vehicle treatment at 5s intervals.

		F	df	р	Regression slope (b)	standard error (se)
5s Oil:	Intercept	20.392	256.212	<.001	0.337654	0.074773
	Time	59.475	2094.662	<.001	0.064232	0.008329
	Time ²	5.148	3318.274	0.023	-0.002853	0.001257
	Time ³	1.569	3343.975	0.21	6.6587E-05	5.3165E-05
5s EB:	Intercept	5.584	254.097	0.019	0.176471	0.074678
	Time	30.858	2092.489	<.001	0.046217	0.00832
	Time ²	1.136	3282.816	0.286	0.001274	0.001195
	Time ³	3.553	3329.726	0.06	-8.719E-05	4.6258E-05
10s Oil:	Intercept	66.816	237.189	<.001	0.59582	0.072891
	Time	30.029	1896.164	<.001	0.040699	0.007427
	Time ²	10.173	3099.307	0.001	-0.001854	0.000581
	Time ³	1.569	3343.975	0.21	6.6587E-05	5.3165E-05
10s EB:	Intercept	34.637	237.148	<.001	0.428504	0.072809
	Time	54.675	1631.544	<.001	0.052416	0.007089
	Time ²	0.003	3082.354	0.954	-3.41E-05	0.000586
	Time ³	3.553	3329.726	0.06	-8.719E-05	4.6258E-05
15s Oil:	Intercept	88.334	230.58	<.001	0.669824	0.071269
	Time	15.786	1849.595	<.001	0.029968	0.007543
	Time ²	1.262	3307.946	0.261	-0.000663	0.00059
	Time ³	0.912	3337.318	0.34	5.1563E-05	5.3983E-05
15s EB:	Intercept	58.163	223.601	<.001	0.533259	0.069922
	Time	32.207	1680.373	<.001	0.042787	0.007539
	Time ²	3.489	3210.816	0.062	-0.000849	0.000455
	Time ³	2.306	3308.19	0.129	-7.034E-05	4.6316E-05
20s Oil:	Intercept	47.165	213.844	<.001	0.559988	0.08154
	Time	19.248	1308.143	<.001	0.030037	0.006847
	Time ²	0.233	2986.282	0.629	-0.000376	0.000777
	Time ³	0.037	3285.353	0.848	8.0749E-06	4.2065E-05
20s EB:	Intercept	42.04	218.948	<.001	0.528293	0.081478
	Time	18.898	1268.021	<.001	0.028639	0.006588
	Time ²	2.071	2939.866	0.15	-0.001104	0.000767
	Time ³	1.134	3266.122	0.287	-4.312E-05	4.0489E-05
25s Oil:	Intercept	45.023	214.241	<.001	0.516575	0.076987
	Time	49.391	1227.739	<.001	0.045515	0.006476
	Time ²	0.435	2641.484	0.51	-0.000351	0.000531
	Time ³	0.82	2489.824	0.365	-2.762E-05	3.0493E-05
25s EB:	Intercept	37.174	214.908	<.001	0.469009	0.076924
	Time	36.878	1087.451	<.001	0.036739	0.00605
	Time ²	0.014	2587.257	0.907	5.875E-05	0.0005

Table S4.4 (cont'd)

	Time ³	0.26	2925.709	0.61	-1.258E-05	2.4684E-05
30s Oil:	Intercept	52.476	233.594	<.001	0.479592	0.05165
	Time	27.629	1960.103	<.001	-0.051432	0.05165
	Time ²	1.809	2559.404	0.179	0.04709	0.005819
	Time ³	0.453	3287.65	0.501	-0.00033	0.000369
30s EB:	Intercept	53.043	209.425	<.001	0.510698	0.070122
	Time	40.766	749.413	<.001	-0.027905	0.004371
	Time ²	2.649	2532.655	0.104	-0.000507	0.000311
	Time ³	8.261	2562.247	0.004	2.9958E-05	1.0423E-05
35s Oil:	Intercept	32.562	178.834	<.001	0.373779	0.065503
	Time	48.222	755.218	<.001	-0.032968	0.004748
	Time ²	0.653	1743.795	0.419	-0.000132	0.000163
	Time ³	16.356	2468.946	<.001	3.7278E-05	9.2176E-06
35s EB:	Intercept	29.593	186.014	<.001	0.362248	0.066591
	Time	40.064	785.885	<.001	-0.030726	0.004854
	Time ²	0.088	2047.915	0.767	-5.74E-05	0.000194
	Time ³	8.261	2562.247	0.004	2.9958E-05	1.0423E-05
40s Oil:	Intercept	52.476	233.594	<.001	0.531024	0.073305
	Time	27.629	1960.103	<.001	0.044203	0.00841
	Time ²	1.809	2559.404	0.179	-0.000748	0.000556
	Time ³	0.453	3287.65	0.501	4.5083E-05	6.6999E-05
40s EB:	Intercept	10.23	179.537	0.002	0.210928	0.065946
	Time	34.128	825.417	<.001	-0.029053	0.004973
	Time ²	5.716	1396.245	0.017	0.000392	0.000164
	Time ³	8.261	2562.247	0.004	2.9958E-05	1.0423E-05

 Table S4.5
 Results from the overall model examining drug treatment under oil.

	F	df	р
Pre-peak:			_
Drug	0.043	235.045	0.835
Time	62.86	1984.134	<.001
Time ²	4.896	2748.843	0.027
Time ³	0.011	3303.571	0.918
Drug x time	0.21	1984.134	0.646
Drug x time ²	0.033	2748.843	0.856
Drug x time ³	0.508	3303.571	0.476
Post-peak:			
Drug	0.015	179.519	0.903
Time	59.994	812.578	<.001
Time ²	12.039	1141.348	<.001
Time ³	13.452	2284.507	<.001
Drug x time	0.008	812.578	0.927
Drug x time ²	0.168	1141.348	0.682
Drug x time ³	0.003	2284.507	0.959

Table S4.6 Results from the interaction model examining drug treatment under oil.

	F	df	р	Regression slope (b)	standard error (se)
Pre-peak VEH:					
Intercept	58.002	232.982	<.001	0.549409	0.072139
Time	28.918	1941.364	<.001	0.044943	0.008358
Time ²	2.261	2647.08	0.133	-0.000813	0.000541
Time ³	0.386	3285.654	0.534	4.0664E-05	6.5416E-05
Pre-peak CNO:					
Intercept	53.011	237.112	<.001	0.528101	0.072532
Time	33.974	2024.639	<.001	0.050464	0.008658
Time ²	2.635	2831.924	0.105	-0.000959	0.000591
Time ³	0.163	3315.017	0.686	-3.037E-05	7.5213E-05
Post-peak VEH:					
Intercept	8.858	179.132	0.003	0.194592	0.065382
Time	31.21	801.535	<.001	-0.028134	0.005036
Time ²	7.565	1136.688	0.006	0.000453	0.000165
Time ³	6.768	2258.629	0.009	2.8354E-05	1.0899E-05
Post-peak CNO:					
Intercept	9.882	179.905	0.002	0.205932	0.065509
Time	28.83	823.47	<.001	-0.027474	0.005117
Time ²	4.657	1145.984	0.031	0.000357	0.000166
Time ³	6.69	2308.808	0.01	2.9157E-05	1.1273E-05

Table S4.7 Results from the overall models examining drug (VEH, CNO) under oil at 5s intervals.

		F	df	р
E-	Drug	0.07	262 222	0.604
5s	Drug Time	0.27 116.86	263.323 2059.452	0.604 <.001
	Time ²	3.134	3312.538	0.077
	Time ³	0.006	3342.554	0.938
	Drug x time	0.022	2059.452	0.882
	Drug x time ²	1.729	3312.538	0.189
	Drug x time ³	2.917	3342.554	0.103
10s	Drug X time Drug	0.038	239.745	0.846
103	Time	73.819	1886.792	<.001
	Time ²	16.533	3089.808	<.001
	Time ³	0.006	3342.554	0.938
	Drug x time	1.237	1886.792	0.266
	Drug x time ²	0.173	3089.808	0.677
	Drug x time ³	2.917	3342.554	0.088
15s	Drug	1.421	247.703	0.234
	Time	34.256	1916.4	<.001
	Time ²	11.668	3303.758	<.001
	Time ³	0.067	3339.375	0.796
	Drug x time	0.049	1916.4	0.825
	Drug x time ²	4.036	3303.758	0.045
	Drug x time ³	2.278	3339.375	0.131
20s	Drug	0.116	214.733	0.734
	Time	44.995	1306.89	<.001
	Time ²	0.293	2971.81	0.588
	Time ³	0.031	3268.426	0.86
	Drug x time	0.291	1306.89	0.59
	Drug x time ²	0.028	2971.81	0.867
	Drug x time ³	0.008	3268.426	0.928
25s	Drug	0.036	227.944	0.85
	Time	73.863	1711.661	<.001
	Time ²	2.182	2652.467	0.14
	Time ³	0.185	3247.976	0.667
	Drug x time	0.043	1711.661	0.835
	Drug x time ²	0.372	2652.467	0.542
	Drug x time ³	0.076	3247.976	0.783
30s	Drug	0.1	237.002	0.752
	Time	57.804	1998.143	<.001
	Time ²	3.768	2616.35	0.052

Table S4.7 (cont'd)

	Time ³	0.132	3292.072	0.717
	Drug x time	0.086	1998.143	0.77
	Drug x time ²	0.012	2616.35	0.913
	Drug x time ³	0.256	3292.072	0.613
35s	Drug	0.1	237.002	0.752
	Time	57.804	1998.143	<.001
	Time ²	3.768	2616.35	0.052
	Time ³	0.132	3292.072	0.717
	Drug x time	0.086	1998.143	0.77
	Drug x time ²	0.012	2616.35	0.913
	Drug x time ³	0.256	3292.072	0.613
40s	Drug	53.965	234.793	0.752
	Time	27.868	1998.143	<.001
	Time ²	1.821	2616.35	0.052
	Time ³	0.441	3292.072	0.717
	Drug x time	46.884	1998.143	0.77
	Drug x time ²	29.937	2616.35	0.913
	Drug x time ³	1.949	3292.072	0.613

Table S4.8 Results from the interaction model examining the effects of drug (VEH, CNO) under oil at 5s intervals.

		F	df	р	Regression slope (b)	standard error (se)
5s VEH:	Intercept	21.014	259.382	<.001	0.337325	0.073586
00 72	Time	60.059	2067.725	<.001	0.064296	0.008297
	Time ²	5.142	3312.566	0.023	-0.002849	0.001256
	Time ³	1.556	3343.664	0.212	6.6283E-05	5.3144E-05
5s CNO:	Intercept	14.467	267.264	<.001	0.282978	0.074399
	Time	56.824	2051.207	<.001	0.062562	0.008299
	Time ²	0.097	3312.513	0.756	-0.000421	0.001354
	Time ³	1.392	3341.222	0.238	-7.263E-05	6.1566E-05
10s VEH:	Intercept	69.093	239.799	<.001	0.595876	0.071687
	Time .	30.413	1868.812	<.001	0.040781	0.007395
	Time ²	10.213	3076.714	0.001	-0.001854	0.00058
	Time ³	1.556	3343.664	0.212	6.6283E-05	5.3144E-05
10s CNO:	Intercept	64.617	239.691	<.001	0.576195	0.07168
	Time	43.585	1902.216	<.001	0.052909	0.008014
	Time ²	6.554	3102.243	0.011	-0.00151	0.00059
	Time ³	1.392	3341.222	0.238	-7.263E-05	6.1566E-05
15s VEH:	Intercept	95.854	243.514	<.001	0.67282	0.068722
	Time	16.141	1814.232	<.001	0.029936	0.007451
	Time ²	1.318	3299.395	0.251	-0.000674	0.000587
	Time ³	0.906	3332.906	0.341	5.1154E-05	5.3739E-05
15s CNO:	Intercept	113.078	251.336	<.001	0.793772	0.074646
	Time	18.129	2019.483	<.001	0.032294	0.007585
	Time ²	11.783	3306.278	<.001	-0.002597	0.000757
	Time ³	1.375	3342.429	0.241	-7.236E-05	6.1708E-05
20s VEH:	Intercept	48.759	215.791	<.001	0.560826	0.080316
	Time	19.365	1286.476	<.001	0.02991	0.006797
	Time ²	0.238	2964.181	0.626	-0.000377	0.000774
	Time ³	0.036	3277.869	0.851	7.8976E-06	4.1902E-05
20s CNO:	Intercept	42.121	213.686	<.001	0.522088	0.080444
	Time	25.807	1326.959	<.001	0.035143	0.006918
	Time ²	0.074	2980.288	0.786	-0.000199	0.000731
	Time ³	0.004	3258.497	0.951	2.5635E-06	4.21E-05
25s VEH:	Intercept	49.844	222.827	<.001	0.517712	0.07333
	Time	51.337	1170.748	<.001	0.045476	0.006347
	Time ²	0.436	2547.704	0.509	-0.000347	0.000526
	Time ³	0.948	2428.379	0.33	-2.934E-05	3.0142E-05
25s CNO:	Intercept	44.698	233.068	<.001	0.497966	0.074483
	Time	29.459	2088.145	<.001	0.047728	0.008794
	Time ²	1.916	2730.95	0.166	-0.000835	0.000603

Table S4.8 (cont'd)

	Time ³	0.007	3307.415	0.934	-6.428E-06	7.7562E-05
30s VEH:	Intercept	53.965	234.793	<.001	0.515161	0.051337
	Time	27.868	1932.587	<.001	0.016271	0.051337
	Time ²	1.821	2524.81	0.177	0.046006	0.006051
	Time ³	0.441	3280.631	0.507	-0.000793	0.000409
30s CNO:	Intercept	59.997	205.993	<.001	0.531771	0.068653
	Time	35.484	652.231	<.001	-0.025283	0.004244
	Time ²	9.729	2246.42	0.002	-0.000925	0.000297
	Time ³	16.243	2404.209	<.001	4.0898E-05	1.0148E-05
35s VEH:	Intercept	33.446	179.482	<.001	0.37312	0.064517
	Time	48.911	740.757	<.001	-0.032968	0.004714
	Time ²	0.633	1710.729	0.426	-0.000129	0.000162
	Time ³	16.407	2429.377	<.001	3.7234E-05	9.1924E-06
35s CNO:	Intercept	35.076	184.044	<.001	0.387344	0.065402
	Time	43.117	743.791	<.001	-0.031466	0.004792
	Time ²	2.873	1714.504	0.09	-0.000312	0.000184
	Time ³	16.243	2404.209	<.001	4.0898E-05	1.0148E-05
40s VEH:	Intercept	53.965	234.793	<.001	0.531432	0.072342
	Time	27.868	1932.587	<.001	0.044235	0.008379
	Time ²	1.821	2524.81	0.177	-0.000749	0.000555
	Time ³	0.441	3280.631	0.507	4.443E-05	6.6924E-05
40s CNO:	Intercept	12.237	179.229	<.001	0.22734	0.064988
	Time	41.399	781.99	<.001	-0.031513	0.004898
	Time ²	3.511	1260.857	0.061	0.000302	0.000161
	Time ³	16.243	2404.209	<.001	4.0898E-05	1.0148E-05

 Table S4.9 Results from the overall model examining drug treatment under EB.

		ır	
	F	df	р
Pre-peak:			
Drug	0.009	222.865	0.923
Time	81.818	1942.567	<.001
Time ²	0.195	2705.888	0.659
Time ³	2.74	3294.305	0.098
Drug x time	0.061	1942.567	0.806
Drug x time ²	0.015	2705.888	0.902
Drug x time ³	0.028	3294.305	0.867
Post-peak:			
Drug	38.734	921.003	<.001
Time	20.829	1337.277	<.001
Time ²	3.32	2540.751	0.069
Time ³	0.078	178.725	0.78
Drug x time	0.306	921.003	0.58
Drug x time ²	0.023	1337.277	0.879
Drug x time ³	0.315	2540.751	0.575

 Table S4.10 Results from the interaction model examining drug treatment under EB.

	F	df	р	Regression slope (b)	standard error (se)
Pre-peak VEH:					
Intercept	34.532	221.254	<.001	0.44632	0.075951
Time	39.413	1916.266	<.001	0.050933	0.008113
Time ²	0.056	2643.801	0.813	0.000113	0.000477
Time ³	1.236	3288.703	0.266	-6.044E-05	5.4361E-05
Pre-peak CNO:					
Intercept	32.638	224.479	<.001	0.435864	0.076294
Time	42.413	1968.226	<.001	0.053783	0.008258
Time ²	0.146	2756.678	0.702	0.000201	0.000525
Time ³	1.503	3298.63	0.22	-7.408E-05	6.0419E-05
Post-peak VEH:					
Intercept	5.127	179.467	0.025	0.15958	0.070476
Time	22.678	930.479	<.001	-0.025616	0.005379
Time ²	9.345	1360.386	0.002	0.000559	0.000183
Time ³	2.705	2554.415	0.1	2.053E-05	1.2482E-05
Post-peak CNO:					
Intercept	3.521	177.982	0.062	0.131802	0.070238
Time	16.282	911.418	<.001	-0.021436	0.005312
Time ²	11.601	1312.691	<.001	0.000598	0.000176
Time ³	0.837	2525.654	0.36	1.0863E-05	1.1877E-05

Table S4.11 Results from the overall models examining drug (VEH, CNO) under EB at 5s intervals.

		F	df	р
-	D	0.00	044.000	0.704
5s	Drug Time	0.09 63.403	244.206 2168.748	0.764 <.001
	Time ²	03.403	3311.441	0.324
	Time ³	4.539	3342.405	0.324
		0.052	2168.748	0.033
	Drug x time Drug x time ²	0.032	3311.441	0.609
	Drug x time Drug x time ³	0.262	3342.405	0.609
10s	•	0.203	229.523	
105	Drug Time	99.858	1737.485	0.786 <.001
	Time ²	0.271	3147.197	0.603
	Time ³	4.539	3342.405	0.033
	Drug x time	0.111	1737.485	0.739
	Drug x time ²	0.111	3147.197	0.768
	Drug x time ³	0.265	3342.405	0.607
15s	Drug X time	0.002	213.623	0.964
103	Time	57.87	1781.731	<.001
	Time ²	5.509	3269.353	0.019
	Time ³	2.942	3331.564	0.086
	Drug x time	0.137	1781.731	0.711
	Drug x time ²	0.018	3269.353	0.892
	Drug x time ³	0.17	3331.564	0.68
20s	Drug	0.063	218.898	0.802
	Time	43.789	1328.744	<.001
	Time ²	4.795	3037.792	0.029
	Time ³	3.442	3295.643	0.064
	Drug x time	0.309	1328.744	0.578
	Drug x time ²	0.056	3037.792	0.814
	Drug x time ³	0.159	3295.643	0.69
25s	Drug	0.161	213.274	0.689
	Time	85.052	1209.903	<.001
	Time ²	0.006	2703.579	0.938
	Time ³	1.456	2688.1	0.228
	Drug x time	1.032	1209.903	0.31
	Drug x time ²	0.006	2703.579	0.938
	Drug x time ³	0.354	2688.1	0.552
30s	Drug	0.021	224.479	0.885
	Time	77.208	1949.524	<.001
	Time ²	0.141	2590.732	0.708

Table S4.11 (cont'd)

	Time ³	2.687	3287.285	0.101
	Drug x time	0.048	1949.524	0.827
	Drug x time ²	0.013	2590.732	0.908
	Drug x time ³	0.027	3287.285	0.869
35s	Drug	0.021	224.479	0.885
	Time	77.208	1949.524	<.001
	Time ²	0.141	2590.732	0.708
	Time ³	2.687	3287.285	0.101
	Drug x time	0.048	1949.524	0.827
	Drug x time ²	0.013	2590.732	0.908
	Drug x time ³	0.027	3287.285	0.869
40s	Drug	31.201	222.957	0.885
	Time	37.391	1949.524	<.001
	Time ²	0.037	2590.732	0.708
	Time ³	1.213	3287.285	0.101
	Drug x time	28.675	1949.524	0.827
	Drug x time ²	39.82	2590.732	0.908
	Drug x time ³	0.111	3287.285	0.869

Table S4.12 Results from the interaction model examining the effects of drug (VEH, CNO) under EB at 5s intervals.

		F	df	р	Regression slope (b)	standard error (se)
5s VEH:	Intercept	5.131	245.411	0.024	0.177785	0.078484
	Time	29.935	2169.769	<.001	0.046168	0.008438
	Time ²	1.104	3306.932	0.294	0.001263	0.001202
	Time ³	3.482	3338.758	0.062	-8.675E-05	4.6493E-05
5s CNO:	Intercept	7.273	243.003	0.007	0.211043	0.078254
	Time	33.517	2167.728	<.001	0.04889	0.008445
	Time ²	0.114	3315.801	0.735	0.0004	0.001183
	Time ³	1.312	3343.947	0.252	-5.301E-05	4.6281E-05
10s VEH:	Intercept	31.377	229.559	<.001	0.429353	0.07665
	Time	52.567	1716.271	<.001	0.05229	0.007212
	Time ²	0.004	3145.399	0.948	-3.843E-05	0.000591
	Time ³	3.482	3338.758	0.062	-8.675E-05	4.6493E-05
10s CNO:	Intercept	35.798	229.487	<.001	0.458864	0.076693
	Time	47.328	1759.575	<.001	0.048913	0.00711
	Time ²	0.453	3149.008	0.501	-0.000395	0.000587
	Time ³	1.312	3343.947	0.252	-5.301E-05	4.6281E-05
15s VEH:	Intercept	51.55	212.905	<.001	0.527972	0.073535
	Time	31.285	1749.575	<.001	0.042904	0.007671
	Time ²	3.342	3239.281	0.068	-0.000838	0.000458
	Time ³	2.268	3320.974	0.132	-7.023E-05	4.6635E-05
15s CNO:	Intercept	51.95	214.337	<.001	0.532733	0.073913
	Time	26.643	1815.587	<.001	0.038919	0.00754
	Time ²	2.268	3291.284	0.132	-0.000746	0.000496
	Time ³	0.847	3338.923	0.357	-4.298E-05	4.6708E-05
20s VEH:	Intercept	39.844	217.982	<.001	0.526342	0.083385
	Time	18.772	1315.816	<.001	0.028823	0.006652
	Time ²	2.002	2985.858	0.157	-0.001091	0.000771
	Time ³	1.099	3281.894	0.294	-4.262E-05	4.0644E-05
20s CNO:	Intercept	44.406	219.819	<.001	0.555911	0.083423
	Time	25.188	1341.268	<.001	0.034111	0.006797
	Time ²	2.811	3082.604	0.094	-0.001354	0.000807
	Time ³	2.454	3306.976	0.117	-6.593E-05	4.2086E-05
25s VEH:	Intercept	34.497	213.1	<.001	0.46814	0.079705
	Time	35.967	1145.385	<.001	0.036842	0.006143
	Time ²	0.013	2673.176	0.91	5.7302E-05	0.000504
	Time ³	0.239	2981.275	0.625	-1.215E-05	2.4845E-05
25s CNO:	Intercept	28.06	213.448	<.001	0.42292	0.079838
	Time	49.27	1270.38	<.001	0.045962	0.006548
	Time ²	0	2730.289	1	3.1457E-07	0.000536

Table S4.12 (cont'd)

	Time ³	1.331	2487.083	0.249	-3.581E-05	3.1037E-05
30s VEH:	Intercept	31.201	222.957	<.001	0.418593	0.054111
	Time	37.391	1926.526	<.001	0.007851	0.054111
	Time ²	0.037	2530.854	0.848	0.051191	0.005826
	Time ³	1.213	3283.648	0.271	0.000136	0.000363
30s CNO:	Intercept	38.771	201.475	<.001	0.455466	0.073148
	Time	39.609	745.48	<.001	-0.027857	0.004426
	Time ²	0.996	2569.14	0.318	-0.000301	0.000302
	Time ³	6.139	2661.264	0.013	2.5397E-05	1.025E-05
35s VEH:	Intercept	26.92	182.424	<.001	0.36421	0.070197
	Time	37.924	837.968	<.001	-0.03065	0.004977
	Time ²	0.111	2163.455	0.739	-6.532E-05	0.000196
	Time ³	8.12	2685.022	0.004	3.0014E-05	1.0533E-05
35s CNO:	Intercept	19.883	180.495	<.001	0.311823	0.06993
	Time	34.515	821.138	<.001	-0.028966	0.00493
	Time ²	0.177	2028.637	0.674	7.9572E-05	0.000189
	Time ³	6.139	2661.264	0.013	2.5397E-05	1.025E-05
40s VEH:	Intercept	31.201	222.957	<.001	0.426444	0.076345
	Time	37.391	1926.526	<.001	0.04992	0.008164
	Time ²	0.037	2530.854	0.848	9.4153E-05	0.00049
	Time ³	1.213	3283.648	0.271	-6.154E-05	5.5888E-05
40s CNO:	Intercept	6.122	176.211	0.014	0.172159	0.069578
	Time	27.328	859.386	<.001	-0.026265	0.005024
	Time ²	7.731	1452.05	0.005	0.000461	0.000166
	Time ³	6.139	2661.264	0.013	2.5397E-05	1.025E-05